TUMOR NECROSIS FACTOR ALPHA ENHANCED CYROSURGERY:
IN VITRO AND IN VIVO MECHANISMS

A THESIS

SUBMITTED TO THE FACULTY OF THE GRADUATE SCHOOL OF
THE UNIVERSITY OF MINNESOTA

BY

JING JIANG

IN PARTIAL FULFUILLMENT OF THE REQUIREMENTS FOR THE
DEGREE OF DOCTOR OF PHILOSOPHY

JOHN CHRISTOPHER BISCHOF, PHD, ADVISER

JULY 2010

ACKNOWLEDGMENTS

i

ABSTRACT

Cryosurgery has shown potential as a minimally invasive technology for tumor treatment. However, the partial destruction of tissue at the iceball edge not only potentiates the later recurrence of the tumor, but also limits the ability of imaging techniques to predict outcomes. A variety of adjuvants have been investigated to improve the efficacy of cryosurgery and the correspondence between the imaged iceball and the destroyed tissue. The most effective of these adjuvants is tumor necrosis factor alpha (TNF-α), however, the precise role of TNF-α on cryosurgery enhancement is not well understood. Prostate cancer was selected as the tumor model to investigate the mechanisms of the combinatorial treatment both *in vitro* and *in vivo*. In the *in vitro* system, increased cryosensitivity in human microvascular endothelial cells (MVEC) was noted compared to human prostate cancer cells (LNCaP Pro 5) with or without TNF-α pre-treatment. This suggests that injury to the endothelium may help govern the extent and enhancement of cryoinjury *in vivo*. In the *in vivo* model system, prostate tumor (LNCaP Pro 5) was grown in a dorsal skin fold chamber implanted in a male nude mouse. Four hours pre-treatment of TNF-α was observed to induce vascular pre-conditioning, including inflammation (NF-κB) and apoptotic (caspase) pathways upregulation. This acted to convert tumor vascular endothelium from a non-thrombotic non-adhesive barrier to a pro-adhesive surface that encouraged inflammatory cell infiltrate from the blood. After TNF-α pre-conditioning a large increase in host inflammatory infiltrate within the cryolesion was observed over cryosurgery alone. Apoptosis, subsequent to inflammatory infiltrate, was also enhanced by TNF-α through leukocyte-endothelium interaction at the periphery of the cryolesion at day 1. This contributed to vascular injury and microvascular shutdown (perfusion defect) from day 1 to 7. However, caspase and NF-κB inhibition studies show that the inflammation (NF-κB) instead of apoptotic (caspase) pathway played a dominant role in TNF-α cryosurgical enhancement *in vivo*. Finally, this combinatorial approach was tested in ELT-3 uterine leiomyoma hindlimb tumor system allowing timing, delivery, sex and tumor type to vary. This work shows the potential of this combinatorial approach for general tumor treatment with cryosurgery.

TABLE OF CONTENTS

LIST OF TABLES

LIST OF FIGURES

CONTRIBUTION OF THE AUTHOR AND OTHERS

This dissertation describes the accumulated doctoral research of the author and includes the contribution of several collaborators. The advisor, Dr. John C. Bischof worked closely with the author on the experimental planning and data analysis for the research. He also worked with the author on the writing of each published paper. A brief description of the contributions made by the author and others towards the data and text of each chapter of the thesis is detailed below.

Chapter 1: The literature review was mainly conducted by the author, modified and augmented from the previous review papers including Hoffmann et al., 2002, Goel et al., 2009 and Gage et al., 1998.

Chapter 2: This Chapter was published as: Jing Jiang, Raghav Goel, M.Arif Iftekhar, Rachana Visaria, John D. Belcher, Gregory M. Vercellotti, and John C. Bischof. Tumor necrosis factor-α-induced accentuation in cryoinjury: mechanisms in vitro and in vivo. Molecular Cancer Therapeutics 2008; 7(8): 2547-55. In this paper, the present author and Raghav Goel contributed evenly and were both first authors for the published paper. The present author planned and performed the in vitro experiment, and the in vivo experiment was performed by Raghav Goel. The author participated in data analysis and creation and edition of the manuscript for publication. Dr. Gregory M. Vercellotti helped with research planning. Julia Nguyen isolated the primary cells (MVECs) from the human foreskin and provided the MVECs culture media.

Chapter 3: This Chapter was submitted as: Jing Jiang, Raghav Goel, Stephen C. Schmechel, Gregory M. Vercellotti, Colleen Forster and John C. Bischof. Combinatorial cryosurgery: cellular and molecular mechanisms and dynamics of TNF-α enhanced cryosurgical therapy in an *in vivo* prostate cancer model system. This manuscript was

submitted to Cryobiology at the time of this dissertation submission. The author performed major experimental work of DSFC implantation, tumor treatment and vascular imaging. The H&E and IHC staining were performed by Colleen Forester. Jonathan Henriksen scanned the H&E and IHC slides, and assisted with data acquisition. Dr. Stephen C. Schmechel helped with histological analysis and quantification measurement.

Chapter 4: This Chapter was submitted as: Jing Jiang and John C. Bischof. Effect of timing, delivery and dose of tumor necrosis factor alpha in combinatorial adjuvant cryosurgery treatment of ELT-3 uterine leiomyoma (fibroid) tumor. Cryoletters, 2010; 31(1):50-62.The present author performed all experimental work and data analysis and created and edited the manuscript for publication.

Chapter 5: This Chapter was summarized by the present author. The future work was proposed by Dr. John C. Bischof, Mithun Shenoi, Neha Shah and the present author for a previous RO1 submission.

Chapter 1 Introduction

1.1 Cryosurgery Techniques

Cryosurgery (also called cryotherapy) is the use of extreme cold usually produced by cryogens to destroy abnormal tissue. For internal tumors, cryogens are circulated through a hollow instrument called a cryoprobe, which is placed in contact with the tumor. Imaging techniques, such as ultrasound or MRI, are used to guide the cryoprobe and monitor the freezing of the tissue, thus limiting the damage to nearby healthy tissue. A ball of ice crystals (ice ball) forms around the probe, freezing the cells within the iceball. Sometimes more than one probe is used to deliver the cold to various parts of the tumor. The probes may be put into the tumor during surgery or through the skin. After cryosurgery, the frozen tissue thaws and is either naturally absorbed by the body (for internal tumors), or dissolves and forms a eschar scab (for external tumors) [1].

Cryosurgery was first performed in England in the 1840s by James Arnott using iced saline [7, 222] to treat gynaecological tumors. This technique has been limited to treatment of superficial surface malignancies (i.e. nonmelanoma dermatologic conditions) due to the inability to deliver cryogens to subdermal organs [151]. It was not until 1960s that a cryosurgical probe system was developed to deliver liquid nitrogen to a cryosurgical probed placed within the body. Since then, the cryosurgery technique has been widely applied to the treatment of deep tissue diseases (i.e. prostate, liver, uterus, bone and eye) [37-39]. From the 1980s to 1990s, significant advances in cryosurgical technique were achieved including: 1) real-time monitoring and imaging techniques, such as ultrasonography (US), magnetic resonance imaging (MRI) and computed tomography (CT), to guide the surgeons to place the cryoprobe into the tumor and monitor the freezing process [85, 203, 238], and 2) the placement of multiple cryoprobes to create a desired shape of the frozen region that conforms to the complex anatomy of a diseased tissue such as the prostate [12, 254]. Due to these probe and imaging improvements, clinical application of cryosurgery has increased markedly in the last decade.

Cryosurgery is now widely applied as a treatment for a variety of cancer and noncancerous conditions (Fig. 1-1) as summarized in Table 1-2. One of the most important uses of cryosurgery in cancer is for prostate cancer. This cancer is the second leading cause of cancer-related deaths among males America with about 218,890 new cases and 27,050 prostate cancer-related deaths expected for 2007. Originally accepted primarily for salvage following local failure of radiotherapy, cryosurgery is now used more often as primary treatment for prostate cancer. It was estimated that 6,680 cryoablation procedures were performed for prostate cancer treatment in the United States in 2005 with more than 15,000 procedures projected in 2010 [66]. An online database COLD (Cryo On-Line Data) Registry consisting of case report forms was designed to collect relevant pre-treatment and post-treatment information for patients undergoing whole gland prostate cryoablation. This data shows that five-year biochemical diseases free status of whole gland cryoablation is consistent with results published for radiation and surgery [128]. Cryosurgery has been recognized by the American Urological Association (AUA) as a therapeutic option for carcinoma of the prostate and is also considered an alternative treatment for a number of other cancer including liver, kidney and breast [173, 189, 200, 201]. Recently, there has been a surge in the use of cryosurgery to treat abnormal cardiac tissue and vascular diseases [71, 140, 158, 226, 256]. The major advantage of cryosurgery is its minimal invasive nature requiring only small incision or insertion of the cryoprobe through the skin. This is also an important advantage over open surgical techniques. Compared to other minimally invasive probe technologies such as RF (radiofrequency) ablation, cryosurgery has additional advantages including painless applications, enhanced catheter stability and a smaller propensity for thrombosis [158]. However, there are still limitations for the clinical application of cryosurgery as summarized below.

The main impediment in widespread clinical use of cryosurgery is the inability of the technique to destroy cells at the periphery of the iceball. The current critical threshold for

complete destruction is usually assumed to be around -40 °C in cancer [78]. Whereas the edge of the iceball (-0.5 °C) can be visualized using US, CT or MRI, there is no means to predict the treated region or the "kill zone" within the iceball edge (Fig. 1-6). Therefore, under-freezing will result in viable cancer cells which can lead to recurrence of the tumor due to the incomplete destruction of tumor tissue at the periphery of the iceball. On the other hand, over-freezing may result in freezing of surrounding critical structures leading to various complications and morbidities. This problem is particularly severe in organs such as the prostate. Prostate cancer occurs principally in the peripheral zone of the prostate near a number of structures that the surgeon would prefer to spare from injury, including the rectum, bladder, external sphincter and the cavernosal nerves, which are responsible for erectile function.

In order to better predict the outcome and to achieve greater control of the cryosurgical procedure for prostate cancer treatment, research in the field has focused on two approaches. The first approach is the use of computational modeling to predict temperature isotherms within an iceball and to estimate the tissue volume reaching temperatures lower than -40°C [12, 271, 310]. The second approach, and also the focus of this thesis, is the use of molecular adjuvants to increase cryosensitivity of the tissue at the periphery of the iceball (-40 to -0.5°C) [104]. Use of molecular adjuvants would expand the "kill zone" to the periphery of the iceball (-0.5°C) which would have remained viable otherwise [94]. For this purpose, fundamental understanding of the impact of cryosurgery on tissue, especially the biophysical and biological mechanisms involved during and after cryosurgery, becomes critical and continues to be studied [44, 76, 114, 137, 237, 245]. Cells inside the iceball can be affected by freezing in three different ways [78]: 1) cells near the cryoprobe face the most severe thermal conditions (below -40°C) and are damaged completely beyond repair, 2) cells at the edge of the iceball (above -0.5°C) survive the mild thermal history and remain viable, 3) cells between the viable and dead zones (-40 to -0.5°C), which are injured but may choose to die or repair depending on several factors such as cell type, cell-cell and cell-ECM interaction, thermal history,

microcirculation etc. A further understanding of the nature of immediate and delayed injury mechanisms in prostate cancer especially between the viable and dead zones, at both the cellular and molecular levels is a current challenge in the field of cryosurgical research [68, 78, 114, 232]. This also potentiates the enhancement of these mechanisms by selecting appropriate molecular adjuvants, thereby extending the complete kill zone up to the iceball edge. This work specifically explores the mechanisms by which cryosensitivity can be enhanced by molecular adjuvants.

1.2 Mechanisms of Cryosurgery

The freezing of tumor tissues is a complicated phenomenon as analyzed by histology. Immediately after cryosurgery, a central necrosis area caused by direct cell injury is observed [201, 227]. The same immediate cell injury mechanisms that destroy tumor cells also destroy endothelial cells of the microvasculature. This results in post-thaw platelet aggregation and vascular stasis. Thrombosis and ultimately ischemia occur within the treated area, leading to ischemic necrosis of the frozen tumor within a few hours post cryosurgery [244, 298]. At the peripheral zone of the cryolesion, where the temperature may not have been cold enough to kill all the cells, some of the cells show signs of apoptosis which peak at 24 hours [79, 242]. A distinct inflammatory zone also appears at the demarcation of the frozen and untreated tissue from 6 hours to 3 days [227]. Wound repair begins at the periphery of the cryolesion from day 7 to a few weeks, followed by inflammatory cell infiltrate and new blood vessels growth into the injured tissue from surrounding viable tissue, and ultimately fibroblasts and new collagen formation within the lesion [123, 269]. The evolution of the histological changes as the lesions progressed over time post cryosurgery is highly correlated with the mechanisms of cryoinjury. Many people have reviewed the cryoinjury mechanisms, including Goel et al [91], Hoffman and Bischof [114], and Gage and Baust [78]. Here these mechanisms are rearranged into immediate and delayed mechanisms (Fig. 1-2).

1.2.1 Immediate Injury

a. *Cellular Impact:*

The most immediate injury caused by freezing is cellular necrosis either by intracellular ice formation (IIF) or dehydration mechanism (Fig. 1-3). Necrotic cell death is considered an accidental type of death, caused by gross cell injury, and results in death of groups of cells within a tissue. The immediate cellular injury mechanisms attributed to this mode of cell death are dependent on the thermal history defined by four parameters: cooling rate, end temperature, hold time and thawing rate. Enhanced cryoinjury is achieved by faster cooling rate, lower end temperature, longer holding time and slower thawing rate [21, 259]. However, end temperature is the most important parameter usually used to evaluate the overall effectiveness of cryosurgery[78]. Cooling rate is also critical as it will determine which cellular injury mechanism (intracellular ice formation vs. dehydration) occurs during freezing.

1) Intracellular Ice Formation (IIF):

If the cooling is too rapid, insufficient water is removed osmotically to eliminate supercooling. As a result, water trapped in the cells nucleates and grows into intracellular ice which can cause injury to the organelles and membranes by mechanical effects [133, 182].

2) Dehydration:

On the other hand, slow cooling can also be injurious as well. As ice forms outside the cells, the withdraw of water from the extracellular system by freezing creates a hyperosmotic environment, inducing dehydration of the cells [181]. The high concentration of solute has been hypothesized to injure the cell in several ways, including damage to the enzymatic machinery [166] and destabilization of the lipid-protein complexes within the cell membrane [263].

b. _Tissue Impact_

The IIF and dehydration not only destroy the tumor cells, but also destroy the endothelial cells along the blood vessel, the circulating erythrocytes and leukocytes within the vessel or in the interstitial space of the tissue. This is manifested in histology with a large central necrotic area around the cryoprobe with an intense eosinophilic staining of cells, and a loss of nuclear and cytoplasmic detail [218]. This is often referred to as the complete destruction zone (usually below -40°C) where all types of cells experience a severe freezing insult. In the partially damaged zone (between -40°C to -0.5°C), these direct injury mechanisms still occur but are attenuated. Importantly, endothelial cells have been shown to be more cryosensitive to direct cell injury than several tumor cell lines [19]. Therefore, even though the tumor cells experiencing the mild freezing are not completely destroyed, the ice crystals form and propagate along the vascular system and mechanically induce damage to the blood vessel wall causing endothelial sloughing, subsequently leading to delayed ischemic injury as described in the next section. In addition, the mechanical destruction of cells leaves a large amount of cell debris and cytokines in the injury site, sending out a signal for host inflammatory cell recruitment and adaptive immunological response.

1.2.2 Delayed Injury

In addition to the immediate effects of ice formation *in vivo* (cellular and vascular ice formation and dehydration), the tissue continues to be injured by several delayed mechanisms from hours to days after cryosurgery, which are considered to be critical to the creation of the cryolesion. These delayed mechanisms are governed by a series of local vascular events (ischemia/reperfusion), the recruitment of host cells and the interaction of host-local mechanisms in both non-tumor specific (inflammation) and tumor specific manner (adaptive immune response).

1.2.2.1 Local Injury

Delayed Local injury takes place at the cellular and vascular level. At the cellular level, apoptotic cells appear from few hours and peak at 24 hours after cryosurgery [242]. At the vascular level, both ischemia/reperfusion injury and endothelium and wall injury occur hours to days after cryosurgery, which leads to the dysfunction of vasculature and deprives the tumor tissue from oxygen and nutrient supply. Loss of nutrients and inability to remove waste yields a mature cryolesion at roughly 3 days after cryotreatment.

    a.   *Cellular Impact*

Apoptosis is recognized as another mode of cell death at the periphery of the iceball [79]. Generally speaking, there are 2 types of cell death: apoptosis and necrosis. Different than necrosis, apoptosis, or programmed cell death, is an essential physiologic process required for normal development and maintenance of tissue homeostasis. Its role in freezing is that a cell can be injured without immediate cell death leading to a possible choice. The cell may choose to repair itself and survive, or it may commit "suicide" by choosing gene-regulated or programmed cell death through apoptosis. This has been mainly investigated *in vitro*, by showing that inhibition of apoptosis in frozen cells leads to an increase in cell viability and functionality in cell culture [16, 264]. The temperature range at which apoptosis has occurred is from as high as 6 °C to as low as -10 °C and perhaps lower [193, 230]. The time spent at these temperatures required to induce apoptosis is on the order of minutes to hours [193]. The molecular pathways underlying apoptotic initiation post freeze-thaw are not completely known, however, caspase activation and mitochondrial dysfunction appear to play a role [239, 307]. Some data suggests apoptosis occurs after freezing due to transmigration of leukocytes through the endothelium during post-thaw inflammation [185, 242]. However, *in vivo* evidence of the importance and the role of apoptosis in the induction of the cryosurgical lesion and the factors stimulating apoptosis onset is still lacking in the field and thus requires further investigation [242]. In addition, there is no *in vivo* evidence so far to show if apoptosis occurs in tumor cells, endothelial cells or host infiltrated cells.

b. *Tissue Impact*

1) Ischemia/Reperfusion

During freezing procedure, the blood flow within the vasculature ceases. As the tissue thaws, the blood flows back to the recently frozen tissue. The brief period of hyperemia causes vasodilatation, increased permeability of vascular wall, edema and aggregation of platelets. Transient stasis occurs during the first 20 min due to obstruction by platelet aggregation (microemboli) [217]. Over the course of an hour blood flow will return to near normal levels. After this period, usually an hour post thaw, stasis will begin in the most affected regions. Permanent stasis occurs mainly due to the damage of endothelial cells and exposure of basement membrane, subsequently leading to edema, platelet aggregation, and microthrombus formation [302, 303] (Fig. 1-4). Small venules are completely occluded by thrombi 4 hours after thawing [4]. The loss of blood supply deprives all cells of oxygen and nutrients and allows waste to build up. This results in ischemic necrosis of tissue [178, 217]. Endothelial damage is considered as a key step in the initiation and maintenance of permanent stasis and ischemic necrosis post cryosurgery.

2) Endothelium and Wall Injury

Endothelial cell damage is caused by the immediate effects of IIF and dehydration as already discussed and the delayed effects of free radical formation during reperfusion as will be discussed here. In time the cells die from these insults by necrosis or apoptosis. When microvasculature is shut down, cells become hypoxic. During reperfusion, the high oxygen delivery to the frozen area causes free radical formation [14]. These free radicals peroxidate the lipids and create pores in the cell membrane, therefore destroying endothelial cells. Various studies done by injecting free radical inhibitors before freezing and during thaw have shown a reduction in injury [178]. Free radicals are likely to be important particularly at the periphery of the lesion during cryosurgery, which

experiences milder direct cell injury (immediate injury) conditions. The free radical formation during ischemia/reperfusion not only leads to direct endothelial injury, but also contributes to the initiation of inflammation mechanism.

1.2.2.2 Host Mediated Immunological Injury

In addition to the successful cryoablation of the primary tumor, reports of metastatic tumor destruction have suggested that an inducement or augmentation of "host resistance", possibly immunologic in nature, may occur as a result of cryosurgical destruction [75, 219, 260] (Fig. 1-5). Key elements of the host response are: to destroy tumor cells, prevent the spread of tissue damage, contain imbalances of homeostasis, remove dead damaged/altered tissue, and ultimately restore tissue function [147]. The interaction of the host immunological response with the local tumor tissue enhances the cryoinjury at the local site, and also elicits a prolonged anti-tumor mechanism that has a distant effect on metastatic tumor and second tumor challenge. The host immunological response is first orchestrated by the innate immune response in a non-antigen specific manner, which subsequently facilitates adaptive immune response, an antigen specific immunological response [235].

a. _Innate Immune Response (Inflammation)_

Besides the local injury mechanisms (IIF, dehydration, ischemia/reperfusion and apoptosis), a "host mediated" inflammatory response is also observed, which essentially governs the extent of the cryolesion. This mechanism induces accumulation of inflammatory cells in the border area between frozen and incompletely frozen tissue [198, 242]. The interaction of this "host inflammatory response" with the local tumor tissue is initiated by several mechanisms. First, necrosis releases endogenous danger signals including: 1) intracellular contents, such as pro-inflammatory cytokines(e.g. TNF-α, IL-1 and 6), heat shock proteins (HSP), DNA and RNA uric acid and the chromosomal protein

HMGB1 (high mobility group box chromosomal protein and 2) disruption of tissue architecture, such as fibrinogen, oligosaccharides of hyaluronan, extra domain A (EDA)-containing fibronectin and heparin sulfate proteoglycan [49, 257, 258, 276]. These "danger signals" can initiate recruitment of circulating leukocytes to the injury site, and further activate the innate immune response [235]. Secondly, during ischemia/reperfusion post cryosurgery free radicals formed in the vasculature induce NFκB-dependant transcription of gene encoding adhesion molecules (ICAM, VCAM, E-selectins and P-selectins) [11, 36, 290] that further mediate leukocyte transendothelial migration from circulation to the interstitium. Therefore, it is not surprising that leukocytes originally accumulate mainly at the margin of the lesion where reperfusion occurs, but not in the center.

The neutrophil is by far the most prevalent leukocyte in the early (up to 3 days) inflammatory infiltrate. Neutrophils are called to clean up the debris from the cells that died or were injured during the freeze. In the process, they adhere to the endothelium and release enzymes designed to digest the dead cells. However, with the large insult that comes from the tissue freezing, the neutrophils become over activated and can destroy live cells in the process. Several studies found neutrophils in the region of injured vessels [24, 113, 224]. Intravital techniques have shown neutrophil adhesion to the wall of vessels after freezing the injury [6, 313]. The endothelium is damaged in particular because the activated neutrophils must migrate through the endothelial lining [60]. Neutrophils also play a central role in this host inflammatory response by initiating the coagulation cascade [268], acting as chemoattractants for inflammatory cells [59, 268], beginning the debridement of devitalized tissue, and phagocytosis of foreign bodies by releasing toxic agents (myeloperoxidase, free radicals, cationic peptides, eicosanoids and proteases) [131, 300].

  b. *Adaptive Immune Response:*

The second stage of immunological response occurs by activating the adaptive immune system. Immunostimulation is mainly induced by cell lysis releasing tumor antigens into the blood stream. These antigens are taken up by antigen presenting cells (APC) (dendritic cells and macrophages), the maturation of APC further leads to B cell mediated humoral response (the generation of antigen-specific antibody) or T cell mediated cellular response [235], depending on the cytokines released by APC, the helper T-cells and other cells within the microenvironment. Cytotoxic T-cells are mainly activated by the cytokines released from the Th1 helper T-cell (IL-2, IFN-γ, TNF-α, GM-CSF). A second cascade can occur when Th2 helper T-cells are activated and the secretion of B-cell stimulatory cytokines (IL-4, IL-5, IL-10), which stimulate the B-cell to proliferate and differentiate into plasma cells for antibody production [91, 115, 235].

Among these steps, maturation of APC, especially dendritic cells, is a prerequisite to determine whether the tumor debris is able to induce adaptive immune response [46]. Both necrosis and apoptosis generated by cryosurgery are considered as endogenous "danger signals" which have significant impact on the immune response [235]. Necrosis not only induces the innate immune response as described in last section, but also leads to increased dendritic cell maturation and macrophage activation [80, 240], which could further activate adaptive immune response. The role apoptosis plays in immune response is not completely clear yet. In fact, several studies have suggested that apoptotic cells are recognized and phagocytosed as "self" cells instead of "non-self" cells, which prevents pro-inflammatory cytokine release and dendritic cells maturation [63, 163, 241, 265], therefore contributing to immunosuppresion verses immunostimulation [212]. As both necrosis and apoptosis play a role in tumor cell death after cryoablation, the relative contribution of necrosis and apoptosis in the death of the tumor cells may shift the immune response from stimulatory to suppressive. It is therefore evident that the ability of cryoablation to generate an anti-tumor response and the nature of that response will be dependent on: 1) the availability of antigens, 2) "danger signal" triggered by cryoablation, 3) the mode of cell death (apoptosis vs. necrosis), 4) the recruitment and maturation of

APC. However this theory is still controversial as cryosurgical ablation of tumors is known to induce both immunostimulation and immunosuppresion in animal models and in patients.

1.2.3 Interaction of Mechanisms

It is worth noticing that all these immediate and delayed injury mechanisms (local vs. host mediated injury) are highly interrelated and overlapping in their effects. Inflammatory cell infiltrate is considered as a key step in enhancing the local injury through a host-local interaction at the vascular level, and also an important linkage to activate a tumor-specific immunological response. As mentioned above, immediate cell damage due to freezing causes release of certain chemotactic factors which direct inflammatory cells to the site of injury. Formation of free radicals also contributes to recruitment of more inflammatory cells. Inflammatory cells produce free radicals, and also adhere to the endothelium and plug microvessels, further amplifying the damage to endothelium and therefore tissue ischemia [183]. Also, recruitment of inflammatory cells and release of inflammatory cytokines elaborate the tumor microenvironment, which subsequently facilitates the activation of adaptive immune response. The importance of these mechanisms and their enhancement by adjuvants post cryosurgery continue to be investigated at the cellular, molecular and host level in this study.

1.3 Adjuvants for Cryosurgical Enhancement

In recent years, new adjuvants are being sought to increase the destructive effect of freezing. The reason for this is due to the incomplete destruction of tumor tissue at the periphery of the iceball with cryosurgery alone. This makes the modern monitoring techniques for the iceball imaging (US, CT or MRI) unable to predict the outcome of the cryosurgical procedure [85, 203]. Two critical limitations remain in the use of cryosurgery for prostate cancer: 1) tumor recurrence after under freezing 2) morbidity

associated with over freezing of adjacent critical structures which subsequently lead to complications such as rectal and uretheral fistulas [237]. Therefore, cryosurgical adjuvants are being investigated to destroy the tumor more effectively by overlapping the iceball and kill zone. This effectively increases the ability of iceball monitoring technologies to predict injury (Fig. 1-6). These adjuvants are designed to accentuate the tissue injury mechanisms known to be induced by cryosurgery. Four non-exclusive categories of cryoadjuvant are reviewed by Goel et al. [91], including 1) thermophysical adjuvants, 2) chemotherapeutics, 3) proinflammatory cytokines or vascular based agents, and 4) immunomodulators. These adjuvants used for cryosurgical enhancement have been summarized in Table 1-3 (*in vitro*) and Table 1-4 (*in vivo*).

1.3.1 Thermophysical Adjuvants

Thermophysical adjuvants modify the shape of ice crystals during freezing thereby enhancing the mechanical destruction of the cell membranes connective tissue [148, 149, 191, 215]. These adjuvants include antifreeze proteins (AFP) creating spicular ice, salts (i.e. NaCl, KCl), and some amino acids (i.e. glycine) to create separate eutectic phases that damage cells. These adjuvants can enhance the threshold injury temperature up to -5°C [103, 104, 215, 294]. However, a major challenge of using these adjuvants is delivering sufficiently high concentration of adjuvant locally to achieve the desired effect without causing toxicity to the surrounding normal tissue.

1.3.2 Chemotherapeutics

The synergistic effect of cryosurgery and ancicancer drugs (chemotherapeutics) was discovered in tumor model systems by using peplomycin and adriamycin [122]. This is due to the fact that vascular volume and vascular permeability increases immediately after cryosurgery, therefore frozen tumor preferentially traps the anticancer drugs as compared to untreated tumor. Recently, as apoptosis is recognized as another mode of cell death at the periphery of the iceball, many studies used apoptosis inducer combined

with cryosurgery at the mild temperature (-40 to -0.5°C). These apoptosis inducers include 5-fulorouracil, cisplatin, doxorubicin, mitomycin and bleomycin, vinorelbine, navelbine and TRAIL (tumor necrosis factor-related apoptosis-inducing ligand) [32, 34, 68, 70, 156, 186, 308]. However, most of these studies are *in vitro* and their impact *in vivo* still requires verification. Importantly, chemotherapeutics have not shown the ability to enhance the cryodestruction up to the iceball edge.

1.3.3 Pro-inflammatory Cytokines and Vascular Agents

Studies in our lab demonstrated pro-inflammatory cytokine TNF-α with appropriate dose and timing can dramatically improve cryosurgical destruction even completely destroy up to the iceball edge (-0.5 °C). As TNF-α is a multifunctional cytokine which can induce complicated effects to the tumor cells, vasculature and immune cells by activating different intracellular pathways (apoptosis vs. inflammation), the exact mechanisms of TNF-α enhancement on cryosurgery is poorly understood and will be further investigated in this study. In addition, as systemic toxicity induced by TNF-α is a limitation for its clinical application, thus targeted delivery of TNF-α to the tumor site becomes another challenge for this work.

1.3.4 Immunomodulators

As APCs (especially dendritic cells) play a pivotal role in the induction of adaptive immune response, several studies showed the ability to enhance cryosurgical destruction by inducing and stimulating dendritic cells in the injury site, including imiquimod, CpG-oligodeoxynucleotides, BCG-CWS (bacillus calmette-guerin cell wall skeleton) and GM-CSF (macrophage-colony-stimulating factor) [51, 83, 221, 281]. The future selection and identification of immunomodulators still requires a better understanding of the immunological mechanisms stimulated by cryosurgery.

1.4 TNF-α for Cancer Treatment

TNF-α stands for tumor necrosis factor, for its antitumor properties when originally discovered 30 years back in 1975 [25]. Since then, many other functionalities of this multi-functional cytokine have been ascertained and are still being investigated. TNF-α is secreted mainly by macrophages, NK cells and T-lymphocytes and other cell types such as fibroblasts, astrocytes, smooth muscle cells and most tumor cells [95, 267]. It is a vital cytokine involved in inflammation, immunity, apoptosis cell differentiation and proliferation [65, 109, 187, 267, 285, 295, 297] (Fig. 1-8). It can act in many different ways, depending on the cell type, dose and presence of other molecules in the environment [41].

1.4.1 TNF-α as an Anti-Tumor Agent

The use of TNF-α as antitumor agent goes back to 20th century as the main component in the Coley's toxin used for treatment of patients with sarcoma, carcinoma and lymphoma [187]. With the development of recombinant- TNF-α in 1984, a lot of research has been done to study the cytotoxic effects of the protein in many different cancers [255]. There appear to be a number of mechanisms by which TNF-α induces an anti-tumor effect (Fig.1-7). When given at high doses, it starts a chain of complex reactions culminating in destruction of the tumor. In 1988, Watanabe et al [295] demonstrated that it can promote coagulation and destroy tumor vasculature [194]. Through activation of receptors on the surface of endothelial and tumor cells, it can induce killing of tumors by immune cells of the host [5, 55, 65], subsequently causing ischemia to the center of the tumors [108]. It also has direct cytotoxic effects on endothelial cells [229] and many tumor cell lines *in vitro* by production of hydroxyl radicals and induction of apoptosis [187].

To enhance the ability of TNF-α to kill tumors, a number of studies have examined the synergistic effects of TNF-α in combination with cytokines, chemotherapy agents, radio

therapy, hyperthermia and cryosurgery. In conjunction with cytokine IFNγ, TNF-α has been shown to cause haemorrhagic necrosis, inducing vascular engorgement by erythrocytes and adhesion of platelets to tumor vascular endothelium. This then leads to destruction of the tumor vasculature with necrosis and apoptosis [45]. Using L-M cells the addition of a number of commonly used chemotherapy agents to cultures containing recombinant human TNF-α (rhTNF) produced 4-347 fold decrease in the IC50 (the concentration required for 50% inhibition of cell growth) compared to rhTNF alone [296]. The vascular injury induced by TNF-α has lead to its use as an adjuvant to radiation therapy and hyperthermia. Combinations of liposomal-encapsulated TNF-α with radiation have shown some promise in animal models of cancer including prostate cancer [30, 54, 99, 100, 283]. Investigations have begun to assess the ability of TNF-α to enhance low temperature hyperthermic injury. Hiraoka et al explored the combined effects of TNF-α and hyperthermia in a transplanted TNF-α-sensitive Meth-A tumor model [111]. A synergistic effect of TNF-α and hyperthermia was observed when TNF-α was administered 10 min before heating. This thermal enhancement of the action of TNF-α became more prominent with an increase in heating temperature. Visaria et al has combined TNF-α and hyperthermia (42.5°C for 30 minutes) to treat a TNF-α -resistant fibrosarcoma *in vivo* [289]. Individually both the modalities cause a minimal effect on tumor cytotoxicity. However, the combination of both modalities resulted in a marked decrease of tumor doubling time. Necrosis and hemorrhage were the most prominent histopathological alteration in the treated tumors. In summary, these studies have shown that TNF-α enhances hyperthermic injury in part through vascular injury.

1.4.2 TNF-α and Cryosurgery

Our laboratory has generated preliminary work with TNF-α administered *in vivo* showing that 4 hours pre-treatment of the tumor tissue with TNF-α can dramatically accentuate freeze injury over freezing alone [94]. Our initial desire of selecting TNF-α is due to the pro-inflammatory aspect of this cytokine, which is hypothesized to pre-condition the tumor tissue through a vascular inflammation mechanism. The role of TNF-α in

cryosurgery can be multi-factorial due to its inherent complexity as well as the uncertainties associated with mechanisms of cryoinjury. In order to understand the enhancement of cryoinjury by TNF-α at the cellular and molecular level, it is important to assess the potential overlap between freezing injury and TNF-α induced injury in the cells and tissues of cancer.

As already mentioned TNF-α promotes expression of various molecules on the cell membrane thus starting a chain of events inside the cell. TNF-α can directly kill tumor cells by necrosis, or under certain conditions it can also stimulate apoptosis. It also induces formation of free radicals which cause lipid peroxidation and protein damage [297]. TNF-α also has multiple effects on the tissue vasculature. First of all, it produces direct vascular damage by inducing endothelial cell apoptosis and subsequent hemorrhagic necrosis of tumor interstitium [194]. Second, TNF-α induces vascular inflammation by expression of adhesion molecules such as ICAM-1, VCAM-1, and selectins on endothelial cells through NF-κB pathway activation, thus leading to an enhancement in host leukocyte recruitment. Third, TNF-α also activates neutrophils, and monocytes by upregulation of adhesion molecules and promotes coagulation [297]. It's worth noting that the adhered neutrophils migrate to interstitium, and the neutrophil-endothelial interaction produce various cytokines (TNF-α, IL-1, IL-8, PDGF) amplifying the vascular inflammation effect, therefore enhancing vascular injury.

The precise mechanisms of TNF-α plays in cryosurgical enhancement is first based on the cells affected. Tumor cells, endothelial cells and host infiltrated leukocytes are the components of tissue, directly affected by the action of cryosurgery as well as TNF-α. Thus, the cellular response after TNF-α combined with cryosurgery needs to be carefully studied in this work. It is hypothesized that TNF-α induces a vascular injury over a direct tumor cell injury, which further potentiates the cryosurgical injury. This vascular injury mechanism is not only a local response, but more importantly, also depends on the host

17

mediated inflammatory infiltrate and its interaction with tumor vasculature. These cellular events are highly associated with the molecular mechanisms activated by TNF-α, and the final response induced by TNF-α followed by cryosurgery depends on the dominance of one molecular pathway over all other (i.e. apoptosis pathway vs. inflammation pathway). The precise role of apoptosis vs. inflammation induced by TNF-α and cryosurgery in different cell types and how these mechanisms link to each other is yet to be defined both *in vitro* and *in vivo*. Overall, it is believed that TNF-α is more pro-inflammatory vs. pro-apoptotic and that will activate endothelium, augmenting the accompanying inflammatory response and inflicting more damage post cryosurgery. Specifically the cells at the periphery of the lesion, which usually survive a freeze, are likely to be the target of a combined TNF-α and freezing assault.

1.4.3 Delivery Systems of TNF-α

The major limitation for the clinical application of TNF-α is the systemic toxicity. It has been administered intravenously to a wide range of tumors in Phase I and II clinical trials with none or limited tumor responses and was associated with severe toxicity particularly hypotension, rigors, fever and hepatotoxicity [23, 43, 74, 248]. The delivery of TNF-α is an important aspect of the proposed treatment. The use of TNF-α and IFN-γ, which had been shown *in vitro* to act synergistically, has also been evaluated in clinical trials, again the toxicity produced was unacceptable [2, 64]. The maximum tolerable dose clinically in human is $300\mu g/m^2$ [187]. TNF-α however, has been shown to be useful in limb perfusion studies for patients with melanoma and soft tissue sarcomas. In these studies, the limb vasculature was isolated from the body and large amounts of systemically toxic TNF-α were infused into these tumor-bearing limbs to necrose the tumor [58]. This strategy is licensed in Europe in combination with melphalan, since the addition of TNF-α to melphalan increased the response rates considerably. The use of TNF-α as an anti-cancer agent has clear limitations due to its systemic toxicity and may even be deleterious in the long term. The safe yet effective delivery of TNF-α is an important aspect of the proposed treatment.

Several technologies exist for the delivery of TNF-α to tumors, including liposomes, gene therapy, and most recently nanoparticle delivery systems [48, 99, 119, 139, 142, 144, 197, 207, 282, 283]. Research in our lab has focused on the CYT-6091, a multivalent drug assembled by covalently binding of TNF-α molecules and PEG-THIOL (thiol-derivatized polyethylene glycol) on 33 nm nanoparticles of colloidal gold [205]. TNF-α molecules act as both the ligand for receptor targeting and the therapeutic. The PEG-THIOL serves to hydrate the colloidal gold nanoparticles and in doing so, shields the nanoparticle drug from detection and clearance by the RES (reticuloendothelial system). Therefore, such delivery systems preferentially extravasate in the leaky tumor vasculature and passively accumulate drug within the tumor microenvironment while concomitantly reducing the accumulation in healthy organs [177, 192, 207, 210, 304]. CYT-6091 just successfully finished a phase I clinical trial as a stand-alone delivery vehicle (publication is pending). Our laboratory has developed collaboration with CytImmune, Inc. the company who provided the CYT-6091 for all of the *in vivo* experiments.

We recently have reported on the safe use of CYT-6091 (250 μg/kg), 4 hours before cryosurgery significantly increased tumor growth delay in a LNCaP Pro 5 prostate cancer grown in athymic nude mice [289]. Similar results were found with the addition of CYT-6091 prior to hyperthermia in our murine model of breast cancer [94]. However, the effect of pre-treatment time, dose and delivery methods of TNF-α on cryosurgical enhancement in different tumor model systems are still required for the clinical translational of this combinatorial cryosurgical treatment.

1.5 Overview of Ph.D Dissertation

1.5.1 Research Goal

To determine the cellular and molecular mechanisms whereby TNF-α enhances cryosurgical injury. In particular, the importance and dynamics of vascular injury and, inflammatory mechanisms in both *in vitro* and *in vivo* tumor model systems will be investigated.

1.5.2 Hypothesis

TNF-α pre-conditioning promotes an inflammatory infiltrate, which enhances vascular injury during cryosurgery, thereby enlarging the cryolesion.

1.5.3 Specific Aims

1. To determine the dominant molecular mechanism (apoptosis vs. inflammation) of TNF-α accentuated cryosensitivity in both *in vitro* and *in* vivo prostate cancer model systems. – Chapter 2

2. To investigate TNF-α induced pre-conditioning events and dynamics of TNF-α on cryosurgical enhancement mechanisms (host-mediated inflammation) in an *in vivo* prostate cancer model system. – Chapter 3

3. To characterize the timing, dose and delivery methods of combined TNF-α and cryosurgery for cancer treatment in an *in vivo* leiomyoma model system. – Chapter 4

1.5.4 Research Overview

The concept and mechanisms associated with enhanced cryosurgical destruction with an inflammatory adjuvant (TNF-α) are described and characterized in this work. While adjuvant application is not a new topic, this work identifies for the first time the importance of the inflammatory infiltrate in creating vascular injury, a key mechanism in

cryosurgical enhancement. A preclinical characterization of TNF-α delivery regime and methods further promises the translation of TNF-α enhancement of cryosurgery into clinical application. This doctoral dissertation is organized into chapters, each chapter consisting of a specific research project. The aim and end objective of each research project are summarized below.

For Chapter 2, in the case of prostate cancer cryoinjury augmentation, the effect of using TNF-α as an adjuvant was first characterized *in vitro* in appropriate isolated cell model that can serve as the basis for molecular studies of the pertinent biological mechanisms. The cells studied were LNCaP Pro 5, a human prostate carcinoma subline, which is non metastatic in nude mice and androgen-dependent [214]. The second cell type studied was human mircovascular endothelial cells (MVEC) isolated from human foreskin neodermis in primary cultures [17]. These cells were chosen as representative of the tumor epithelial and microvascular endothelial cells in human prostate cancer. A controlled cryotreatment protocol with and without TNF-α was administered in cell monolayers. In addition, a unique *in vivo* prostate tumor xenograft model (LNCaP Pro 5) grown in a dorsal skin fold chamber (DSFC) on a male nude mouse was constructed to investigate and compare TNF-α effect of cryosurgical enhancement. First, the effect of TNF-α dose on cryoinjury (viability, DNA damage and threshold injury temperature) was compared *in vitro* and *in vivo*. Finally, the dominant molecular mechanism was investigated by inhibition of apoptotic or inflammatory pathway both *in vitro* and *in vivo*. Although it is evident both *in vitro* and *in vivo* results that the administration of TNF-α before freezing increases the amount of injury significantly, the increase in injury is significantly higher *in vivo* as compared with that *in vitro*. In addition, the inhibition of apoptotic and inflammatory pathways during cryosurgical enhancement with TNF-α presents contrasting results suggesting host-mediated inflammation is responsible for augmentation *in vivo* and while MVEC-mediated apoptosis is a dominant the mechanism *in vitro*. This discovery prompted us to further investigate the role of endothelial cells and more importantly, the host mediated inflammation response in TNF-α induced accentuation in cryoinjury as

described in Chapter 3.

Chapter 3 aims to further investigate the cellular and molecular mechanisms and dynamics of TNF-α pre-conditioning on cryosurgical enhancement *in vivo*. The same tumor xenograft model system (i.e. LNCaP in nude mouse DSFC) as described in Chapter 2 is used here. This model allows comparison of intravital thermography, vascular imaging, and post-sacrifice histological and immunohistochemistry at different time points within the tumor. These assessments allow unprecedented quantification for cryosurgery. Specifically new insights into the importance of TNF-α pre-conditioning, iceball location, and temperature in the destruction of prostate cancer are reported. In concert with the model a new histological method is developed to track spatial and temporal measurement of necrosis, inflammation, thrombosis and granulation dynamics within the tissue after treatment. A powerful new scanning and image analysis system allows us to better characterize and quantify the histology and immunohistochemistry information at the molecular, cellular and tissue level. The results suggest that TNF-α pre-conditioning enhances cryosurgical lesions by vascular mechanisms that lead to direct tumor cell necrosis and indirect tumor cell injury via promotion of inflammation and leukocyte (esp. neutrophil) recruitment.

Finally, Chapter 4 characterizes the effect of pre-treatment time, dose and delivery methods of TNF-α on cryosurgical enhancement in a uterine fibroid system. This is a drift from my previous model system in the following: 1) the prostate cancer model (LNCaP) has been changed to a leiomyoma tumor (ELT-3) model system; 2) Male nude mice in previous prostate cancer study have been changed to female nude mice for this leiomyoma tumor model. Male; 3) a hind limb tumor, a three dimensional and more realistic representation of tumor, has been implanted in a nude mouse instead of a two dimensional tumor xenograft grown in dorsal skin fold chamber. This hind limb tumor system allows the measurement of tumor growth delay post treatment; and 4) the TNF-α

nanoparticle delivery system CYT-6091 has been used (i.v. injection) here to compare to native TNF-α for its efficacy and safety evaluation. Although TNF-α shows promise as an adjuvant to cryosurgery, as a stand alone drug for tumor control TNF-α causes hypotension with dose-limiting toxicity as shown in poor phase I/II clinical trial results [110]. Therefore, the administration regime of TNF-α needs to be carefully characterized based on efficacy and toxicity in 3D tumor model. Recently, we have shown the ability to enhance cryosurgical destruction to the visualized iceball edge without toxicity using nanoparticle delivery of TNF-α at 5 µg dose (CYT-6091) [94, 311]. This promising finding in a prostate cancer model (LNCaP) of male nude mouse prompted us to investigate this combinatorial approach in a different tumor (ELT-3 uterine leiomyoma) with several new dose, timing and delivery approaches for TNF-α introduction. Therefore, a uterine fibroid tumor (ELT-3) xenograft implanted in hind limb of a female nude mouse was used to evaluate the tumor growth delay and toxicity subject to different treatments. Our work suggests that an i.v. dose between 2 and 5 µg CYT-6091 with a 4 hours pre-treatment time and a more aggressive cryosurgical protocol (i.e. freezing beyond the visible edge of the tumor) may accomplish non-toxic and effective enhancement of cryosurgical destruction in ELT-3 (uterine fibroid) tumors. This study also suggested the potential of this combinatorial approach for general tumor treatment allowing sex (male vs. female) and tumor type (prostate tumor vs. uterine fibroid) to vary. In order to translate the use of the adjuvant CYT-6091 enhancement of cryosurgery into enhanced destruction and control of uterine fibroids in the clinic clearly further basic and preclinical work is needed.

Table 1-1: (a) list of cryogens that have been used in cryosurgery instruments [77]; and (b) summary of cryosurgical devices and the various indications for which they are used [91]

Cryogen	Lowest achievable temperature (°C)
(a)	
Ice-saline	−21.2
Dichlorotetrafluoromethane (Freon 114)	3.8
Dichlorodifluoromethane (Freon 12)	−29.8
Chlorodifluoromethane (Freon 22)	−40.8
Solid carbon dioxide (CO_2)	−78.5
Liquid nitrous oxide (N_2O)	−89.5
Argon (compressed)	−185.7
Liquid nitrogen (N_2)	−195.8

Probe	Co.	Cryogen	Shape	Indications	Web
(b)					
Cancer targets					
SeedNet™[a]	Galil Medical, Yokneam, Israel	Argon JT	Probe	Prostate, kidney cancers, and uterine fibroids	www.galil-medical.com
CryoCare CS™[a]	Endocare, Irvine, CA	Argon JT	Probe	Prostate, kidney, lung, and liver cancers	www.endocare.com
Visica 2™	Sanarus, Pleasanton, CA	Liquid N_2	Probe	Breast fibroadenomas	www.sanarus.com
Various Systems	BryMill, Ellington, CT	Liquid N_2	Probe, spray	Dermatologic lesions	www.brymill.com
Erbokryo CA™	Erbe Medical, Leeds, UK	N_2O or CO_2 JT	Probe	General surgical use	www.erbe-med.com
			Noncancer targets		
CryoMaze™	ATS Medical, Minneapolis, MN	Argon JT	Steerable catheter	Cardiac arrythmia	www.atsmedical.com
FrostByte™	ATS Medical, Minneapolis, MN	Argon JT	Clamp probe	Atrial fibrillation	www.atsmedical.com
Arctic Front™	Cryocath,[b] Montreal, QC, Canada	Liquid N_2O	Balloon catheter	Atrial fibrillation	www.cryocath.com
Freezor™	Cryocath, Montreal, QC, Canada	Liquid N_2O	Steerable catheter	Cardiac arrythmia	www.cryocath.com
CryoCor™	Boston Scientific, Natick, MA	Liquid N_2O	Steerable catheter	Atrial flutter	www.cryocor.com
PolarCath™	Boston Scientific, Natick, MA	Liquid N_2O	Balloon catheter	Peripheral arterial disease	www.bsci.com
HerOption™	American Medical Systems, Minnetonka, MN	Mixture of cryogens	Probe	Endometrial bleeding	www.americanmedicalsystems.com
CryoPac™ Systems	Cryomed LLC, Layton, UT	N_2O or CO_2 JT	Probe	Chronic pain	www.cryomed.us

[a]Purchased by Medtronic, Inc. in 2008.
[b]Merging in 2008–2009.

24

Table 1-2: Summary of the current patient base for various diseases that have cryosurgery as one treatment option [91]

Targets	New cases/deaths[a]	Cryosurgical outcomes	Alternatives	References
Cancer targets				
Skin cancer[b]	65,000/10,900	95-98% cure rates	Surgery, rad and chemo	[8, 26, 83, 96, 132, 221, 275]
Prostate cancer	218,900/27,000	1-2 years no PSA	Surgery, rad, chemo, and heat	[9, 105, 137, 164, 246]
Breast cancer	180,510/40,910	Size reduction	Surgery, rad, chemo, and heat	[20, 138, 162, 199]
Liver (colon[d]) cancer	19,200 (112,300)/16,800 (52,200)	5 year survivals	Surgery and heat	[47, 52, 129, 137, 155, 202, 247]
Kidney cancer	51,200/12,900	5 year survivals	Surgery and heat	[86-88, 116, 223, 299]
Lung and bronchus	213,400/160,400	Palliation	Surgery and heat	[18, 170-172]
Noncancer targets				
Skin: keloids/scars	Unknown	Cosmetic	Excision/ grafting	[106, 107, 233]
Uterus: abnormal bleeding	Unknown	Improved lifestyle	Surgery and heat	[31, 234, 278]
Uterus: uterine fibroids	>60% in women above 45	Maintain uterus	Surgery	[10, 236, 251, 314]
Cardiac arrhythmia	>2.2 million	Improved lifestyle	Surgery and heat	[134, 141, 188, 220]
Vascular disease	12-20% above 65	Reduce arteriosclerosis	Angioplasty and stenting	[77, 226]

[a]Sources of incidence: ACS statistics 2007 and AHA statistics 2007.

[b]Cure rates apply to nonmelanoma skin cancers.

[c]Fibroadenomas – a nonmalignant tumor.

[d]Many liver cancers in the western world are metastatic from colon carcinoma.

Table 1-3: *In vitro* adjuvant for cryosurgical enhancement [91]

Mechanism	Model	Adjuvant	Dose	Time	Reference
(1) Thermophysical Adjuvant: Ice Crystals	Normal Rat Liver	ATP-1	10 mg/ml	0-5 mins before FT	[148]
	Rat Prostate	Eutectic Salts	Eutectic conc.	0-5 mins before FT	[103]
	Human Breast	Glycine	10 g/ml		[294]
(2) Chemotherapeutics: Apoptosis, Antiproliferative	Human Prostate	5-FU	25 µg/ml	2-4 days before FT	[32]
	Human Prostate	5-FU*	25 µg/ml	2 days before FT	[33]
	Human Prostate	TRAIL	500 ng/ml	0-5 mins before FT	[34]
	Human Hepatoma	Doxorubcin**	55 µg/ml	24 hrs before FT	[308]
(3) Inflammatory Cytokines: Apoptosis, Inflammation	Human Prostate	TNF-α	1-1000 ng/ml	4 hrs before FT	[126]
	Human Endothelial	TNF-α	1-1000 ng/ml	4 hrs before FT	[126]
	Human Breast	Imiquimod	100 ng/ml	24 hrs before FT	[15]
	Human Prostate	TNF-α	1 µg/ml	4 hrs before FT	[84]

* Enhancement was also reported with other drugs : cisplatin, etoposide and taxotere.
** Enhancement was also reported with other drugs: mitomycin, 5-fluorouracil, cisplatin.

Table 1-4: In vivo adjuvant for cryosurgical enhancement [91]

Mechanism	Model	Adjuvant	Dose	Time	Reference
(1) Thermophysical Adjuvant: Ice Crystals	Human Prostate	AFP-1	10 mg, local	0-5 mins before FT	[215]
	Rat Prostate	Flounder AFP	0.5 mg, local	0-5 mins before FT	[191]
(2) Chemotherapeutics: Apoptosis, Antiproliferative	Human Lung	Navalbine	120 µg, i.v	Multiple time points	[68]
	Human Lung	Vinblastine	120 µg, i.v	20 hrs after FT, 15 days after FT	[70]
	Human Prostate	5-FU	15-20 ng, local	0-5 mins after FT	[156]
(3) Inflammatory Cytokines: Apoptosis, Inflammation	Human Prostae	TNF-α	0.2-1 µg, local 5 µg, i.v	4 hrs before FT 4 hrs before FT	[94, 126] 2.
(4) Immunomodulators	Mouse Melanoma	Imiquimod	3.12 mg, local	Up to 10 days after FT	[221]
	Mouse Melanoma	CpG-ODN	100 µg, local	1 hour after FT	[51]
	Mouse Colon	BCG-CWS			[281]
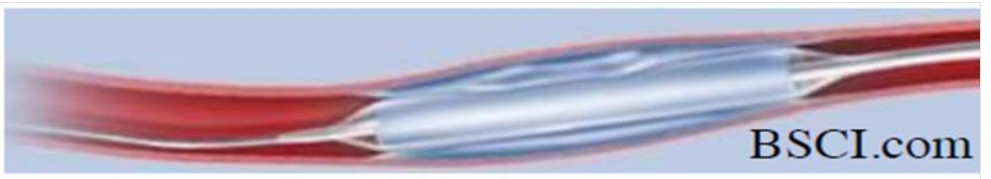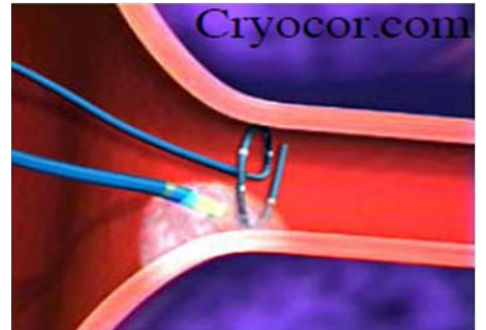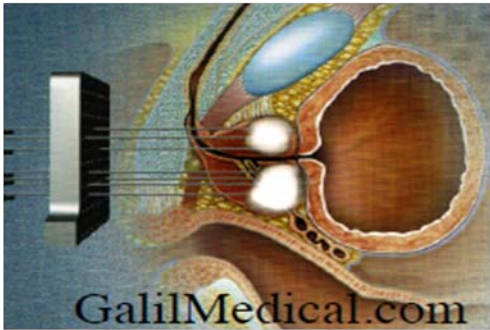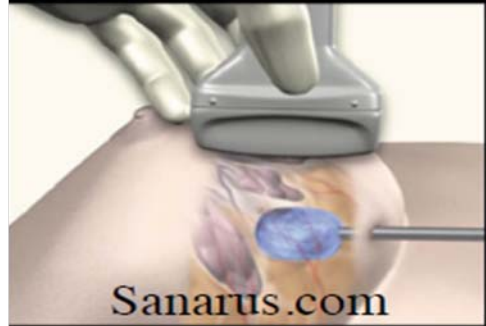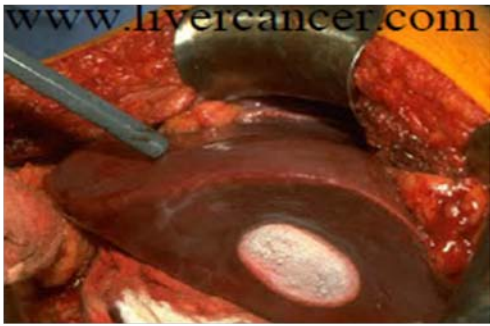
Figure 1-1: Cryosurgery in different organs
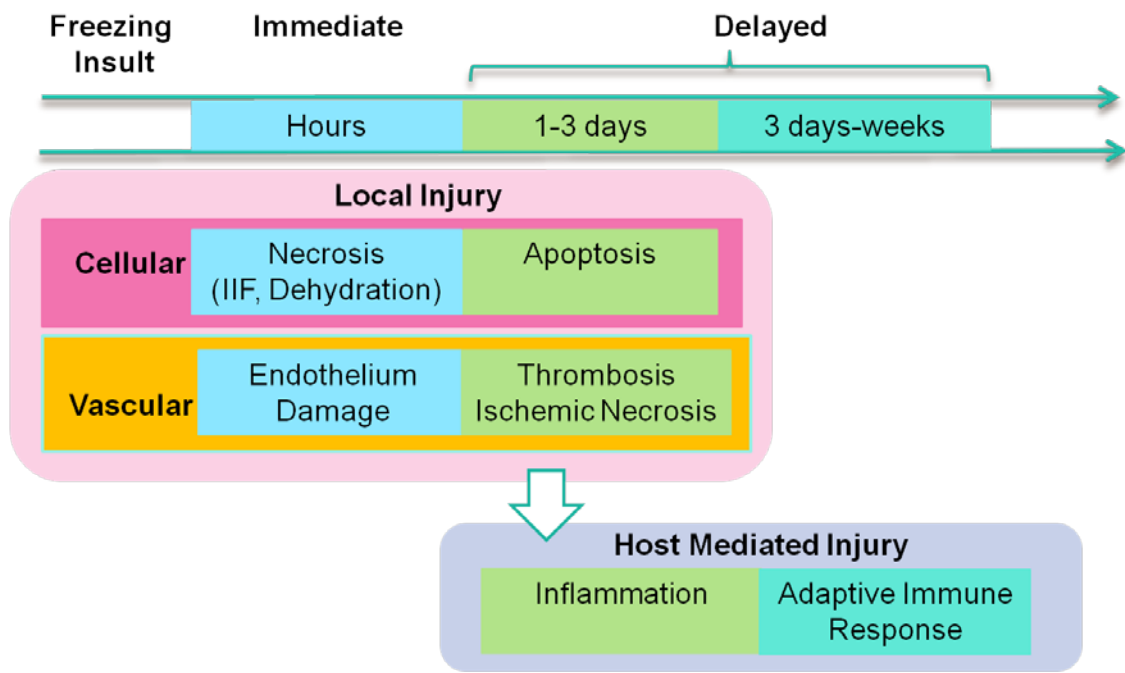
Figure 1-2: Schematic of cryoinjury mechanisms

Figure 1-3: Mechanisms of immediate local injury (modified from [91])
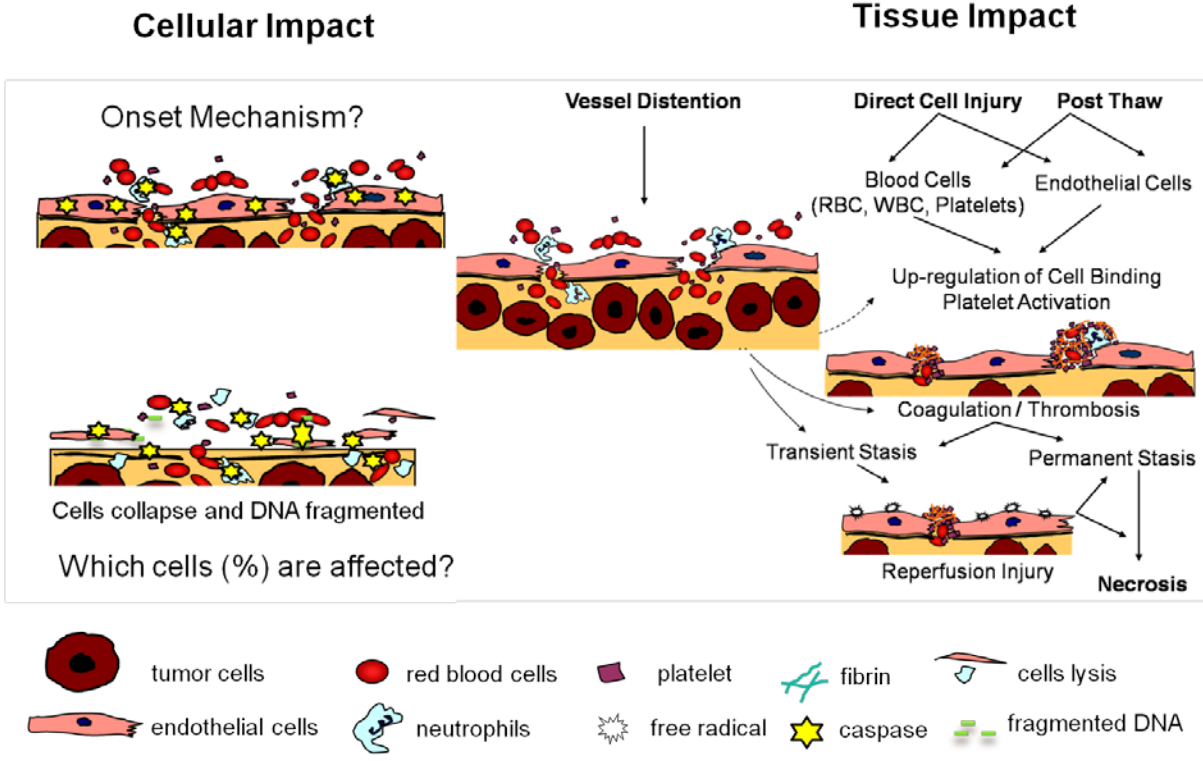
Figure 1-4: Mechanisms of delayed local injury (modified from [91])
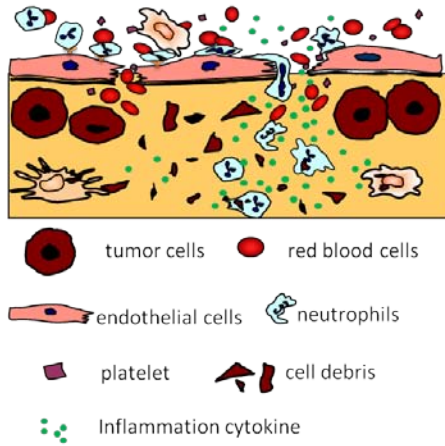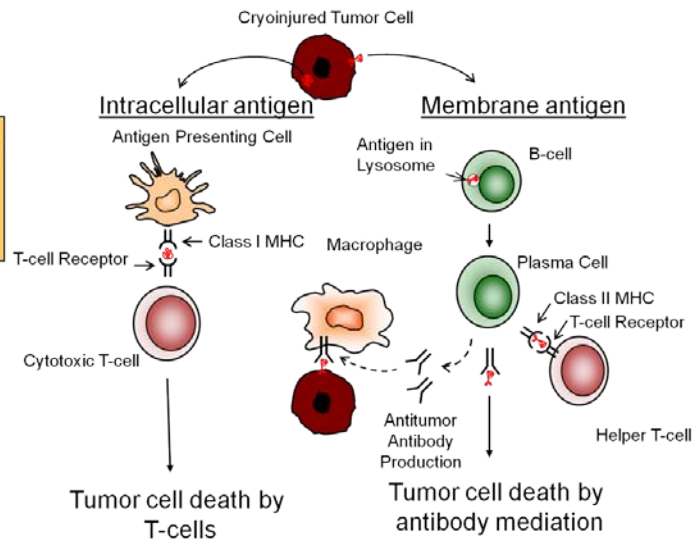
Figure 1-5: Mechanisms of delayed host mediated injury (modified from [91])
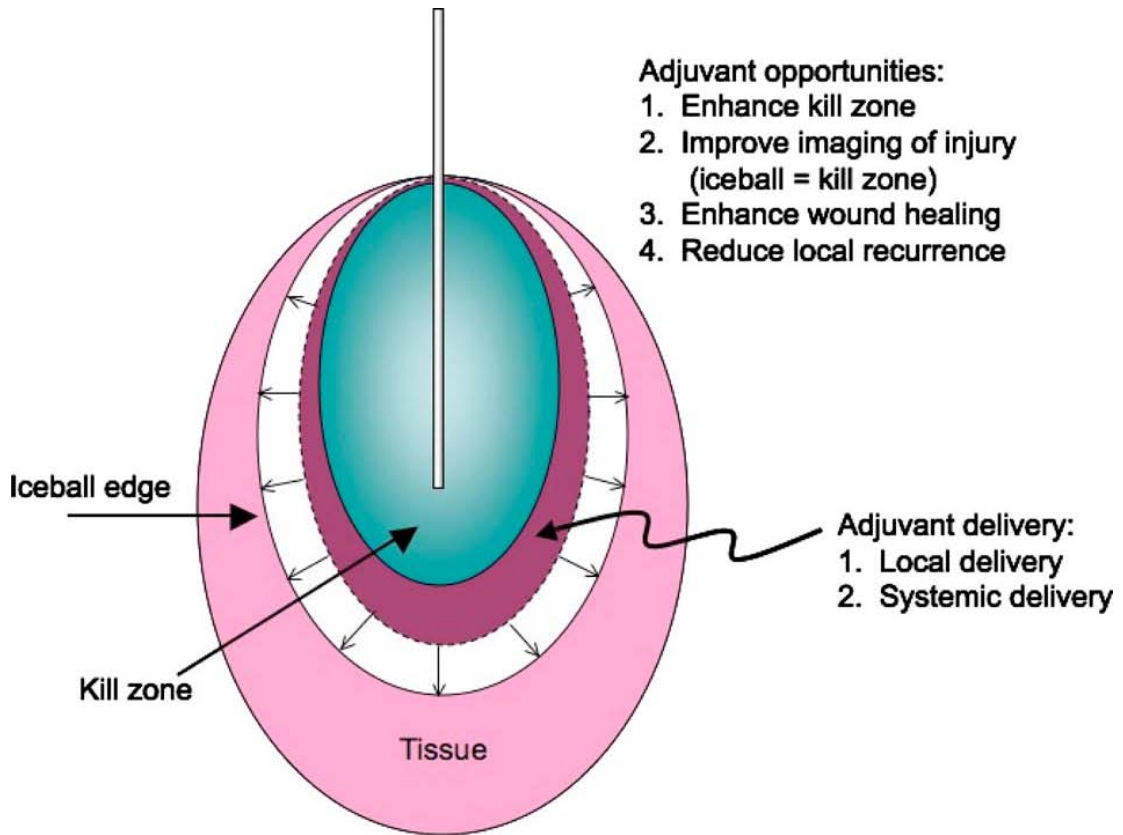
Figure 1-6: Improvements in cryosurgical procedure by the use of adjuvants [91]
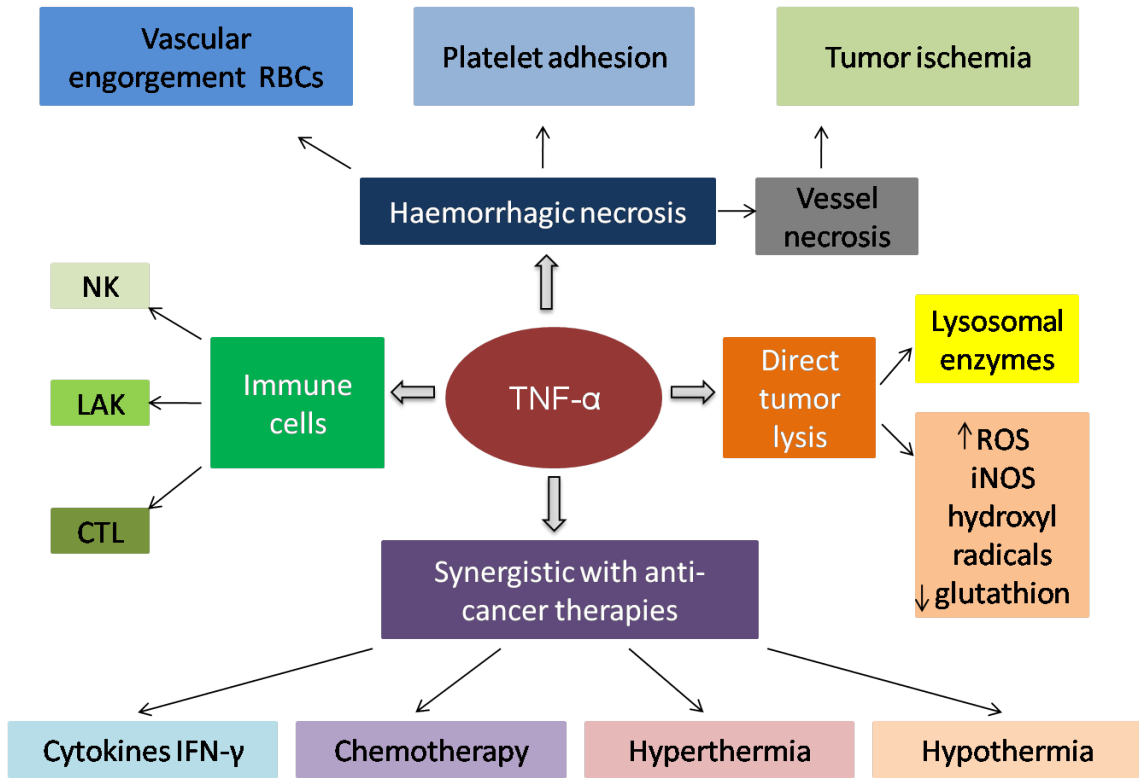
Figure 1-7: Schematic diagram of anti-tumor effect of TNF-α (modified from [297])
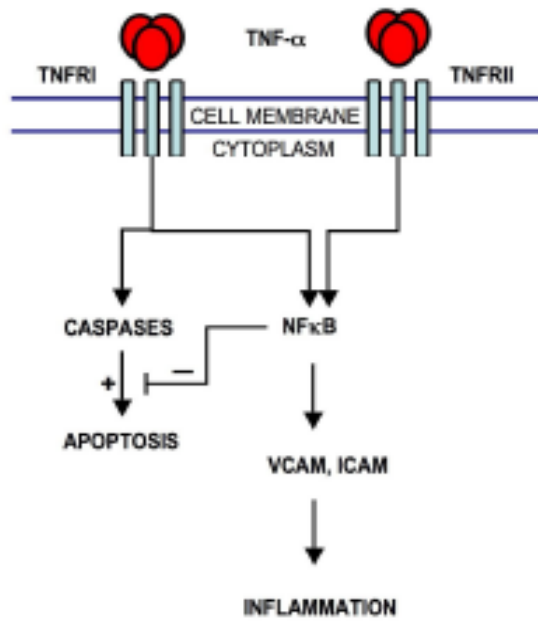
Figure 1-8: TNF-α signaling pathway (modified from [267, 284])
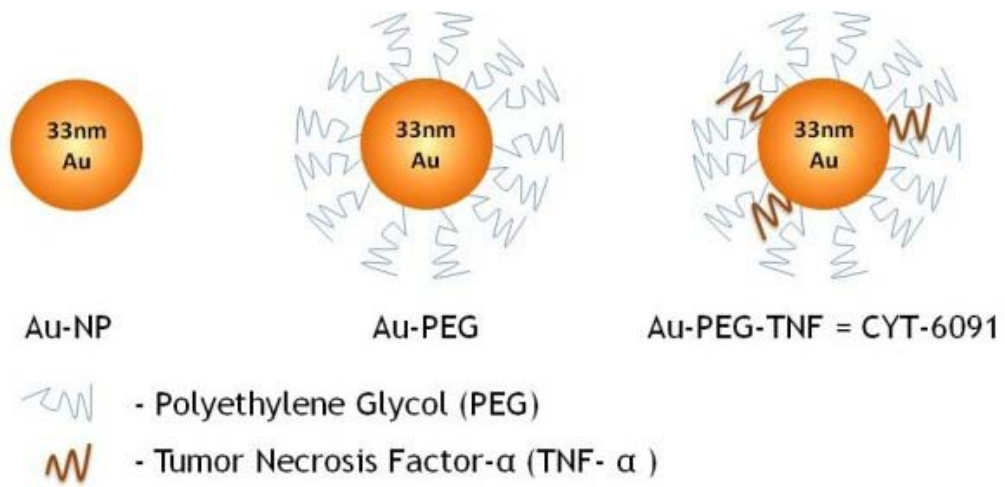
Figure 1-9: Schematic of nanoparticles coated with TNF-α and PEG [92]

Chapter 2 TNF-α Induced Accentuation in Cryoinjury: Mechanisms *In Vitro* and *In Vivo*

2.1 Background

Cryosurgery is a surgical technique that utilizes extreme cold temperatures to treat diseased tissues such as tumors in the body. The finding that clinical imaging [Ultrasound (US), Computed Tomography (CT) and Magnetic Resonance (MR)] can be used to monitor the growth of an iceball *in vivo* has made cryosurgery an important minimally invasive thermal therapeutic modality [211, 232]. Despite advantages including ease of operation, low morbidity and low cost, the use of cryosurgery is limited by its inability to destroy the entire tissue within an iceball as reflected in local recurrence of cancer after freezing [165]. The clinical guideline to ensure complete cell death by this technique alone is -40°C, which limits the control and predictability of the procedure [165, 232]. Thus, whereas the edge of the iceball (-0.5°C) can be visualized using US, CT or MR, the means to enhance or predict the "kill zone" within the iceball are urgently needed. Recent research in cryosurgery has focused on the use of molecular adjuvants to increase tissue cryosensitivity at the periphery of an iceball (0 to -40°C), which would otherwise remain viable [28, 32, 94, 122, 186]. It was shown recently for the first time in an *in vivo* prostate cancer model, that a cytokine, TNF-α, could enhance cryosensitivity and achieve tissue destruction up to the edge of an iceball (-0.5°C) [94]. This study focuses on understanding the dose-dependency and mechanisms of TNF-α induced cryosurgical augmentation at both the cellular (*in vitro*) and tissue level (*in vivo*). The results are very significant as they suggest the involvement of contrasting injury mechanisms *in vitro* as compared to *in vivo*.

Several theories have been put forth as to the mechanisms of tissue injury by freezing alone and grouped mainly under direct cellular effects and vascular effects [78]. Direct cell injury during freezing can occur by intracellular ice formation (IIF) at higher cooling rates near the cryoprobe or solution effects injury at low cooling rates present at the

periphery of the iceball. While IIF directly damages cells by mechanical interaction with large stable ice crystals, solution effects causes cellular dehydration with an increase in both intracellular and extracellular solute concentrations leading to destabilization of the cell membrane [78, 114, 182]. Post-thaw analysis of injury suggests that both apoptosis and necrosis can occur [32, 114]. A second theory regarding the mechanism of damage at the tissue level is vascular injury due to the shutdown of microvasculature after freezing and the resultant ischemic necrosis [115, 178, 217]. Damage to the endothelium, ischemia-reperfusion injury, inflammation and the resultant loss of microcirculatory support is considered critical in defining the edge of the cryolesion [115, 217]. At molecular level, studies have shown the activation of NF-κB and the expression of cell adhesion molecules such as selectins, ICAM and VCAM after endothelial insult, leading to an enhanced inflammatory response [57]. Accentuation of either cellular or vascular mechanisms of injury is a goal in adjuvant-enhanced cryosurgery.

Adjuvants aiming to accentuate established cryoinjury mechanisms can be grouped into several categories: (1) thermophysical adjuvants such as antifreeze protein (AFP) and chemicals (i.e. salts and some amino acids), which work directly on cells, (2) chemotherapeutics such as peplomycin, adriamycin, 5-fluoracil, bleomycin and navelbine, which are established cytotoxic drugs and (3) cytokines or vascular based agents [32, 69, 122, 186, 273]. While all of these approaches have shown some accentuation of injury at temperatures >-40°C, particularly *in vitro*, none have been able to show an overlap of the iceball edge with the edge of the cryolesion *in vivo*.

Recent research in our laboratory has focused on the accentuation of vascular injury during freezing using a vascular targeting cytokine, TNF-α [28, 94]. For the first time it was shown that with the proper dose and delivery of TNF-α, it is possible to achieve an overlap of the kill zone and the iceball edge, allowing imaging feedback of injury and attain control of the procedure [94]. TNF-α is a well-known cytokine for its role in

inflammation, immunity and for its anti-tumor properties [187, 267, 295]. At the cellular level, TNF-α can lead to direct cell death by apoptosis or induce inflammation by the activation of NF-☐B, which is important, particularly in tissues, due to the presence of immune cells [267, 284]. It now remains to be determined which one (or both) of these pathways are active at the cellular and tissue levels in enhancing cryosurgical injury.

The aims of this study are to investigate and compare both *in vitro* and *in vivo*: 1) the effect of TNF-α dose on cryoinjury and; 2) the mechanisms of TNF-α induced accentuation in cryoinjury. Cryoinjury was assessed *in vitro* using viability and DNA fragmentation assays and *in vivo* by measuring perfusion defects. Specific inhibitors were used to target caspase-mediated apoptosis and NF-kB-mediated inflammatory pathways to investigate the molecular mechanisms. The results demonstrate a direct dose-dependency of TNF-α on cryoinjury both *in vitro* and *in vivo* but contrasting cell injury mechanisms responsible for the observed augmentation.

2.2 Material and Methods

2.2.1 *In Vitro*

2.2.1.1 Cell Culture

Both LNCaP Pro 5 (LNCaP) cells and MVECs released form newborn human foreskin (29) were grown as adherent monolayers in 25cm^2 T-flasks as previously described. All treatments were performed when flasks were 80% confluent.

2.2.1.2 TNF-α and Inhibitor Treatments

Recombinant human TNF-α (A gift from Cytimmune Sciences, Rockville, MD) was diluted with Dulbecco's phosphate buffered saline (DPBS) (BioWhittaker Inc,

Walkersville, MD), and reconstituted to a final concentration (1 ng/ml, 10 ng/ml, 100 ng/ml, 1000 ng/ml) with fresh media. Pan caspase inhibitor Z-VAD-FMK (R&D Systems, Minneapolis, MN) and NF-κB inhibitor BAY 11-7085 (EMD Biosciences, La Jolla, CA) were dissolved in DMSO and diluted to final concentrations of 100 μM and 10 μM respectively in fresh media before application. The cells were incubated with media containing TNF-α for 4 hours. The inhibitors were present in the media until injury assay.

2.2.1.3 Freeze/thaw (FT) of Monolayer Cultures

Cell monolayers in 25cm^2 flasks were frozen in an ethanol bath maintained at constant temperatures (-5 ℃ or -10 ℃), and spontaneously nucleated when the temperature reached -1 °C. LNCaP cells were frozen until the culture temperature reached -10℃ and then held on a copper block maintained at -10 ℃ for 5 minutes. MVECs were frozen till they reached -5℃. Cells were allowed to thaw passively at room temperature for 15 minutes and then incubated at 37°C until injury assessment.

2.2.1.4 Cell Counting and Viability Assay

Cells were mixed with 9 M of Hoechst 33342 (Sigma-Aldrich, St. Louis, MO) and 7 M of propidium iodide (PI) (Sigma-Aldrich, St. Louis, MO) and assessed at 200X by fluorescent microscopy (Olympus BX-50, Tokyo, Japan). At least seven representative fields and a total of 200-300 cells/sample were counted in each monolayer culture. Cell viability was calculated at several time points after treatments.

2.2.1.5 DNA Fragmentation Assays

Cells were collected and fixed with 70% ethanol at 4 °C overnight. After centrifugation, cells were washed twice with 1ml DPBS. One ml of staining solution (containing 3.8 mN

sodium citrate and 50 µg/ml PI in DPBS) and 50 µl of 10 µg/ml RNAse A (Worthington Biochemicals, Lakewood, N.J.) was added to the pellets. The pellets were stored in dark for 1 hour at 37°C and kept covered until further analysis. The PI fluorescence was measured using about 1×10^4 cells in a FACSCalibur E4513 flow cytometer. The fraction of the cells in various cell cycle stages was estimated from DNA content of the cells [208].

2.2.2 *In Vivo*

2.2.2.1 DSFC Implantation

The dorsal skin fold chamber (DSFC) allows intravital two dimensional, controlled growth and visualization of tumors as described previously [113, 206]. This model was adapted by our lab to perform controlled freezing and has since been used in several cryosurgery studies [28, 94, 113]. Briefly, the dorsal skin of each nude mouse was sandwiched between two anodized aluminum frames with 10 mm diameter viewing windows, separated by a distance of 450 µm, maintained by spacers on the screws [113, 206]. The epidermis was removed from the viewing side along with excess fascia to permit better visualization of the microvasculature.

2.2.2.2 Tumor Implantation

One-two million LNCaP cells were suspended in 30 µl of matrigel matrix (matrigel diluted 3:1 in serum free media; BD Biosciences, Bedford, MA) and inoculated into the DSFC chamber window on both day 0 and day 4 of implantation. The experiments were performed on day 12 following DSFC implantation, when the tumor covered the entire chamber [28, 94].

2.2.2.3 TNF-α and Inhibitor Treatments

On the day of the study, the glass window was removed and soluble TNF-α (2 ng, 200 ng, 500 ng or 1 g) dissolved in 30 l saline was applied topically in the DSFC. The glass window was replaced after 15 minutes and cryosurgical treatment was performed 4 hours later. Specific NF-κB inhibitors BAY 11-7085 and andrographolide were dissolved in DMSO at concentrations of 10 mg/ml and 15 mg/ml respectively. BAY 11-7085 at a dose of 0.4 mg/kg was applied topically in the DSFC 15 minutes before TNF-α application, while andrographolide was administered twice, intraperitoneally (i.p.) at a dose of 30 mg/kg each at 2 hours and 15 minutes before TNF-α application [29, 168, 216, 305]. Pancaspase inhibitor Q-VD-OPH (MP Biomedicals, Aurora, OH) was administered i.p at a dose of 50 mg/kg, 15 minutes before TNF-α application [29, 168, 216, 305].

2.2.2.4 Freeze/thaw (FT) of the DSFC

The normal skin control (i.e non-tumor subcutaneous tissue within the DSFC) was frozen 3 days after chamber implantation to allow the tissue to recover from surgery. The tumor implanted DSFCs were allowed 12 days to grow in the DSFC prior to cryosurgery.

The freezing procedure in the DSFC has been described in detail previously [94]. Briefly, a 1 mm diameter brass fin fitted to a 5 mm cryoprobe (Endocare, CA) was inserted in the center of the DSFC and allowed to attain a temperature of -100°C for 55 seconds, followed by a passive thaw at room temperature. The temperature was monitored throughout the procedure by the use of thermocouples placed at 2, 3 and 4 mm radius from the center respectively and also by an infrared (IR) camera (FLIR, Boston, MA). The thermocouple measured temperatures and IR measured temperatures correlated well with each other and were also validated by a quasi steady state mathematical model, as shown in our previous publications [28, 94, 113].

2.2.2.5 Injury Measurement in the DSFC

The effects of TNF-α and/or cryosurgery on vascular damage were visualized using a 10 mg/ml 70 kD fluorescein isothiocyanate (FITC) - labeled dextran intravenously by tail vein injection at 3 days post-treatment [28, 94, 113]. Stasis was defined as the lack of blood flow (i.e perfusion defects) as evidenced by the lack of fluorescence signal within a vessel. The chamber was traversed radially in the four perpendicular directions (N, S, E, W) and radial locations of stasis (i.e. perfusion defects) noted using a micrometer scale fixed on the stage with the chamber center as the origin. Temperatures at the four measured radii of stasis were then extrapolated from the respective IR image taken after cryosurgery and averaged to obtain the temperature threshold (defined as minimum temperature for complete cell death) of injury for that particular animal [94].

2.2.2.6 Statistical Analysis

Comparison of the effect of different treatment conditions on the cells was performed using one way ANOVA followed by Bonferroni's multiple comparison test or a t-test. Each group consisted of at least n of 3.

2.3 Results

2.3.1 Cell Injury *In Vitro*

2.3.1.1 Viability

MVECs were found to be more sensitive than LNCaPs to cryoinjury at similar FT conditions (data not shown). Therefore, the freezing protocols were adjusted to produce similar viability (approximately 50%) in both the cell lines thereby allowing comparison after TNF-α addition, and also to simulate the thermal conditions present near the edge of the iceball. A direct dose dependency on cell viability was observed in the cells after the

application of TNF-α (0.1 ng -1000 ng/ml), before FT. A 4-hour treatment of TNF-α at 1000 ng/ml dose reduced the cell viability to $64.2 \pm 6.1\%$ and $72.3 \pm 4.8\%$ for MVECs and LNCaP cells respectively (Fig. 2-1A and 2-1B). FT alone reduced the cell viability in MVECs to $39.3 \pm 5.5\%$ and in LNCaP cells to $56.7 \pm 5.4\%$. Pre-treatment of cells with 1000ng/ml TNF-α for 4 hours before FT showed a significant augmentation in cell injury when compared to FT alone with viability reducing to $23.7 \pm 3.8\%$ and $27.2 \pm 6.6\%$ ($p < 0.05$) for MVECs and LNCaP cells respectively.

2.3.1.2 DNA Fragmentation

DNA fragmentation analysis was performed to provide evidence supplemental to viability analysis of TNF-α enhanced cryoinjury. The data from DNA fragmentation assay is shown in Fig. 2-2A and 2-2B. PI intensity (x-axis) corresponds with DNA content of sub G1, G1, S and G2/M phase cells. In this assay, sub G1 phase cells were cells with reduced DNA content due to either apoptosis or necrosis. Typical histograms of DNA content per 10^4 cells in LNCaP cells and MVECs are shown at different TNF-α doses. In addition, % of sub G1 cells was calculated to compare percentage of DNA fragmented cells after each treatment. TNF-α at a dose of 1000 ng/ml had a minimal effect on LNCaP cells (5% enhancement), but dramatically augmented the DNA damage in MVECs to 76.6 ± 1.6 % from $26.2 \pm 2.1\%$ observed in control cells ($p < 0.001$). Freezing alone showed a DNA fragmentation of $14.5 \pm 1.6\%$ and $64.6 \pm 5.0\%$ for LNCaP cells and MVECs respectively. On pre-treatment with 1000 ng/ml of TNF-α before freezing, the DNA fragmentation increased by 16.7% in LNCaP cells and 17.5% in MVECs ($p < 0.05$). The trends in the results suggest that the drop in the viability as seen in Fig. 2-2A and 2-2B is likely due to the presence of cells in sub G1 state (i.e apoptotic or necrotic).

2.3.2 Tissue Injury *In Vivo*

Injury in the DSFC was assessed by intravital fluorescence of perfusion and post-mortem histology (see Chapter 3). All control unfrozen normal skin and tumor DSFC's demonstrated blood flow throughout the chamber as visualized by FITC-dextran fluorescence. Sham treatment displayed patent vasculature beyond the probe insertion site at 0.5 mm radius. The chambers frozen with or without TNF-α intervention displayed a central static region surrounded by perfused tissue in the rest of the chamber. There was increased permeability (not quantified) at the edge of the injury evident as blurriness due to the leakage of dye. White blood cell rolling and adhesion, indicative of enhanced inflammation, was observed just before cryotreatment in all TNF-α pre-treated animals as previously noted [28, 73]. Post treatment analysis of histology showed a centrally necrotic region surrounded by a transition region, which was comprised of both viable and dead cells, inflammatory cells and thrombosed, dilated vessels as previously described by Hoffman et al., 2001 [301]. Surrounding the transition region, normal tissue morphology (untreated) could be seen. We have previously shown using a fluorescent dye $DiOC_7$, that the boundary of blood perfusion coincided very well with the edge of necrosis on H & E stained slides [94]. Thus, the average temperature measured at the edge of stasis in the DSFC by vascular imaging represents the temperature threshold for tissue necrosis by cryosurgery for that particular animal.

Fig. 2-3 shows the temperature threshold of necrosis as measured at the edge of stasis for different groups in both normal skin and tumor. The temperature threshold increased with the addition of TNF-α in a dose dependent manner for both normal skin and tumor as seen in Fig. 2-3. In normal skin it increased significantly from -27.7 ± 5.0ºC for cryo (FT) only to -13.0 ± 2.5ºC, -2.6 ± 2.7ºC and -4.0 ± 3.1ºC with pre-treated doses of 2, 200 and 500 ng TNF-α respectively (Fig. 2-3A). As expected, tumor was found to be more sensitive to cryoinjury when compared to normal skin with a temperature threshold of -14.5 ± 1.5ºC by FT alone treatment (Fig. 2-3B). With pre-treated doses of 2, 200 and 1000 ng TNF-α, the temperature threshold increased considerably ($p < 0.01$) to -7.0 ±

1.6ºC, 2.1 ± 2.7ºC and 5.1 ± 1.9ºC respectively (Fig. 2-3B). Thus, at a total dose of 200 ng or greater, it was possible to obtain an overlap between the kill zone and the iceball edge in the tumor tissue.

2.3.3 Apoptosis and NF-κB Pathways *In Vitro*

To elucidate the molecular mechanisms involved in TNF-α enhanced cryoinjury by experiment, pan-caspase inhibitor Z-VAD-FMK (ZVAD) and NF-κB inhibitor BAY 11-7085 (BAY) were added before TNF-α pre-treatment. As shown in Fig. 2-4A, inhibition of apoptosis with ZVAD had no significant effect on LNCaP viability in any of the treatments (TNF-α, FT, or TNF-α + FT). However, inhibition of NF-κB with BAY decreased LNCaP viability by 26.1% after FT ($p < 0.05$). Contrastingly in MVECs (Fig. 2-4B), ZVAD had a survival effect rescuing 25.3% cells after TNF-α treatment ($p < 0.05$), 17.2% after FT ($p < 0.05$), and 26.0% after TNF-α + FT ($p < 0.05$). Inhibition with BAY reduced MVEC viability by 16.9% after FT ($p < 0.05$). The combined treatment of ZVAD + BAY showed some rescue compared with BAY alone in MVECs with statistical significance only in TNF-α treatment group ($p < 0.05$), and significantly reduced MVEC viability compared with ZVAD alone in FT treatment group ($p < 0.05$). These results indicate an active NF-κB pathway after FT in both MVECs and LNCaP cells and active caspases in MVECs in the presence of TNF-α.

2.3.4 Apoptosis and NF-κB Pathways *In Vivo*

The inhibition experiments *in vivo* were performed at a TNF-α dose of 200 ng, where a significant accentuation in cryoinjury was observed, in both normal skin and tumor after FT (Fig. 2-5). Andrographolide (ANDRO), an NF-κB inhibitor, significantly reduced the TNF-α enhancement in cryoinjury for both normal skin and tumor (Fig. 2-5). In normal skin, the temperature threshold was reduced from -2.6 ± 2.7ºC to -18.3 ± 5.2ºC ($p < 0.01$), closer to the injury obtained with FT alone at -27.7 ± 5.0ºC (Fig. 2-5A). A similar

reduction was seen in tumors where the temperature threshold changed considerably to -7.5 ± 2.2°C from 2.1 ± 2.7°C (p < 0.01) (Fig. 2-5B). Pre-treatment of tumor tissue with BAY, another NF-κB inhibitor, reduced the temperature threshold after TNF-α + FT to -8.0 ± 3.1°C, which was statistically different (p < 0.01) from TNF-α + FT alone (Fig. 2-9B).

In contrast, inhibition with Q-VD-OPH, a caspase inhibitor, had a minimal effect on the accentuation of cryoinjury by 200 ng TNF-α for both normal skin and tumor. The temperature threshold with caspase inhibitor was measured to be -7.4 ± 1.9°C and 1.0 ± 2.1°C for normal skin and tumor, respectively (Fig. 2-5A and B). Although caspase inhibition was statistically significant (p < 0.05) in normal skin when compared to TNF-α + FT without inhibition, the reduction was significantly less than what was obtained after NF-κB inhibition with ANDRO (p < 0.05). None of the inhibitors (BAY, ANDRO, Q-VD-OPH) had a significant effect on temperature threshold obtained by FT alone (data not shown). Therefore, *in vivo* inhibition studies with NF-κB and caspase inhibitors show the presence of NF-κB-mediated inflammatory pathways in TNF-α-induced accentuation of cryoinjury.

2.4 Discussion

It is evident from both *in vitro* and *in vivo* results, that the administration of TNF-α before freezing increases the amount of injury significantly. This increase in injury is considerably higher *in vivo*, where complete cell destruction could be obtained up to the edge of the iceball (-0.5°C). Inhibition of apoptotic or inflammatory pathways during cryosurgical enhancement with TNF-α presents contrasting results suggesting host-mediated inflammation responsible for augmentation *in vivo* and MVECs mediated apoptosis as the mechanism *in vitro*.

The *in vitro* data provides compelling evidence to suggest the role of endothelial cells in TNF-α induced accentuation in cryoinjury. MVECs are more sensitive to freezing injury than LNCaP cells and therefore milder freezing conditions (-5ºC and 0 minute hold time) were used for this cell line as compared to LNCaP cells (-10ºC and 5 minutes hold time) [19]. Increasing amount of cryoinjury to both MVECs and LNCaP cells was obtained in a dose dependent manner with the addition of TNF-α. The sensitivity of MVECs to cell death in the presence of TNF-α was greater than LNCaP cells both with and without freezing. The resistance to TNF-α induced cell death in LNCaP cells as compared to MVECs could be due to the constitutive expression of anti-apoptotic proteins (ex. Inhibitor of Apoptosis Proteins), shown to be present in most tumor cell lines [56]. The presence of PI3K/Akt survival pathway, could be another mechanism for the resistance of LNCaP cells to TNF-α induced injury [250].

Increased cryosensitivity of endothelial cells (with or without TNF-α) suggests that injury to the endothelium may help govern the extent and enhancement of injury *in vivo*, where many cell types are present. In fact several *in vivo* studies have shown endothelial injury and ensuing inflammation to be critical in governing the kill zone at the periphery of an iceball [113, 178, 217]. The addition of TNF-α *in vivo* is suggested to cause even more endothelial cell death at higher subzero temperatures as observed *in vitro*, thereby increasing the extent of the vascular shutdown within the iceball.

The *in vivo* cryosurgical studies performed in the DSFC demonstrated a very significant dose dependency (Fig. 2-3). The temperature threshold of necrosis increased drastically with the addition of TNF-α, for both normal skin and tumor in the DSFC. At a dose of 200 ng, the edge of injury overlapped with the edge of the iceball (-0.5ºC) in tumor tissue, suggesting the ability to destroy all tumor within a cryosurgical iceball. This is clearly an augmentation that is not expected from the *in vitro* studies, where there was still significant viability remaining at -5ºC (in MVECs) and -10ºC (in LNCaP cells). It

suggests the presence of other factors or mechanisms to account for the enhanced injury observed *in vivo* vs *in vitro*.

TNF-α is closely associated with *in vivo* vascular events and injury. Apart from endothelial cell apoptosis, the other reported actions of TNF-α *in vivo* comprise of proinflammatory reactions such as an increase in procoagulant activity, decrease in anticoagulant activity, recruitment and adherence of inflammatory cells such as neutrophils, and production of other cytokines [195, 225, 284, 295]. TNF-α induced activation of NF-κB can promote the transcription of several genes that could increase the inflammatory/procoagulant response in the tissue by the expression of adhesion molecules such as ICAM, VCAM on the endothelium, facilitating leukocytes infiltration, and enhancing tissue factor expression while down regulating thrombomodulin [73, 267, 284]. The increase in direct cell cryoinjury observed *in vitro* may partially be explained due to TNF-α induced apoptosis of endothelial and tumor cells. But the dramatic enhancement in cryoinjury observed *in vivo* also suggests the role of inflammatory prothrombotic events, which follow both after TNF-α and cryosurgical treatments. In order to investigate the significance of apoptosis and inflammation in TNF-α induced accentuation in cryoinjury, specific inhibitors to block caspases (to inhibit apoptosis) or NF-κB (to inhibit inflammation) were used both *in vitro* (cellular level) and *in vivo* (host level).

In vitro inhibition suggests active apoptosis pathway in MVECs in the presence of TNF-α and/or FT and NF-κB pathway in both the cell lines after FT. Caspases inhibition with Z-VAD-FMK showed significant rescue in MVECs, but no rescue in LNCaP cells (Fig. 2-4). This confirmed caspase mediated apoptosis as the injury mechanism in endothelial cells under TNF-α and FT insult. On the other hand, activation of NF-κB, results in the prevention of apoptosis through several anti-apoptotic proteins, including Bcl-XL (to inhibit cytochrome c leakage from the mitochondria), IAP (to inhibit caspase 3 and

49

caspase 8 activation) and FLIP (to inhibit caspase 8 activation) [98, 167, 184]. NF-κB inhibitor BAY 11-7085 reduced the viability of LNCaP cells and MVECs after both cryo and combined treatments (Fig. 2-4), confirming the activation of NF-κB as a protective mechanism after FT *in vitro*. The selection of inhibitors and dosage used in this work is based on previous literature on *in vitro* and *in vivo* models of NF-κB and caspase inhibition [29, 97, 120, 169, 216, 231, 305].

In vivo blocking of apoptotic or inflammatory pathways suggests the role of TNF-α mediated inflammatory response to be the mechanism of observed enhancement in cryoinjury. In the DSFC both NF-κB inhibitors, BAY 11-7085 and andrographolide, produced a remarkable reduction in the TNF-α induced increase in temperature threshold of necrosis of cryoinjury for both normal skin and tumor (Fig. 2-5). On the other hand, treatment with Q-VD-OPH, a caspase inhibitor, didn't produce a significant change in the temperature threshold of necrosis (Fig. 2-5). This is in contrast to *in vitro* results, where the application of caspases inhibitor reduced injury (in MVECs), and NF-κB inhibitor to the contrary, enhanced cell injury (in LNCaP cells).

The results using apoptosis and inflammatory inhibitors observed both *in vitro* and *in vivo* supports our initial hypothesis of TNF-α induced apoptosis to be the mechanism for increased cell death observed *in vitro* but TNF-α induced host-mediated inflammatory response to be critical *in vivo* (Fig. 2-6). Although these in vitro and *in vivo* adjuvant augmentations are apparently divergent and affect two phenomena mediated by two distinct mechanisms, these contrasting results may represent two levels of the same *in vivo* phenomenon, ischemic necrosis, due to TNF-α effects at the cellular and tissue level. Previous work with cryoadjuvants (particularly chemotherapeutics) has shown augmentation of cryoinjury, but fall short of obtaining an overlap of the kill zone with the edge of the iceball [32, 68, 122, 186]. These studies have focused on increasing cryosurgical efficacy by using drugs to activate apoptotic based cell death pathways

50

specifically near the edge of the iceball. The bulk of this work has been performed *in vitro* and none of the studies thus far have shown synergistic effects *in vivo*, as observed in this study. Though very few studies have confirmed the presence of apoptosis *in vivo* after a FT treatment, the overall significance of this mechanism of cell death in a cryosurgical procedure is not well defined and still under interrogation [69, 262].

Host-mediated vascular changes such as inflammation have been observed and implicated in a large number of studies related to freezing induced injury [78, 114]. This work is the first effort to investigate the underlying mechanisms of vascular targeting drugs such as TNF-α in the augmentation of cryosurgical injury. The results show that though apoptotic based cellular level pathways may augment cryoinjury *in vitro*, the host-mediated vascular inflammatory pathways are more critical and produce a synergistic effect in cryoinjury augmentation *in vivo*. Future work is needed at the molecular level to determine the critical factors in the NF-κB pathway that produce the observed synergistic augmentation *in vivo*. This study advocates the use of vascular targeting drugs such as TNF-α, or perhaps less toxic molecules that activate the NF-κB pathway in order to produce an augmentation in cryoinjury. Further work is in a translational model is also needed to advance the clinical goal of complete cell death within a cryosurgical iceball.
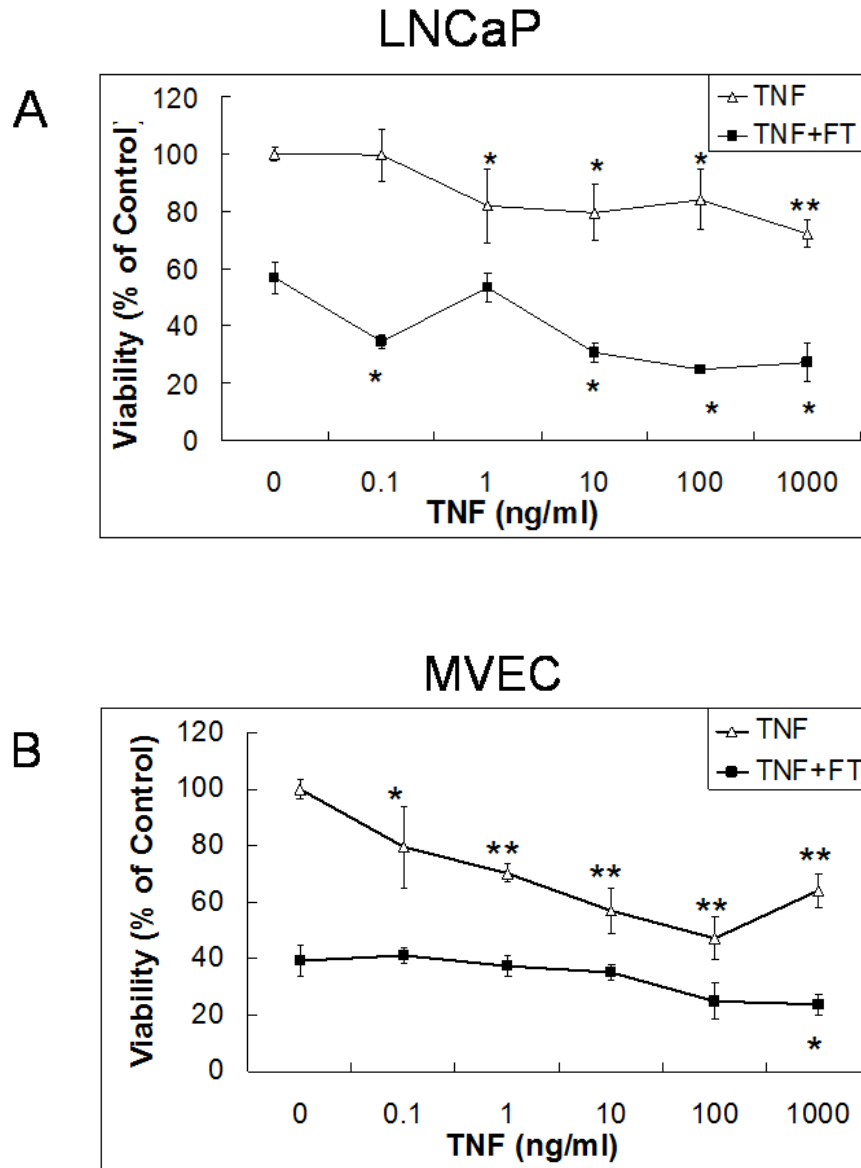
Figure 2-1: *In vitro* effect of TNF-α concentration on the viability of **(A)** LNCaP monolayers with freezing to -10°C, 5 min hold time, and **(B)** MVEC monolayers with freezing to -5°C, 0 min hold time. Cells were treated with TNF-α at concentrations of 0.1, 1, 10, 100, 1000 ng/ml for 4 hours prior to freezing. Values presented are the means ± standard error mean from 3 independent experiments, and control indicates untreated cells. Significant effects of TNF-α compared to control and TNF-α + FT compared to FT alone (*, $p<0.05$; **, $p<0.001$)
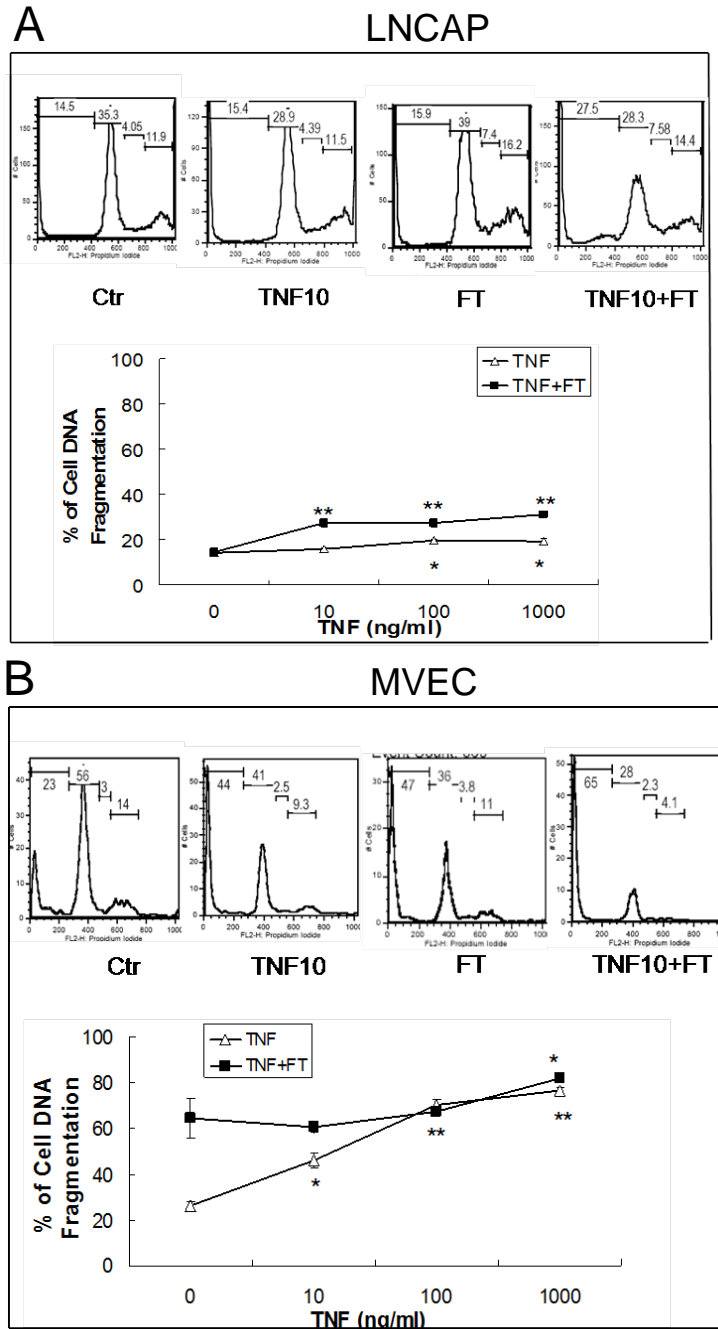
Figure 2-2: *In vitro* effect of TNF-α concentration on DNA fragmentation of (C) LNCaP monolayers with freezing to -10°C, 5 min hold time, and (D) MVEC monolayers with freezing to -5°C, 0 min hold time. Cells were treated with TNF-α at concentrations of 10, 100, 1000 ng/ml for 4 hours prior to freezing. Viability and DNA fragmentation were assessed at 48 hours (LNCaP cells) or 24 hours (MVECs) after freeze/thaw (FT). Values presented are the means ± standard error mean from 3 independent experiments, and control indicates untreated cells. Significant effects of TNF-α compared to control and TNF-α + FT compared to FT alone (*, p<0.05; **, p<0.001).

A Normal Skin
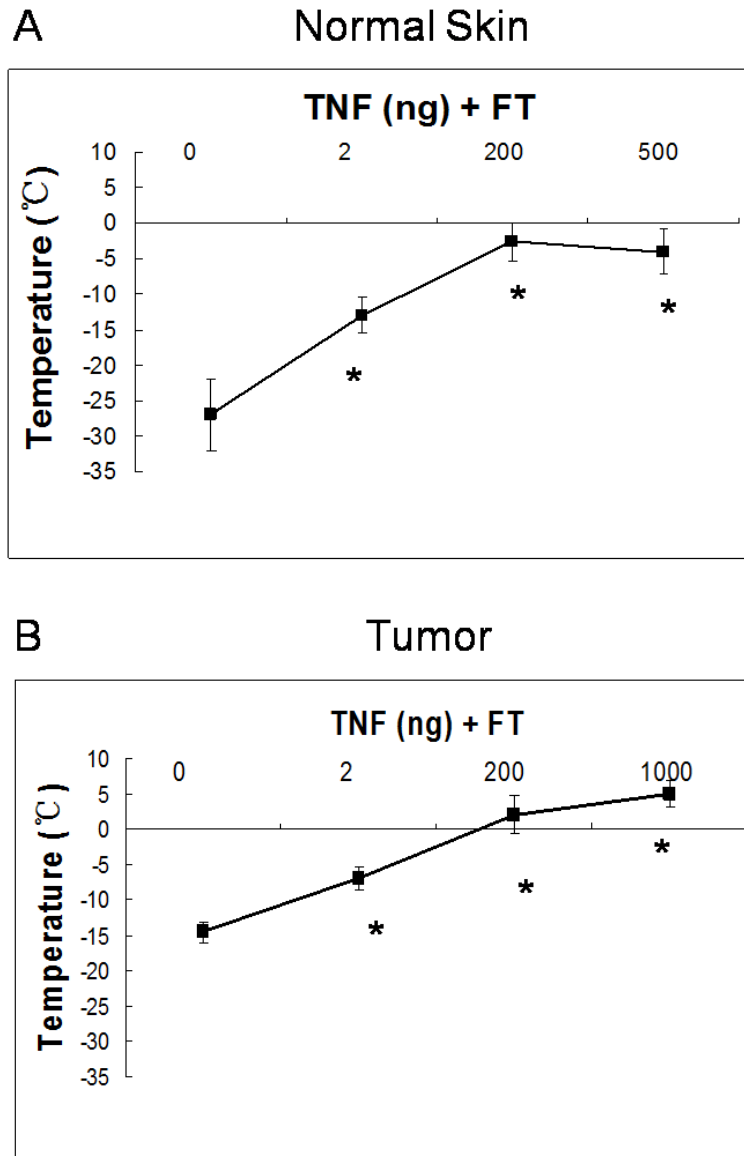
B Tumor

Figure 2-3: *In vivo* effect of TNF-α dosage in normal skin (A) and LNCaP pro 5 tumor (B) grown in a dorsal skin fold chamber. Tissues were incubated with TNF-α for 4 hours prior to freezing. The minimum temperature required for complete cell death was measured at the edge of perfusion defect from the infra-red image taken during the treatment. Values presented are mean ± standard deviation from 5-8 animals in treated groups were statistically different than□each group. All TNF-α untreated freeze alone groups (*, p < 0.01).
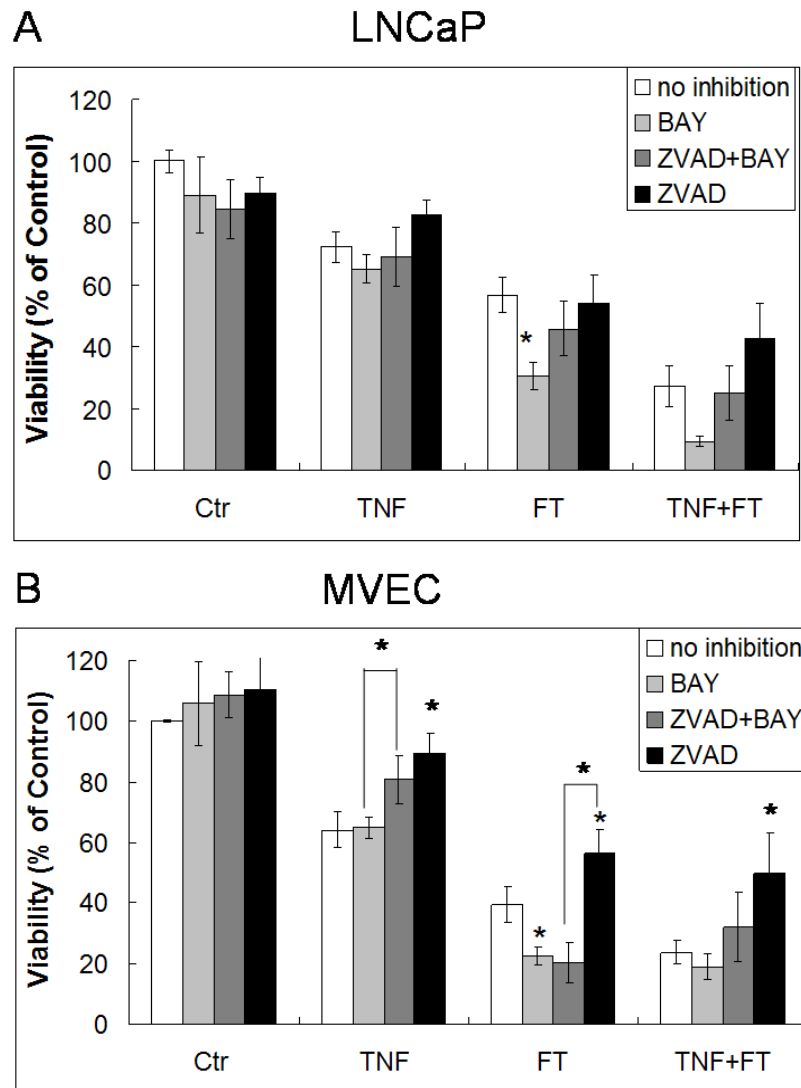
Figure 2-4: *In vitro* effect of caspase inhibitor Z-VAD-FMK (ZVAD) and NF-κB inhibitor BAY 11-7085 [112] on (A) LNCaP monolayers with freezing to -10°C, 5 min hold time, and (B) MVEC monolayers with freezing to -5°C, 0 min hold time. TNF-α treatment was at 1000 ng/ml for 4 hours prior to freezing. 100 μM ZVAD and 10 μM BAY were present in the medida until viability assay. Viability was assessed at 48 hours (LNCaP cells) or 24 hours (MVECs) after freeze/thaw (FT). Values presented are the means ± standard error mean from 3 independent experiments, and control indicates untreated cells. Significant effect of inhibitors compared with no inhibitor (*, $p < 0.05$). Significant effects of BAY compared with ZVAD+BAY, and ZVAD compared with ZVAD+BAY were shown in brackets (*, $p < 0.05$).

A Normal Skin
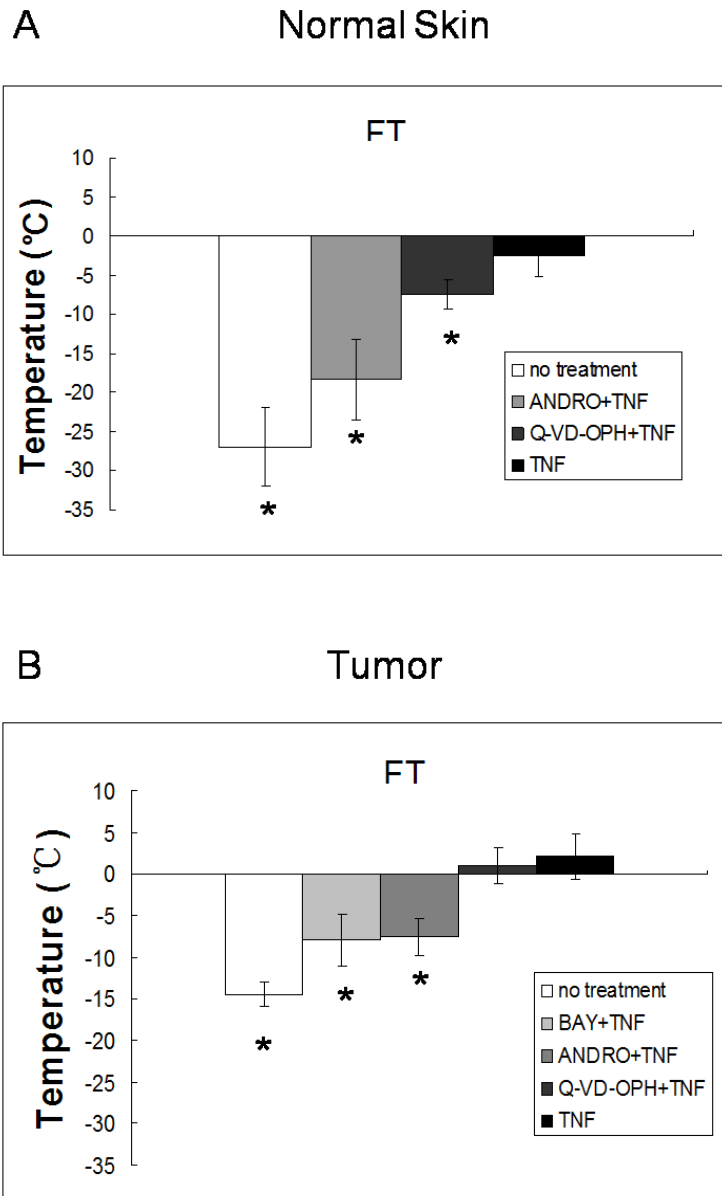
B Tumor

Figure 2-5: *In vivo* effect of using NF-κB inhibitors BAY 11-7085 (BAY), andrographolide (ANDRO) and Caspases inhibitor Q-VD-OPH in normal skin (A) and tumor (B) grown in a dorsal skin fold chamber. The inhibition was performed at TNF-α pretreated dose of 200 ng for both normal skin and tumor. Values presented are mean ± standard deviation from 5-8 animals in each group. Groups were statistically different than groups pretreated with TNF- α (*, $p < 0.01$).
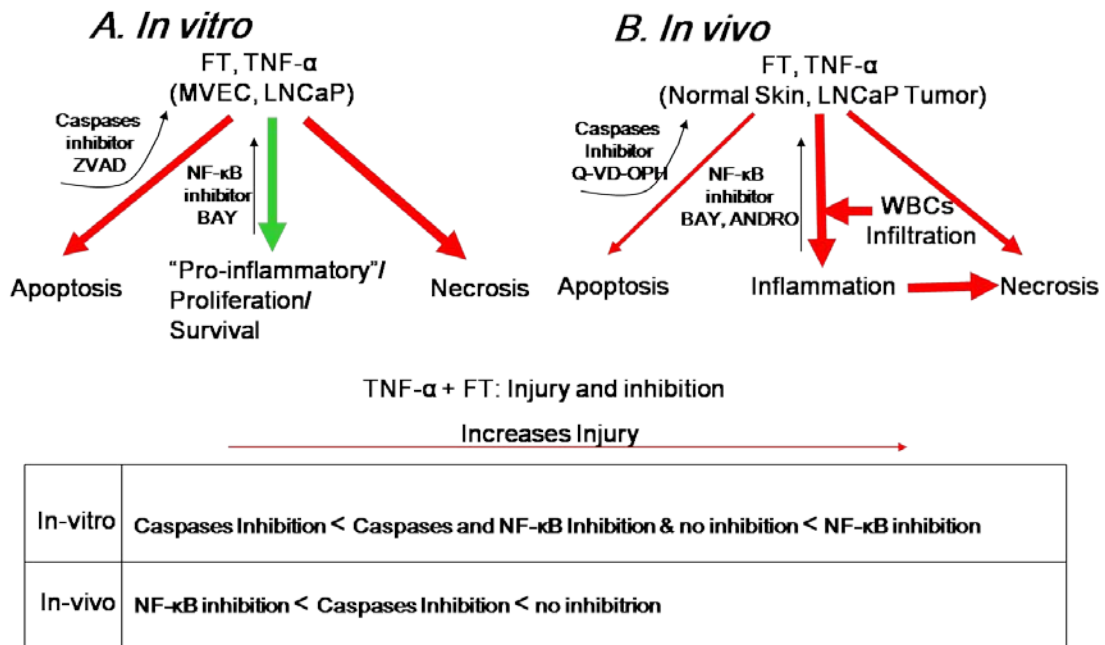
Figure 2-6: Summary of *in vitro* and *in vivo* pathways of TNF-α enhanced cryoinjury. (A) *In vitro* response showing a prominent apoptotic vs. pro-inflammatory enhancement of injury which can be blocked by caspases (leading to rescue in MVECs) and NF-κB inhibition (leading to even greater death in LNCaP cells) respectively. (B) *In vivo* response showing a predominantly inflammatory vs. apoptotic enhancement of injury *in vivo* which can be blocked by NF-κB inhibition and to a less extent of caspases inhibition. An important part of the blockable inflammatory enhancement is suggested to be the inflammatory infiltrate (neutrophils and macrophages) recruited to the wound site.

Chapter 3 Pre-conditioning Cryosurgery: Cellular and Molecular Mechanisms and Dynamics of TNF-α Enhanced Cryotherapy in an *In Vivo* Prostate Cancer Model System

3.1 Background

Prostate cryosurgery using intra-operative iceball imaging and modern Argon Joule-Thomson probe technology has increased markedly in the last decade [211, 232]. Although mostly accepted for salvage following local radiotherapy failure, it is now increasingly used as a primary treatment for locally advanced disease [136]. It is estimated that 6,680 cryoablation procedures were performed in the United States in 2005 with 15,000 procedures projected in 2010 [66]. Five-year biochemical disease free status for cryosurgery is now comparable to published results for radiation and surgery in the prostate [128]. However, reproducible clinical application of cryosurgery continues to suffer from the inability of the technique to destroy cells at the periphery of the lesion (i.e. at the iceball edge) where the temperatures are above -40°C [78]. Clearly, sublethal injury at the iceball edge may lead to cancer recurrence. However, over-freezing (creating an iceball beyond clinically apparent cancer) may result in damage of surrounding normal structures such as nerves and vessels, leading to complications [237]. As both under and over-freezing outcomes are undesirable, much research has focused on controlling destruction within the iceball by cellular, vascular and immunological mechanisms [28, 33, 83, 215]. It is now clear that one important approach to controlling disease at the edge of the prostate, where both the cancer and the iceball edge co-exist, is to augment these mechanisms with cryosurgical adjuvants [91].

TNF-α, isolated 30 years ago, is a multifunctional cytokine that plays a key role in apoptosis and cell survival as well as in inflammation and immunity. There are a number

of mechanisms by which TNF-α can induce an anticancer effect, including: apoptosis [209], pro-coagulation and acute hemorrhagic necrosis [110], activation and mediation of macrophage and natural killer (NK) cell destruction [110], and occasionally the initiation of tumor specific immunity [22, 108, 174]. Our earlier results suggest that inflammation and vascular injury are critical specifically to TNF-α-mediated enhancement of cryosurgery [126]. However, further description of the timing and mechanisms of TNF-α pre-conditioning and enhancement of combinatorial treatment are needed for optimal translation to clinical use.

In the current study, we investigate the time course of TNF-α pre-treatment effects in tumors, and of combinatorial treatment (TNF-α pre-treatment + cryosurgery). We found that combinatorial treatment, relative to cryosurgery alone, enhanced histological zones of destruction and vascular stasis. Immunohistochemical studies revealed that TNF-α-mediated enhancement of these histologic zones correlated with translocation of NF-κB, VCAM expression and upregulated expression of caspase 3 (a marker of apoptosis) in the cells and vasculature of the tumor.

3.2 Materials and Methods

3.2.1 Cell Culture

LNCaP Pro 5 cells were transfected with plasmid DNA encoding the DsRed-express (Clontech, Mountain View, CA) fluorescent protein to permit monitoring of tumor growth in dorsal skin fold chambers (DSFCs) as described previously [94]. DsRed-LNCaP cells were cultured as adherent monolayers in Dulbecco's modified Eagle's medium (DMEM)/F12 media (BD Biosciences, San Jose, CA) supplemented with 10% of fetal bovine serum, antibiotics, and 10^{-9} mol/L dihydrotestosterone (DHT) as previously described [28].

3.2.2 Animals

Athymic male NU/J mice were obtained from the Jackson Laboratory (Bar Harbor, ME) and housed according to an approved IACUC and University-approved standard operating procedures. Experiments were performed when mice were 6-8 weeks old. Animals with DSFCs were housed under conditions of higher humidity and temperature than normal to maintain tissue microvasculature[94]. When appropriate, animals were anesthetized by an i.p. injection of ketamine (100 mg/kg) and xylazine (10 mg/kg).

3.2.3 DSFC and Tumor Cell Implantation

A DSFC was implanted in each nude mouse as previously described [94, 113]. Immediately after DSFC implantation and on day 4 after implantation, DsRed-LNCaP cells (1-2 million cells/mouse; suspended in 30 µL Matrigel (BD Biosciences, San Jose, CA) that had been diluted 3:1 in serum-free medium) were seeded into the DSFC chamber window. Intravital imaging of tumor cells was performed using a Nikon inverted fluorescent microscope equipped with a 20× objective (Nikon, Melville, NY) and silicon intensified transmission camera (Hamamatsu, Bridgewater, NJ) as previously described [28, 113, 206]. Experiments were performed on day 12 following DSFC implantation, when tumor cells were found to cover the entire chamber window as previously reported [28, 94, 126].

3.2.4 Treatment with TNF-α, NF-κB Inhibitor and Cryosurgery

On the day of the study, the glass windows of DSFCs were removed. The NF-κB inhibitor Bay 11-7085 (EMD Biosciences, San Diego, CA; dissolved in DMSO at 10 mg/ml) was topically applied in the DSFC at a dose of 0.4 mg/kg for 15 min. After Bay treatment, or without pre-treatment with Bay, 200 ng/mouse of TNF-α (a gift from

CytImmune Science, Inc., Rockville, MD; dissolved in 30 µl saline), or a sham mixture of saline, were topically applied for 15 min. The glass windows were replaced and animals were treated with cryosurgery 4 hours later as described previously [94, 126]. Briefly, DSFC windows were removed and a 1 mm diameter brass extension tip fitted to a 5 mm cryoprobe (Endocare, Irvine, CA) was inserted into the center of the DSFC for 55 s (to attain temperatures of -100°C) followed by passive thawing at room temperature. The temperature was monitored throughout the procedure by the use of infrared thermography and thermocouples placed at 2, 3 and 4 mm radial positions around the DSFC center [94].

3.2.5 Intravital Measurements of Vascular Flow

On days 1, 3 or 7 following cryosurgery (with or without prior TNF-α pre-treatment), 0.1 ml of 10 mg/ml 70-kDa FITC-labeled dextran (Sigma, St. Louis, MO) was injected into the tail vein of each animal. Using the inverted fluorescent microscope and camera described above, the average radius of signal in the FITC channel was measured at four perpendicular radial directions relative to the chamber center. Vascular stasis was defined as the lack of fluorescence signal (signifying lack of blood flow, or perfusion defect). Leukocyte interactions with vascular endothelium were visualized following injection of 10 ml/kg body weight of saline containing 1 mg/ml of the nuclear dye rhodamine 6G (Sigma, St. Louis, MO), which labeled leukocyte nuclei intravitally [53]. Slow moving/rolling leukocytes near microvessel walls and fast moving leukocytes in central vascular flow were videotaped during their passage through vessels with a 20× objective using the imaging set up described above.

3.2.6 Histology and Immunohistochemistry

Animals were sacrificed 4 hours post TNF-α treatment or at day 1, 3 and 7 post cryosurgery immediately after vascular imaging. The entire tumor tissue from the

viewing area of the dorsal skin fold chamber was bisected: one-half of each specimen was fixed in 10% buffered formalin (Sigma, St. Louis, MO), embedded in paraffin, sectioned at 4-7 µm and stained with hematoxylin-eosin (H&E). The other half was frozen and stored at -80 °C for immunohistochemistry (IHC). Cryostat sections were acetone-fixed, blocked with serum and incubated with optimal dilutions of anti-mouse antibodies. NF-κB p65 (Gene Tex, Inc., Ivrine, CA) and VCAM (Vector Laboratories, Burlingame, CA) primary antibodies were used for staining of specific molecules. This was followed by ASA-horseradish peroxidase (Covance, Dedham, MA) application and finally 3,3'-Diaminobenzidine (DAB) chromagen that yields a brown color reaction. CD31/PECAM (Biocare Medical, Concord, CA) for endothelial cells and caspase 3 (Biocare Medical, Concord, CA) primary antibodies were co-stained, and dual chromogen imaging was used for CD31/PECAM (Biocare Medical) and caspase 3 (Biocare Medical) to co-localize apoptosis and endothelium.

Histologic sections were digitized using a whole slide digital imaging system, ScanScope (Aperio, Vista, CA), and analyzed using Spectrum software (Aperio, Vista, CA). From prints of whole slide images, distinct histologic layers corresponding to the zones of central necrosis, inflammation, thrombosis/ischemic necrosis, granulation tissue and viable tumor were measured and averaged. Measurements were performed at angles of 30º, 60º and 90º relative to a plane perpendicular to the long axis of the mouse (which was the plane of bisection of tissue pieces removed from each DSFC). Shrinkage was found to be uniform and accounted for as previously reported [94], yielding an average of 18.9 ± 7.7% at each radial location. For quantification of VCAM and caspase 3 IHC staining intensity, digital annotation regions were applied in representative areas of each tumor section and pixels that exceeded threshold limits were quantified (as a ratio of total) using Positive Pixel Count v9 software (Aperio, Vista, CA). NF-κB activation was characterized by the translocation of the p65 (labeled with brown precipitate) from the cytoplasm to nucleus and presented as number of NF-κB activated cells / number of total cells in the representative areas.

3.2.7 Statistics

Statistical significance was determined using the paired student's t test. If the difference was at the level of $p < 0.05$, it was determined significant. Otherwise, the difference between two measurements was not significant, i.e., $p > 0.05$.

3.3 Results

3.3.1 Histological Zones Following Cryosurgery without TNF-α

The maximum cryosurgical lesion without TNF-α pre-treatment presented at day 3. Cryoinjury was characterized by five histological zones extending radially outward from the probe location (Fig. 3-1). Zone 1: immediately surrounding the cryoprobe a central necrotic zone was formed, characterized by intense eosinophilic staining of cells, loss of hematoxylin staining and loss of cellular detail. Blood vessels in this central necrotic zone were destroyed. In some specimens, scattered neutrophils were present in this zone. Zone 2: surrounding the central necrotic zone, a marked band of inflammation was present. Neutrophils were the dominant cells in this band, with lesser numbers of lymphocytes and histocytes also present. Zone 3: centrifugal to the inflammatory band was a zone of thrombosis and resulting hemorrhage and ischemic necrosis. Zone 4: surrounding the zone of thrombosis/ischemic necrosis was a zone of granulation tissue characterized by fibroblast/myofibroblast infiltration and proliferation, new collagen deposition and nascent capillary formation [293]. The granulation tissue zone was found only on day 3 and later. The five zones from central necrosis to granulation tissue were defined as the cryolesion. Zone 5: Peripheral to the cryolesion was a zone of viable tumor.

3.3.2 TNF-α Pre-conditioning is Mediated at the Vascular Level

Histological features following topical TNF-α treatment were analyzed. Acute vascular injury events, including microvascular dilatation, thrombosis/congestion and hemorrhage (Fig. 3-2A) were first observed and reached the maximum as early as 4 hours after TNF-α treatment and notably decreased from day 1 to day 7. An acute inflammatory response was observed at 4 hours, characterized by an influx of neutrophils, many adherent to the endothelial layer and infiltrating into the interstitial space (Fig. 3-2B). Later, tumor cell necrosis in some areas with thrombosis/congestion became notable and peaked between day 1 and 3, likely due to diminished blood supply and cytotoxic effects of the inflammatory infiltrate. These histological observations are summarized in Table 3-1. Immunocytochemistry of these same samples revealed that TNF-α treatment alone induced NF-κB and caspase 3 activity 4 hours after administration ($p < 0.05$), although both were suppressed later at 24 hours (Fig. 3-2C). VCAM expression was increased over the same period, although the changes were not statistically significant.

3.3.3 Histologic Evolution of Cryolesion Zones and TNF-α Modification of Evolution

One day after cryosurgery, the small central necrosis zone and a surrounding large zone of scant inflammation and thrombosis were difficult to distinguish by H&E staining. Blood vessels were severely damaged at the center, evidenced by fibrin deposition within vessels and extravasation of erythrocytes. Toward the edge of the cryolesion, vascular damage was less severe, characterized by microvascular dilatation. Viable tumor was present in this zone at day 1, such that it was difficult to distinguish the cryolesion edge. No significant TNF-α enhancement was notable at day 1. At day 3, the cryolesion histologic zones were established, including a marked band of inflammation, chiefly neutrophils, surrounding the central necrotic zone, and early granulation tissue formation. At day 3, the radius of the histologically identified cryolesion correlated well with the radius of the vascular stasis visualized by intravital imaging (Fig. 3-3C, Table 3-2). TNF-

α significantly enlarged the cryolesion radius from 3.3 ± 0.6 to 4.3 ± 0.3 mm by histology (Fig. 3-3B, Table 3-2). Specific zones were also enhanced by TNF-α. The inflammatory zone was significantly increased by TNF-α, from 1.9 ± 0.8 mm with cryosurgery alone to 3.0 ± 0.5 mm with combined TNF-α pre-treatment followed by cryosurgery (Fig. 3-3B, Table 3-2). Further, a thin zone of granulation tissue (0.6 ± 0.5 mm in width) peripheral to the zone of thrombosis/ischemic necrosis was formed at day 3 following combinatorial therapy, which was not clearly formed after cryosurgery alone (Fig. 3-3B, Table 3-2). At day 7, the inflammatory and granulation tissue zones continued to expand. Granulation tissue became notable with cryosurgery treatment alone (0.8 ± 0.3 mm in width) and was expanded centripetally into the ischemic necrosis layer with TNF-α pre-treatment (1.2 ± 0.5 mm in width) (Fig. 3-3B, Table 3-2). Importantly, pre-treatment of TNF-α completely destroyed the tumor tissue up to the iceball edge (3.9 mm, -0.5°C) at day 1 and 3, which could not be achieved by cryosurgery alone.

3.3.4 Intravital Imaging Evaluation of TNF-α Enhanced Vascular Injury

The stasis radius modified by TNF-α post cryosurgery was measured by FITC-dextran fluorescence at day 1, 3 and 7 post cryosurgery in both tumor tissue and normal skin (Fig. 3-3C, Table 3-2). With cryosurgery alone, the stasis radius increased from 2.7 ± 0.7 mm at day 1 to 3.3 ± 0.5 mm at day 3 ($p<0.05$) and 3.1 ± 0.1 mm at day 7 in tumor tissue. Whereas, with TNF-α pre-treatment, a large stasis radius was already created at day 1 (3.8 ± 0.8 mm) which remained large at day 3 (4.0 ± 0.4 mm) and day 7 (3.7 ± 0.5 mm). Pre-treatment with TNF-α was observed to increase stasis radius up to the edge of the iceball (3.9 mm) at all time points (day 1, 3 and 7) after cryosurgery compared with cryosurgery alone. This observation was consistent with our previous observation at day 3 post cryosurgery [94, 113], suggesting enhanced vascular damage post cryosurgery induced by TNF-α pre-treatment in tumor. On the other hand, the normal skin showed significant contraction of the radii of vascular stasis from day 1 through day 7 after cryosurgery both with and without TNF-α pre-treatment. TNF-α pre-treatment followed

by cryosurgery in normal skin, yielded a larger vascular stasis early on (day1 and 3) (p<0.05), with a faster reduction in stasis radius at day 7 (1.0 ± 0.3 mm) compared with cryosurgery alone (2.1 ± 0.4 mm) (p<0.05). This suggests an enhanced wound healing process induced by TNF-α in normal skin possibly through enhanced blood flow.

3.3.5 Molecular and Cellular Mechanisms of TNF-α Enhanced Cryosurgery

NF-κB translocation, VCAM expression and caspase 3 signaling pathway induction were altered due to treatment as assessed by IHC at day 1 after cryosurgery with and without TNF-α pre-treatment (Fig. 3-4B). NF-κB translocation and VCAM expression were significantly activated in tumor, endothelial, and the occasional fibroblast cell. Caspase 3 signaling was upregulated in infiltrating leukocytes and endothelial cells. These effects are enhanced by TNF-α pre-treatment at the edge of the cryolesion. At day 3 post cryosurgery, these molecular events decreased to the point where no signal was seen by IHC. Upregulation of VCAM and NF-κB in combinatorial therapy appeared to have a greater biological effect on the lesion. Within the dense inflammatory band, TNF-α pre-treatment greatly enhanced the density of neutrophils infiltrating the tissue from 54.6 ± 18.2 to 121.7 ± 53.3 cells/field (p<0.05, Fig. 3-4D) in the inflammation band. The TNF-α enhanced inflammatory response at day 3 post combinatorial cryosurgery was likely due to VCAM expression mediated by NF-κB since the inflammatory infiltrate was significantly reduced with use of the NF-κB inhibitor Bay, from 121.7 ± 53.3 cells/field without Bay to 40.1 ± 20.5 cells/field with Bay (Fig. 3-4D). This inflammatory infiltrate can also lead to caspase activation in some neutrophils and endothelial cells at day 1 (Fig.4B). Together, these inflammatory and subsequent caspase mediated events lead to the extension of the cryosurgical lesion with TNF-α.

3.4 Discussion

A major challenge of studying the mechanisms of cryoinjury *in vivo* is the differential injury response as a function of the temperature response, especially related to the iceball edge, within the tissue. In this study, we show the distribution of the cellular and molecular activity in tissue using a DSFC model that allows temperature monitoring and quantification of injury responses over time after treatment. Five histological zones were observed post cryosurgery, including central necrosis, inflammation, thrombosis/ischemic necrosis, granulation and viable tumor. TNF-α spatial and temporal modification of these zones and the early molecular mechanisms that affect this response were studied.

Our results suggest that the inflammatory infiltrate is the main mechanism of TNF-α cryoinjury enhancement. Recent evidence has shown that host mediated injury, including vascular and immunological effects, define the edge of a cryosurgical lesion [83, 242]. The host response is orchestrated by the innate immune system in a non-antigen specific manner. Key elements of the host response are: to destroy tumor cells, prevent the spread of tissue damage, contain imbalances of homeostasis, remove dead damaged/altered tissue, and ultimately restore tissue function [147]. The inflammatory infiltrate is an important part of this host response. The interaction of the host response with the local tumor tissue usually takes place during ischemia reperfusion post cryosurgery [90, 175]. Local tissue damage yields "danger signals", including the synthesis of pro-inflammatory cytokines (e.g. TNF-α, IL-1 and 6) and chemokines that initiate recruitment of circulating leukocytes to the injury site [235]. Reperfusion and subsequent re-oxygenation after freeze thaw induce NFκB-dependant transcription of gene encoding adhesion molecules (ICAM, VCAM, E-selectins and P-selectins) and chemokines [11, 36, 290] that further mediate leukocyte transendothelium migration from circulation to the interstitium. Neutrophils play a central role in this host response by initiating the coagulation cascade [268], acting as chemoattractants for inflammatory cells [59, 268], beginning the debridement of devitalized tissue, and phagocytosis of foreign bodies by releasing toxic agents (reactive oxygen species, cationic peptides, eicosanoids and proteases) [300].

Our work suggests that the main effect of TNF-α is to pre-condition the vasculature by activating vascular endothelial cells to recruit inflammatory cells and promote their extravasation. Our results are consistent with published work [147, 204]; however the connection to cryosurgery is new in this work. Vascular pre-conditioning is mediated by NF-κB pathway activation, which peaked at 4 hours, and led to expression of adhesion molecules (VCAM) and adhesion of leukocytes at endothelial surfaces. Combined with cryosurgery, both NF-κB translocation and VCAM activation were significantly enhanced by TNF-α pre-treatment at day 1 (Fig. 3-4B), suggesting that TNF-α pre-treatment mediates later augmented inflammatory infiltration (day 3 post cryosurgery).

In addition, endothelial apoptosis and increased vascular permeability for blood constituents (i.e. cells, proteins) is observed after TNF-α application. This may be either due to TNF-α receptor binding on endothelial cells and caspase activation, and/or reactive oxygen species from pre-recruited inflammatory cells by TNF-α. Finally, infiltrated leukocytes (neutrophils and macrophages) and activated endothelial cells can produce more cytokine (esp.IL-1, 6 and TNF-α,) which amplifies the inflammatory response. All these vascular pre-conditioning events can contribute to the recruitment and retention of an inflammatory infiltrate after cryosurgery.

It has been recently reported that apoptosis was observed at the edge of the cryolesion 24 hours post cryosurgery [242]. Our results are consistent with this evidence and show significant caspase activation after cryosurgery that can be further enhanced by TNF-α pre-treatment. Importantly, caspase activity was mainly found in leukocyte and endothelial cells as confirmed by co-localization of caspase 3 and CD31 staining (Fig. 3-4C), whereas minimal caspase activation was found in tumor cells as described in previous work [262]. This suggests that apoptosis is an outcome of endothelial cell injury due to leukocyte-endothelial cell interaction. This is supported by our previous inhibition

study that showed that NF-κB inhibition, rather than caspase inhibition, significantly reduced the extent of vascular injury post TNF-α enhancement of cryosurgery [126]. The caspase activation within endothelial cells is likely induced by free radicals and proteases released from infiltrating leukocytes [185]. These molecules promote apoptosis of endothelial cells, thereby leading to microvascular damage and subsequent blood flow defects [60, 131]. This enhanced endothelial injury by the inflammatory infiltrate is therefore a result, but not a determinant of, vascular injury and stasis at the cryolesion edge.

An advantage of cryosurgery often cited is that of rapid wound healing and minimal scarring. This has been observed in the management of a wide variety of skin lesions, particularly those affecting the face and skin [160, 253]. However, wound healing after tumor cryoablation has been barely studied. Pre-treatment with TNF-α not only increased the inflammatory infiltrate and the eradication of tumor, but also advanced the initiation of granulation tissue, consisting of endothelial cells, macrophages, and fibroblasts infiltrating to the wound site. This may be due to the fact that TNF-α can stimulate active neutrophils and macrophages [145], angiogenesis [157] and enhance invasive migration of normal fibroblasts [243, 286], therefore promoting the cellular activity during wound healing. In addition, the local environment (cytokines, chemokines and growth factors) modified by TNF-α stimulation can also activate a large transcriptional program, which produces cytokines and growth factors required by wound healing [60, 159, 277]. However, TNF-α promoted wound healing which enhances angiogenesis thereby causing infiltration of tumor cells into the cryolesion site and even recurrence and metastasis of the tumor post cryosurgery [153]. In order to better understand the effect of TNF-α on wound healing (and possible negative effects on tumor recurrence), future studies will need to explore time points beyond 7 days.

The innate immune response is also enhanced by TNF-α and is essential in the development of an adaptive immune response to target the cryotreated tumor [35, 83, 147, 235]. The adaptive immune response begins with antigen uptake and presentation on antigen presenting cells (macrophages and dendritic cells) for recognition by antigen-specific T cells. However, in this study, an athymic mouse model with defective T lymphocyte production was used. Thus, while the innate immune response in our study was vigorous and dominated by neutrophils and macrophages, the contribution of the adaptive immune cells to tissue destruction was underestimated. Future investigation of the effect of TNF-α on adaptive immune response during and after cryosurgery with an immune competent animal model is clearly needed.

In conclusion, these results show the tremendous potential of TNF-α to pre-condition the vascular and immune response of a tumor thereby enhancing cryosurgical efficacy. A strong enhancement of the inflammatory infiltrate within the cryolesion occurred due to TNF-α vascular pre-conditioning. The interaction of this infiltrate with the tumor endothelium and parenchymal cells through a blocking susceptible NF-κB regulated (inflammatory) pathway is thought to be the dominant mechanism of cryosurgical injury and enhancement [126]. Apoptosis was also enhanced by TNF-α; however, this occurred subsequent to the recruitment of an inflammatory infiltrate and, due to the inability to block the effect, is not considered a dominant pathway of cryosurgical injury or enhancement [126]. Finally, granulation tissue formed after cryosurgery is also enhanced by TNF-α pre-treatment, suggesting promotion of wound healing. Further studies are still needed to elucidate the role of TNF-α in the wound healing and adaptive immune response after combinatorial cryosurgery.

Table 3-1: Time course of morphological changes post TNF-α treatment

Time post-treatment	Inflammatory infiltrate[b]	Hemorrhage[c]	Thrombosis & Congestion[d]	Tumor Necrosis[e]
Ctr	-	-	-	-
4hr	++++	+++	++	+
Day 1	+++	-	++	+++
Day 3	+	-	+	+++
Day 7	+	-	+	++

[a] Data correspond to semi-quantitative evaluation in tumor areas of hematoxylin-eosin sections (evaluation was made in five representative fields per sample under 20× magnification). Three to four independent experiments were performed for each treatment.
[b] Average numbers of leukocytes per field.
[c] Percent of tissue area involved by hemorrhage.
[d] Average number of vessels affected by congestion/dilation and thrombosis per field.
[e] Percent of tumor area involved by necrosis.

Table 3-2: Quantitative measurements of the radius of histological zones following cryosurgery

Treatment		Vascular Stasis [b]	Cryolesion (Histology) [c]	Central Necrosis [d]	Inflammation [d]	Thrombosis /ischemic necrosis [d]	Granulation [d]	Viable Tumor [d]
Day 1	Cryo	2.7±0.7	e	0.9±0.6	2.6±0.9	0.1±0.1	NA	1.4±0.3
	TNF+Cryo	3.8±0.8*	3.9±0.6	NA	3.4±0.6	0.5±0.5	NA	1.1±0.2
Day 3	Cryo	3.3±0.5#	3.3±0.6	1.0±0.7	1.9±0.8	0.5±0.4	NA	1.7±0.6
	TNF+Cryo	4.0±0.4*	4.3±0.3*	0.5±0.9	3.0±0.5*	0.2±0.2	0.6±0.5	0.7±0.3*
Day 7	Cryo	3.1±0.1	3.2±0.4	0.5±0.3	1.1±0.7	0.7±0.5	0.8±0.3	1.8±0.4
	TNF+Cryo	3.7±0.5*	3.8±0.5*	NA	2.4±0.5*	0.8±0.4	0.6±0.5	1.2±0.5*

[a] The values represent Mean ± SD of three to four independent experiments for each treatment.
[b] Radius of vascular stasis was measured by intravital microscopic imaging following FITC-dextran injection.
[c] Radii of granulation tissue (outer bound of cryolesion) were measured from digitized H&E-stained sections (corrected for tissue shrinkage after histologic processing as described in Materials and Methods).
[d] Radii of histological zones of central necrosis, inflammation, thrombosis/ischemic necrosis, granulation tissue influx, and viable tumor were measured from digitized H&E-stained sections (corrected for tissue shrinkage after histologic processing as described in Materials and Methods).
[e] Cryolesion edge at day 1 after cryosurgery is imperceptible based on H&E-stained sections.
There was a significant change ($p<0.05$) in radius of vascular stasis from day 1 to day 3 as measured by intravital microscopic imaging.
* Significant changes ($p<0.05$) between combinatorial (TNF-α + cryosurgery) therapy versus cryosurgery alone were seen in the radii of vascular stasis measured by intravital microscopic imaging, and in radii of histologic zones following cryosurgery.
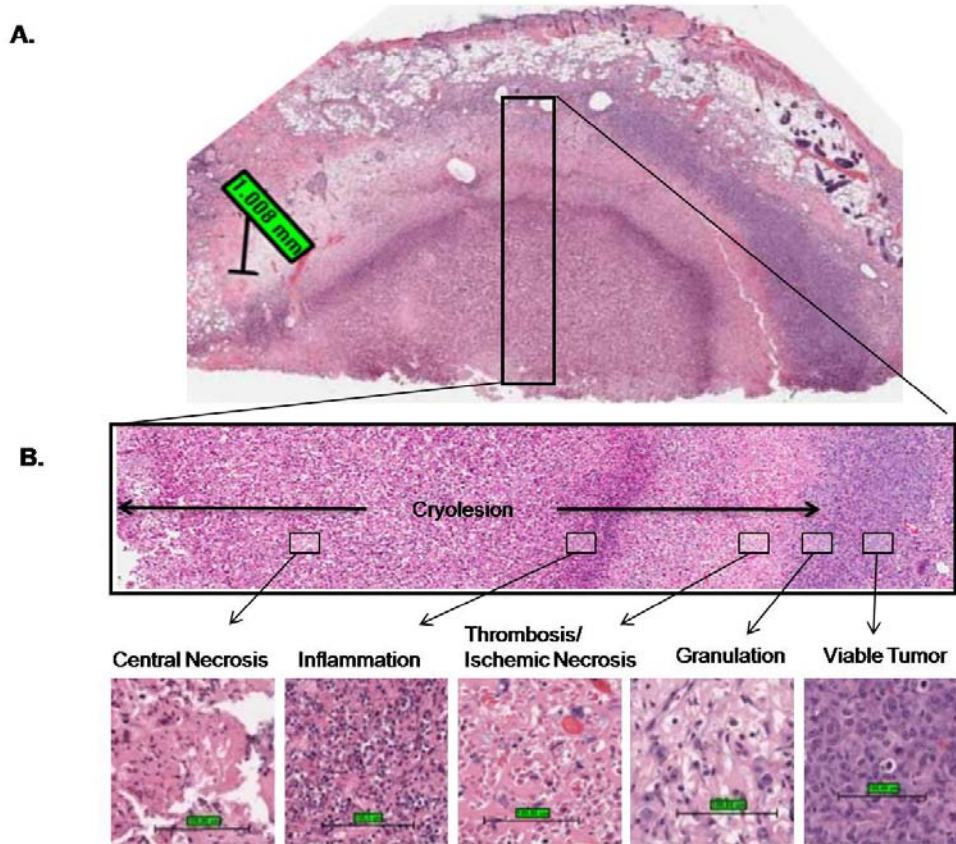
Figure 3-1: Five histological zones were evident after cryosurgery: central necrosis, inflammation, thrombosis/ischemic necrosis, granulation tissue influx, and viable tumor. (A) Demonstration of these histological zones at day 3 post cryosurgery (20× objective; scale bar = 1mm). (B) Demonstration of these histological zones at 40× objective magnification (scale bar = 100 µm).
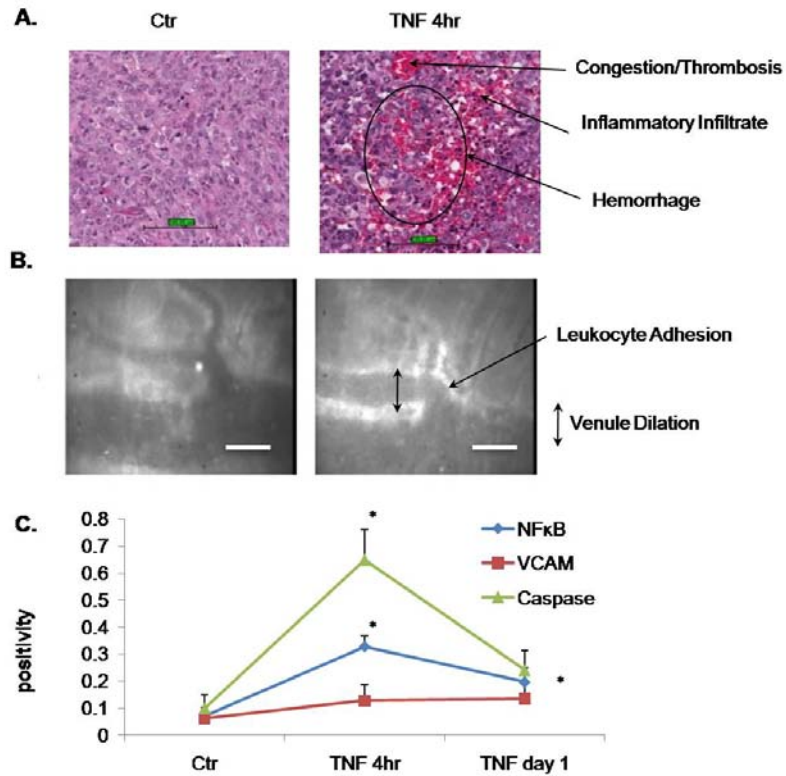
Figure 3-2: TNF-α treatment mediated vascular pre-conditioning events. (A) TNF-α induced histological changes in tumor tissue including congestion/thrombosis, inflammatory infiltrate and hemorrhage (scale bar = 100 µm). (B) TNF-α resulted in microvascular dilatation and enhanced leukocyte association with vessel walls, as visualized by intravital fluorescent videotaping after intravenous administration of the nuclear dye rhodamine 6G (scale bar = 100 µm). (C) TNF-α induced caspase activation in tumor and endothelial cells at 4 hours after treatment (*, $p < 0.05$), and NF-κB activation in endothelial cells at 4 hours and day 1 after treatment (*, $p < 0.05$). Data are presented as the mean (bar height = 1 standard deviation) of three to four independent experiments for each treatment.
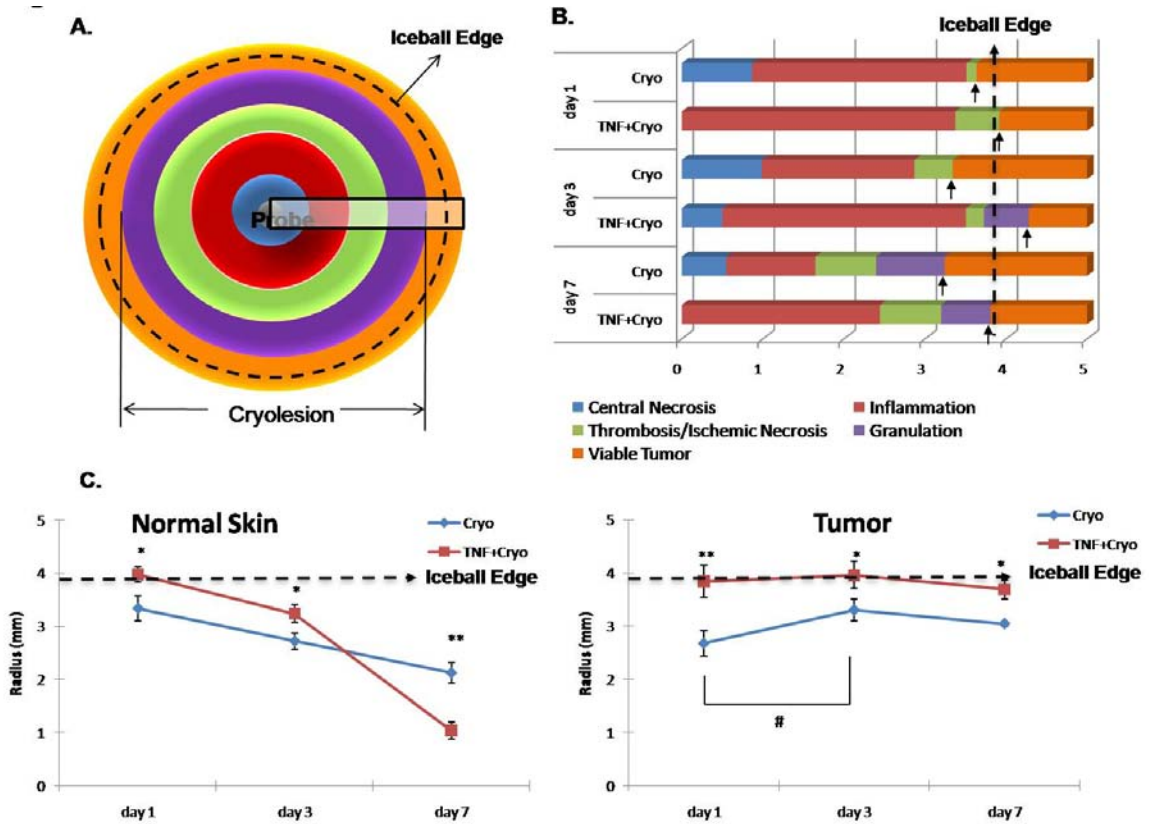
Figure 3-3: Dynamic histological changes following cryosurgery with/without TNF-α pre-treatment. (A) Representation of the iceball formation and five histological zones following cryosurgery (see Fig. 1). (B) Demonstration of changes in the normalized radii of histological zones over time (bar values represent the mean of three to four independent experiments for each treatment; see Table 2 for the mean and standard deviation). Arrows represent histologic cryolesion edge (boundaries of granulation tissue zone) for illustration. Dashed arrows indicate the iceball edge (3.9 mm, -0.5°C) [94]. (C) Stasis radius at days 1, 3 and 7 after cryosurgery measured by intravital microscopic imaging following FITC-dextran injection. Stasis radius was significantly enhanced by TNF-α pre-treatment combined with cryosurgery as compared to cryosurgery alone (*, p<0.05; **, p<0.001). For tumor tissue cryosurgery alone, extension of stasis radius was observed from day 1 to day 3 (#, p<0.05). The bar values represent Mean ± SD of at least four independent experiments for each treatment. Dashed arrows indicate the iceball edge (3.9mm, -0.5°C).
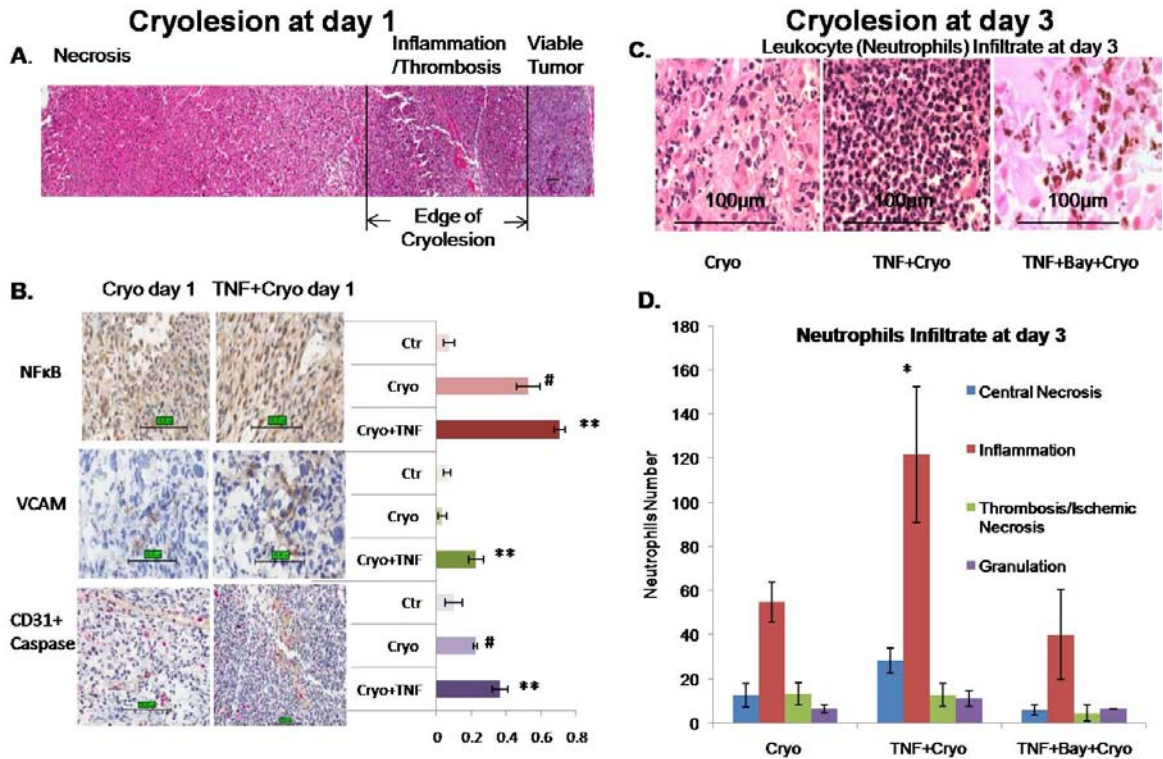
Figure 3-4: Molecular and cellular mechanisms of TNF-α enhanced cryosurgery. (A) Immunohistochemical demonstration of NFκB, VCAM and caspase 3 (red) and CD31 (brown) activation at the edge of the cryolesion at day 1 post cryosurgery (scale bar=100µm). (B) Quantitative immunohistochemistry of NFκB, VCAM and caspase 3 signal in the cryolesion at day 1 post cryosurgery. The average number of positive pixels/total pixels was derived from five representative fields within each sample; values represent mean ± SD of three to four independent experiments for each treatment; there were statistically significant (p<0.05) differences between cryosurgery versus sham control (#), and combinatorial treatment versus cryosurgery alone (**). (C) Leukocyte (neutrophils) infiltrate at day 3 post cryosurgery with or without TNF-α pre-treatment. Animals were treated with cryosurgery alone, TNF-α 4 hours pre-treatment plus cryosurgery, or NF-κB inhibitor Bay followed by TNF-α 4 hours pre-treatment plus cryosurgery. Representative image of neutrophilic infiltrate with H&E staining was taken under high power (100× magnification) within the inflammation zone (scale bar =100µm). (D) Quantification of neutrophils within leukocyte infiltrate within each histological zone under high power field. The average number of neutrophils was measured in five representative fields in each histological layer for each sample. The bar values represent mean ± SD of three to four independent experiments for each treatment. The numbers of neutrophils per field were significantly different between the combinatorial treatment and cryosurgery alone (*, p<0.05).

Chapter 4 Pre-clinical Characterization of TNF-α Dose, Timing and Delivery Methods on Cryosurgical Enhancement in ELT-3 Uterine Fibroid System

4.1 Background

Cryosurgery is a procedure which freezes tissue using a cryogen cooled cryoprobe. Upon thawing, some of the cells of the previously frozen tissue will die leading to a reduction in the size of the tumor. This technique has been used for the treatment of a variety of cancers since the evolution of the first cryogen cooled cryoprobe was introduced in the 1960s [40]. During cryotherapy, direct cell injury first occurs by intracellular ice formation produced near the cryoprobe, and by cellular dehydration present at the periphery of the iceball [78]. Upon thawing host mediated mechanisms including acute (hours to days) vascular injury leading to thrombosis and delayed immunological response (days to weeks) can lead to resolution of remaining tumor cells at the primary and even distant sites [3, 83, 114, 242, 260]. This technique allows both the placement of the minimally invasive cryoprobe and the ensuing iceball growth to be controlled under image guidance, using either ultrasound (US) or magnetic resonance (MR) [42, 62].

Unfortunately, the tissue at the periphery of the iceball is not destroyed completely and hence allows tumor, such as uterine fibroids, to regrow [314]. Thus, the iceball must encompass both the tumor and some adjacent tissue in order to have a satisfactory outcome. Generally, temperatures below -40 °C are recommended at the tumor edge for adequate tumor control [78]. This partial destruction of tissue at the iceball edge not only potentiates the later recurrence of the tumor, but also limits the ability of the imaging techniques to predict outcomes. One potential solution to this problem is the use of cryosurgical adjuvants that improve the correspondence between the imaged iceball and the destroyed tissue, thereby improving image guidance and control during the procedure. A variety of adjuvants have been investigated to accentuate both vascular and

immunological mechanisms of destruction within the cryolesion to more effectively overlap intra-operative cryosurgical iceball imaging and the destructive edge [104]. The most effective of these adjuvants at enhancing the destructive edge of the cryolesion *in vivo* is TNF-α [94, 104, 311]. It should be noted, that TNF-α shows promise as an adjuvant to thermal therapies in general and cryosurgery in particular. However, as a stand alone drug for tumor control TNF-α causes hypotension with dose-limiting toxicity as shown in poor phase I/II clinical trial results [110]. Therefore, the administration regime of TNF-α needs to be carefully characterized based on efficacy and toxicity evaluation. Recently, we have shown the ability to enhance cryosurgical destruction to the visualized iceball edge without toxicity using nanoparticle delivery of TNF-α at 5 µg dose (CYT-6091) [94, 311]. This promising finding in a prostate cancer model (LNCaP) of male nude mouse prompted us to investigate this combinatorial approach in a different tumor (ELT-3 uterine leiomyoma) with several new dose, timing and delivery approaches for TNF-α introduction.

The tumor-derived cell lines from Eker rat leiomyomas (ELT) have been characterized in nude mice [118] and extensively used to identify therapeutic strategies for uterine leiomyoma and to investigate the etiology of this disease [21, 291]. Retention of estrogen responsiveness by ELT-3 cells combined with the fact that spontaneous tumors develop with a high frequency has made this an extremely useful animal model for studies on uterine leiomyoma [118, 291]. Therefore, a study was designed to test TNF-α as an adjuvant to cryosurgery in an *in vivo* model of ELT-3 tumor in female nude mice.

Pre-treatment time, delivery and dose are known to be important parameters to determine TNF-α effect on cryosurgery. It was observed that 4 hours pre-treatment of TNF-α showed a promising effect on the enhancement of both hyperthermia and cryotherapy using nanoparticle delivery of TNF-α [94, 289]. However, for clinical application, a shorter pre-treatment time without reducing efficacy is preferred to reduce time in the operating room and increase patient convenience. Therefore, the efficacy of a 1 and 2 hour pre-treatment time with TNF-α is compared with 4 hours in this study. As systemic

administration of TNF-α has dose limiting toxicity [110], many studies attempted to selectively deliver TNF-α to the tumor site to minimize systemic toxicity, including liposomal delivery, gene delivery, nanoparticle delivery [205, 283]. Other work has found that injecting TNF-α directly into prostate tumor interstitial space, combined with systemically injected interferon-alpha [150], produced a significant reduction of prostate volume in 9 out of 10 cases, implicating the interstitial injection as an effective and a more convenient delivery route for clinical application. This prompts our interest in characterizing the interstitial injection of TNF-α in comparison with systemic injection of CYT-6091 at the same dosage. Two strategies are considered for interstitial injection: intratumoral injection as a single injection at the center of the tumor; and peritumoral as multiple injections at evenly distributed sites at the periphery of the tumor. Finally, the dose range needs to be carefully chosen to minimize the toxicity.

In the present study, TNF-α combined with conservative cryosurgery (i.e. freezing to the visible edge of the iceball) will be investigated for the first time in an ELT-3 tumor grown in a female nude mouse [118]. Specifically this study is designed to characterize the following after freezing to the visible edge of this tumor *in vivo*: 1) the destruction of the ELT-3 tumor over time after cryosurgery; 2) the effect of TNF-α pre-treatment on cryosurgery; 3) the effect of pre-treatment time, mode of delivery and dose on cryosurgery enhancement, and to note any toxicity.

4.2 Materials and Methods

4.2.1 Culture of ELT-3 Cells

ELT-3 cells were cultured as monolayers in 75 cm^2 T flasks as previously described [118], with DMEM/F-12 supplemented with 1.6×10^{-6} mol/l ferrous sulphate (Sigma Chemical Co, St Louis, MO, USA), 1.2×10^{-5} IU/ml vasopressin (Sigma), 1.0×10^{-9} mol/l triiodothyronine (Sigma), 0.025 mg/ml insulin (Sigma), 1.0×10^{-8} mol/l cholesterol

(Sigma), and penicillin/streptomycin 10% fetal bovine serum (FBS). Cells were grown at 37ºC, 5% CO^2 until 80% confluent.

4.2.2 Animals

All animal protocols were reviewed and approved by the University of Minnesota Institutional Animal Care and Use Committee. Female athymic nude mice with NU/J genetic background were purchased from the Jackson Laboratory and housed according to the University approved standard operation procedures. Animals were anesthetized by i.p. injection of ketamine and xylazine at 100 and 10 mg/kg, respectively, and they expired as noted or were sacrificed at day 30 post-treatment.

4.2.3 Hindlimb Tumor Seeding

After reaching 80% confluence, ELT-3 cells were released from the flasks by incubating with 0.05% trypsin and 0.53 mmol/l EDTA for 3 minutes, then neutralized with culture media (described above) and centrifuged at 1400 rpm for 10 minutes. Cells recovered from each 75 cm^2 flask (4 to 6×10^6 cells) were then transferred to an Eppendorf tube in 1ml DMEM/F-12 (Sigma), centrifuged at 1400 rpm for 5 minutes, then resuspended in DMEM/F-12 (Sigma) to 60-80 µl final volume. Two to three volumes of Matrigel matrix (BD Biosciences, San Jose, CA, USA) were added to 1 volume of resuspended cells, and then the suspension was put on ice. Within two hours of cell harvest, 100 µl of the ELT-3 cell suspension (~ 2×10^6 cells in Matrigel matrix) was injected s.c. into the hindlimb of the mouse. Experiments were performed after 5 to 7 weeks, when the tumor diameter was 6 to 8 mm. Animals forming round and symmetrical tumors were randomized into various groups for experiments.

4.2.4 TNF-α Treatment

On the day of the experiment, 2 µg or 5 µg of either native TNF-α (CytImmune Sciences, Inc., Rockville, MD, USA) or TNF-α bound to gold nanoparticles (CYT-6091, CytImmune Sciences, Inc.) [205] was diluted in 100 µl saline, and then injected into the hindlimb tumor or injected i.v. The 5 µg was chosen from previous work with CYT-6091 and the lower dose of 2 µg was chosen in case of toxicity [94, 289]. Native TNF-α was injected directly in to the interstitial space of the tumor either intratumorally or peritumorally. Intratumoral injection was performed by injecting all 100 µl of solution into the center of the tumor. For peritumoral injection, 12.5 µl TNF-α solvent was injected at eight evenly distributed points spanning the circumference of the tumor base. CYT-6091 was administered by i.v. injection only. The TNF-α was administered at 1 hour, 2 hours or 4 hours before cryosurgery. The time intervals and the doses were chosen based on our previous work showing efficacy at 4 hours with TNF-α in cryosurgery [28, 94].

4.2.5 Conservative Cryosurgery

Cryosurgery was performed using a cryosurgical system (Endocare, Inc., Ivrine, CA, USA), as described previously [94], with a 1 mm probe tip modification on a 3 mm tip cryoprobe. A small incision was first made in the center of the tumor with 21-gauge needle to allow insertion of the probe tip without deformation of the tumor. The cryoprobe was activated by allowing the argon cryogen to flow, and the 1 mm probe tip temperature was set at -120 ºC. Freezing was performed conservatively under visual guidance whereby the iceball was allowed to grow just to the visible edge of the tumor (i.e. the tumor edge was at roughly 0 °C a normally non-lethal freeze). The tumor was then passively thawed at room temperature.

4.2.6 Tumor Growth Delay Measurement

Injury was assessed by measuring tumor growth delay after cryosurgery on day 0. Baseline tumor size was measured on day 0 prior to cryosurgery. Tumor growth in fold-changes is reported relative to the size at day 0. Tumor volumes were measured every 3 days through day 30 after treatment. Tumor dimensions were measured using calipers and volumes were calculated and reported as $0.53 \times$ width $\times$ length $\times$ height [280].

4.2.7 Toxicity Assessment

Toxicity was evaluated by changes to survival vs. controls. Survival of the animals was assessed daily and reported every 3 days for up to 30 days after treatment.

4.2.8 Statistics

Comparison of the effect of different treatment conditions on the tumor growth delay was done using one-way ANOVA followed by t test. The tumor growth data from animals that died prior to 30 days were not included for statistical analysis; however, each group still consisted of at least three animals.

4.3 Results

4.3.1 Effect of TNF-α Pre-treatment Time on Cryoinjury Enhancement

In order to determine optimum pre-treatment time, a low dose (2 µg) of native TNF-α was injected peritumorally at 1 hour, 2 hours and 4 hours respectively before cryosurgery (Fig. 4-1). Only the 4 hours pre-treatment significantly reduced tumor volume when compared to cryosurgery alone (Fig. 4-1, *, $p < 0.05$). Shorter pre-treatment times (2 hours

and 1 hour) with the same dose of TNF-α were found to be insufficient to enhance cryoinjury.

4.3.2 Effect of TNF-α Delivery Routes at Low Dose (2 µg) on Cryoinjury Enhancement

Interstitial injection (both intratumoral and peritumoral) of native TNF-α, and i.v. injection of CYT-6091, were compared in terms of cyoinjury enhancement. TNF-α was given at the same dose (2 µg) and pre-treatment time (4 hours before cryosurgery). Only the peritumoral native TNF-α injection route was able to significantly delay tumor growth at 30 days compared with cryosurgery alone (Fig. 4-2, *, $p<0.05$), with the volume reduced from 16.54 ± 1.26 fold with cryosurgery alone to 10.54 ± 2.33 fold. Neither intratumoral injection of native TNF-α nor i.v. injection of CYT-6091 was effective (at this dose and time) in enhancing cryoinjury through day 30 (Fig. 4-2). This suggests that the peritumoral injection, combined with cryosurgery, is the most effective delivery mode for delaying tumor growth for this dose (2 µg). The control tumor with no treatment showed dramatic growth, reaching 22.23 ± 3.13 fold by day 30 (Fig. 4-2). TNF-α alone without cryotreatment, led to a reduction in growth up to day 21 compared to control. However, after 21 days, TNF-α alone did not differ in response (statistically) from control. After cryosurgery without TNF-α, significant tumor growth delay was observed vs. control through day 24, however after day 24, no further delay was noted.

4.3.3 Effect of TNF-α Dose on Cryoinjury Enhancement

The effect of TNF-α dosage on toxicity was then investigated for all three delivery methods. Doses of 2 µg or 5 µg of both native TNF-α and CYT-6091 were administered 4 hours before cryosurgery. Since both peritumoral and intratumoral injection of 5 µg native TNF-α followed by cryosurgery induced high systemic toxicity (100% and 40%, respectively, Fig. 4-5), the least toxic delivery system, i.v. injection of CYT-6091, was

chosen to study TNF-α dose effects on tumor growth delay after cryosurgery (Fig. 4-2). Low dose (2 µg) CYT-6091 combined with cryosurgery showed no toxicity but was not sufficient to delay the tumor growth when compared to cryosurgery alone. In contrast, high dose (5 µg) CYT-6091 with cryosurgery showed some toxicity (33%) but produced a dramatic reduction in tumor volume, from 16.54 ± 1.26 fold with cryosurgery alone to 5.66 ± 2.15 fold change at day 30 (Fig. 4-2, **, $p<0.001$). One animal showed complete tumor regression through day 30 in this treatment group.

4.3.4 Effect of TNF-α on Early Tumor Regression after Cryosurgery

It was observed that the tumor initially regressed for a few days after cryosurgery with or without pre-administration with TNF-α. During this time, eschar formed at the cryosurgery site and remained observable at day 6 (Fig. 4-3). For cryosurgery alone, the tumor grew back to reach the pre-treatment size after roughly 5 days and continued to grow through day 30 thereafter. Pre-treatment with high dose (5 µg) of i.v. injected CYT-6091 created the largest eschar, indicating the maximum cryolesion produced by this treatment. This correlates well with the fact that high dose of i.v. injected CYT-6091 significantly enhanced the early regression from 5.30 ± 1.10 days for cryosurgery alone to 12.54 ± 1.68 days (Fig. 4-4, *, $p<0.05$). One animal in the 5 µg CYT-6091 treatment group showed long term complete regression through day 30 (Fig. 4-3 and Fig. 4-5). With low dose (2 µg), the early regression delay effect was also obtained by peritumoral injected native TNF-α and i.v. injected CYT-6091 (*, $p<0.05$), while intratumoral injected native TNF-α had no effect on early tumor regression compared to cryosurgery alone (Fig. 4-4).

4.3.5 Toxicity of Treatments

Toxicity (lethal effect) of TNF-α treatments combined with cryosurgery occurred within the first 3 days for some of the treatments as summarized in Fig. 4-5. After day 3, all

remaining animals survived until the day of sacrifice. The control group as well as the cryosurgery alone group (no TNF-α) had no toxicity. High-dose (5 µg) native TNF-α peritumoral injection at 4 hours pre-treatment leads to the highest toxicity (100%), followed by intratumoral injection (5 µg, native) (40%), whereas the i.v injection of CYT-6091 (5 µg) remained the safest administration method (33.3%). A similar trend was observed with low dose (2 µg) TNF-α, a dose at which peritumoral injection resulted in 25% toxicity, however no toxicity was observed with either intratumoral injection of native TNF-α or i.v. injection of CYT-6091. Comparing the effect of pre-treatment time on toxicity, both 4 hours and 2 hours pre-treatment with TNF-α by peritumoral injection resulted in 25% toxicity, however the 1 hour pre-treatment resulted in no toxicity.

4.4 Discussion

Our data suggests that pre-treatment with TNF-α before visual guided conservative cryosurgery (i.e. freezing to the visible edge of the tumor) significantly enhances the cryodestruction of uterine fibroid in this combinatorial approach, and that timing, mode of delivery and dose are important variables in optimization of the treatment. A minimum four-hour pre-treatment with TNF-α was needed to obtain enhancement of cryosurgical destruction in this approach. Further, our results show that the most effective delivery method for TNF-α, with maximum enhancement and minimum toxicity, was i.v. injection of CYT-6091.

Pre-treatment time of TNF-α plays an important role in determining the enhancement on cryosurgery. It has been demonstrated that TNF-α targets the tumor-associated vasculature by inducing hyperpermeability and destruction of the vascular lining [284], thrombosis [180], host inflammation infiltration [81] and immune response [279], which are also known as critical mechanisms of delayed injury induced by cryotherapy alone. We observed that at least a 4 hours pre-treatment with native TNF-α combined with cryosurgery was required to effectively delay the tumor growth. This could be explained

87

by the fact that the active mechanisms of TNF-α on the endothelium, including the proinflammatory effects, require de novo protein and RNA synthesis and therefore need 2 to 6 hours to reach the maximum effect [81, 196]. Another major effect of TNF-α is a reduction in blood flow, which otherwise would interfere with iceball expansion during cryosurgery [144, 180, 261]. The vasculature has been observed to shutdown drastically at 4 hours and then partially recover from 4 to 16 hours after i.v. injection of native or gold-bound TNF-α [289]. These factors indicate that 1 to 2 hours pre-treatment times are too short to allow the induction of TNF-α mechanism effects that are responsible for cryoinjury enhancement.

As cryosurgery for large tumors and large dose of TNF-α have demonstrated toxicities [110, 246], it is important to carefully evaluate combinatorial treatments where toxicity needs to be avoided while still maintaining treatment efficacy. Compared with systemic administration of CYT-6091, interstitial injection of native TNF-α allows more concentrated delivery to the tumor vasculature or interstitial space, which allows the exposure of local tumor to a higher TNF-α dosage and thus results in more severe tumor damage. Peritumoral injection was found to be more effective than intratumoral injection. This may be due to the fact that peritumoral injection can more effectively target the periphery of the tumor tissue, the area which is not completely destroyed by cryosurgery alone but which has enhanced cryoinjury with TNF-α pre-treatment, whereas intratumoral injection preferentially affects the center of the tumor tissue, which is already effectively destroyed without TNF-α pre-treatment. Although peritumoral injected native TNF-α was shown to be effective as a cryoadjuvant, it remains the most toxic method, possibly due to the fact that multiple injections increase the chance that native TNF-α will enter the blood stream, and thus induce systemic toxicity. However, i.v. injection of CYT-6091 showed the most dramatic tumor growth delay effect when applied with high dose TNF-α (5 μg). Two mechanisms have been identified for the local tumor effect of CYT-6091. First, it has been shown that CYT-6091 avoids detection and clearance by the reticuloendothelial system, and thus results in passive accumulation of

TNF-α within a solid tumor due to leaky tumor vasculature [205]. Second, it is hypothesized that the cytokine (TNF-α) serves as a targeting ligand that preferentially anchors the vector within the tumor [205].

Finally, some toxicity due to TNF-α occurred with each tested delivery route, but not with every dose. We first tested 5 µg of native TNF-α or CYT-6091 followed by cryosurgery after 4 hours pre-treatment. The toxicity increased sequentially, from CYT-6091 i.v. injection (33%), intratumoral native TNF-α injection (40%) to peritumoral native TNF-α injection (100%). This conflicted with our previous studies which showed that 5 µg CYT-6091 led to 0% toxicity in male mice when followed by either hyperthermia or cryosurgery [94, 289]. This result is thought to be due mainly to a gender related difference, since female mice have been found to be more sensitive to TNF-α toxicity than male mice [146, 306]. In addition, for the same absolute dose (5 µg), the effective dose for female mice was generally higher than for male as females are generally 10–20% smaller by weight than male nude mice. Direct systemic injection of native TNF-α followed by cryosurgery was not attempted as it is presumed more toxic than peritumoral (already 100% at 5 µg with cryosurgery) and it is known to be more toxic than CYT-6091 nanoparticle delivery with heat or cold thermal therapy [94, 289]. Finally, only the peritumoral injection of 2 µg was found to be toxic at 2 and 4 hours pre-treatment times. Thus CYT-6091 is the safest delivery method of an effective dose of TNF-α for enhancement of cryosurgical injury in the ELT-3 tumor.
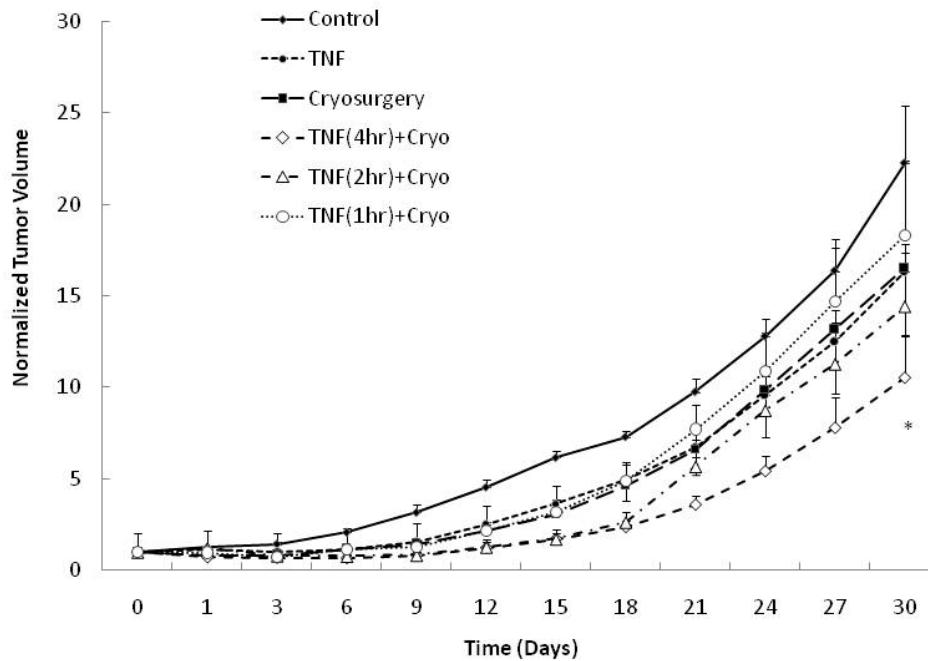
Figure 4-1: Effect of TNF-α pre-treatment on cryoinjury enhancement. Native TNF-α (2 µg) was administered by peritumoral injection, with 1, 2 or 4 hr pre-treatment before cryosurgery. Cryosurgery was performed with a modified 1 mm diameter cryoprobe tip (-120 °C). Injury was assessed by measuring tumor-growth delay after cryosurgery on day 0. Baseline tumor size was measured on day 0; tumor growths in fold-changes in size relative to day 0 are reported. Values presented are the mean ± standard error from 4 independent experiments, and control indicates untreated animals. Only the 4 hr pre-treatment of TNF-α combined with cryosurgery significantly delayed tumor growth compared to cryosurgery alone (*, p<0.05).
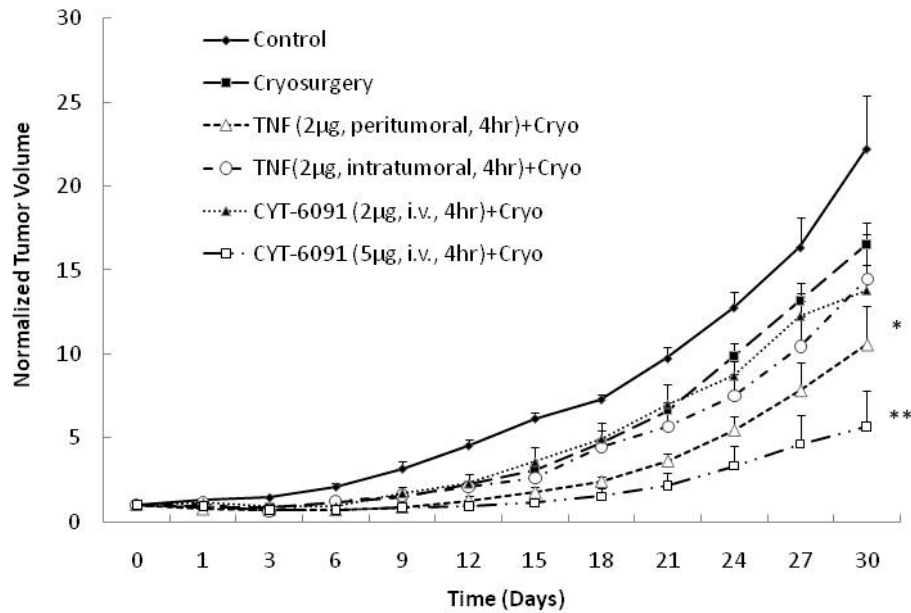
Figure 4-2: Effect of TNF-α dose and delivery mode on cryoinjury enhancement. Native TNF-α (2 µg) was administered locally by either intratumoral injection or peritumoral injection. Nanoparticle bound TNF-α (CYT-6091) (2 µg or 5 µg) was administered systemically by i.v. injection. Cryosurgery was performed with a modified 1mm diameter cryoprobe tip (-120 °C). Injury was assessed by measuring tumor-growth delay after cryosurgery on day 0. Baseline tumor size was measured on day 0; fold-changes in tumor size are reported relative to size at day 0. Values presented are the mean ± standard error from at least 3 independent experiments, and control indicates untreated animals. Either native TNF-α (2 µg, peritumoral, 4 hr) or CYT-6091 (5 µg, i.v., 4 hr) combined with cryosurgery significantly delayed tumor growth compared to cryosurgery alone (*, p<0.05; **, p<0.001).
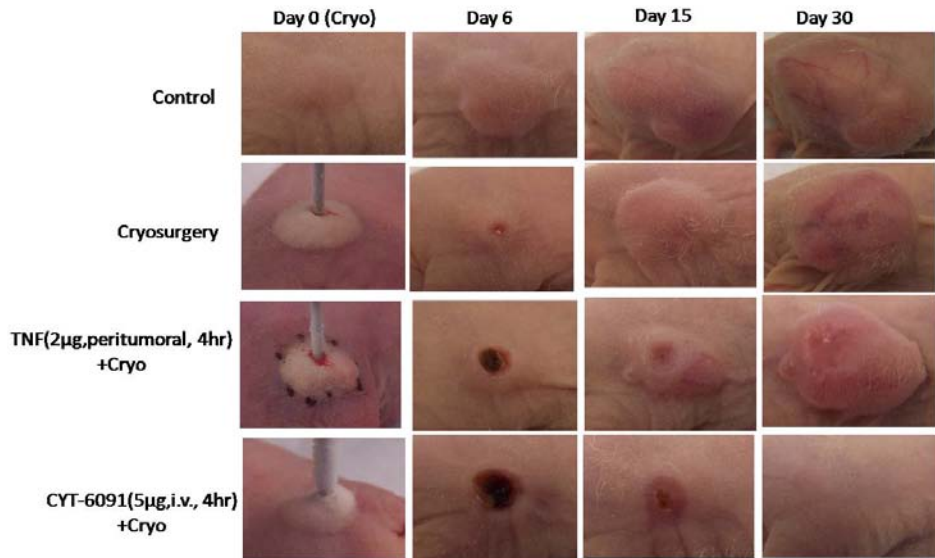
Figure 4-3: Visualization of combinatorial TNF-α cryosurgery treatment outcome. The animals are divided into 4 groups: control (without any treatment), cryosurgery alone, native TNF-α (2 µg, peritumoral, 4 hr pre-treatment) followed by cryosurgery, and CYT-6091 (5 µg, i.v., 4 hr pre-treatment) followed by cryosurgery. A representative animal from each group was imaged immediately after cryosurgery (day 0), and at day 6, 15 and 30 post surgery.
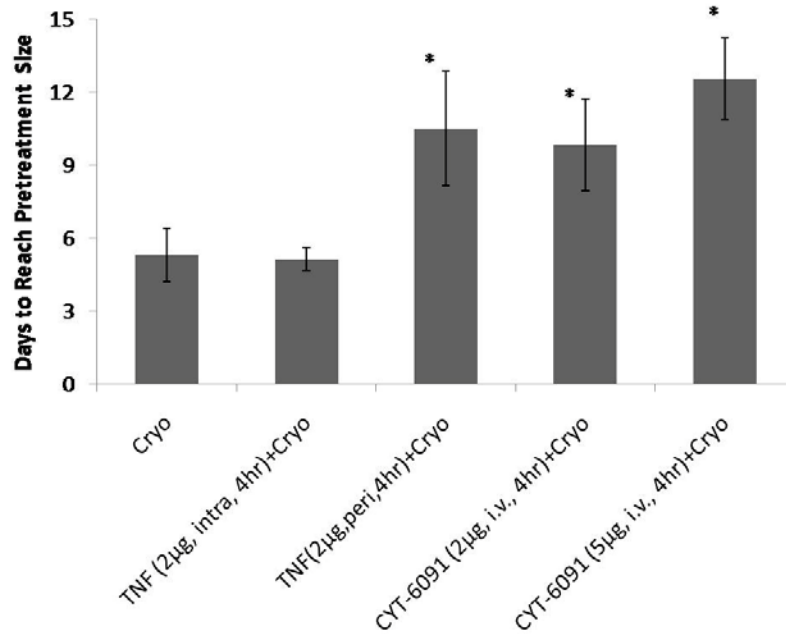
Figure 4-4: The number of days to reach pre-treatment size after combinatorial TNF-α cryosurgical treatment. The animals are divided into 5 groups: cryosurgery alone, native TNF-α (2 µg, intratumoral and peritumoral, 4 hr pre-treatment) and CYT-6091 (2 µg and 5 µg, i.v., 4 hr pre-treatment) followed by cryosurgery. Values presented are the mean ± standard error from at least 4 independent experiments. Early growth was significantly delayed by pre-treatment with 2 µg of peritumoral injected TNF-α, 2 µg and 5 µg of i.v. injected CYT-6091 followed by cryosurgery compared with cryosurgery alone (*, $p < 0.05$).
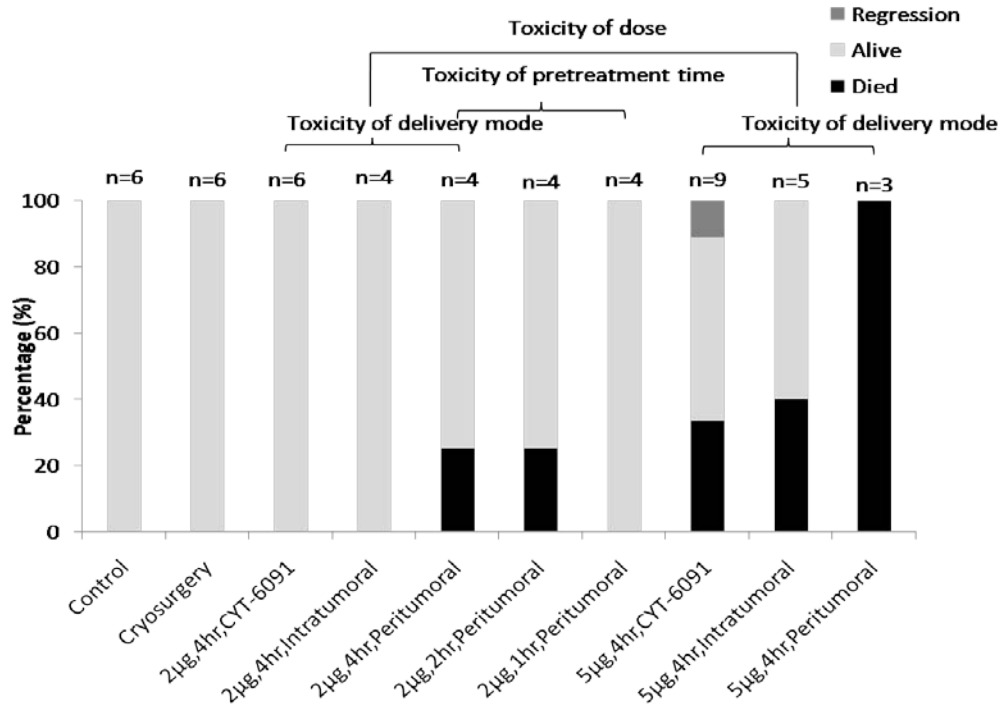
Figure 4-5: Toxicity after cryoadjuvant treatments. Toxicity is shown by the percentage of animals that died post cryosurgery. N denotes the total animal number used in each group.

Chapter 5 Research Summary

5.1 Summary

Prostate cancer is the second leading cause of cancer-related deaths among males in the United States of America with about 218,890 new cases and 27,050 prostate cancer-related deaths expected for 2007. While surgery is the gold standard in the treatment of prostate cancer [292], there is an increasing awareness and need for minimally and non-invasive local techniques such as cryosurgery for poor surgical candidates, or patients with high-grade local disease [176, 190]. The major limitation of cryosurgery is disease recurrence and eventual death in the projected 15,000 patients who are treated with this technology annually in the US [127, 128]. The most comprehensive cryosurgical patient outcome data (COLD Registry) shows that roughly 50% of patients whose high-grade disease is treated by cryosurgery will experience recurrence within 5 years [127, 128]. The major technical problems with cryosurgery that can affect recurrence are: (1) the inability to direct the placement of probes to sites of cancer within the prostate, and (2) the inability to connect the iceball that forms around the probes with the ultimate destruction of the cancer. As a consequence, regions of cancerous tissues will be incompletely destroyed and avoidable complications that reduce the patient's quality of life can result (i.e. rectal and urethral fistulas, incontinence and impotence [127, 128].

In recent years a new research thrust has emerged in cryosurgery that focuses on manipulating and enhancing the biologic response of tissues to cryodestruction [15, 33, 94, 191, 281]. Work in this area has identified adjuvants that typically work through the following mechanisms: 1) thermophysical adjuvants which enhance the injury caused by ice, 2) chemotherapeutic approaches that act at the molecular level or induce apoptosis, 3) cytokines or vascular based agents that modulate the inflammatory response, and 4) immunomodulators that stimulate immune cells to enhance tissue destruction. In this Ph.D work, we have shown that TNF-α, a vascular based agent has the ability to achieve a kill-zone up to the imaged iceball edge in preclinical models. Our work for the first

time demonstrated that the recruitment of a host mediated inflammatory infiltrate at the periphery of the iceball induces enhanced vascular injury thereby extending the cryolesion after freezing injury. This inflammatory infiltrate is mainly mediated by NF-κB inflammation pathway activation. This not only complements the current vascular injury theory that has been well recognized in the field of cryobiology, but also indicates a "host mediated" response over a pure "local" response induced by cryosurgery. The host-local interaction, specifically leukocyte-endothelium interaction, was found to be the main mechanism by which cryosurgery induces delayed tumor destruction, and by which TNF-α enhances cryosurgery. In addition to Fig. 3-4, further evidence for this theory can be found by a VCAM inhibition study (Appendix II) that uses antibody blocking to inhibit leukocyte-endothelial interactions prior to cryosurgery. As expected when these interactions were inhibited the use of TNF-α did not augment the cryosurgical lesion thus again pointing to the importance of the inflammatory infiltrate and it's interaction with the endothelium to enhance cryosurgical injury.

The concept of vascular "pre-conditioning" of tumors prior to cryosurgery has been proposed in this work for the first time. This concept, supported by the data in this dissertation and from our lab, suggests an important link between establishing a pre-conditioning inflammatory process by TNF-α and enhancement of cryosurgical tumor destruction. We believe this approach highlights a tremendous opportunity for new combinatorial approaches using vascular and immunologically active adjuvants with local cancer therapy in general and cryosurgery in particular. Though TNF-α is one of the most potent antitumor cytokines, toxicity in its native form have prevented its systemic administration at therapeutically effective doses. Therefore, improvements in pre-conditioning with local TNF-α delivery will be a continued challenge in this area. One attractive approach to solve this delivery problem is to use a nanoparticle carrier.

To reduce toxicity and increase specific tumor loading, we have investigated a gold nanoparticle conjugated with TNF-α (CYT-6091 – CytImmune, Rockville, MD) for pre-conditioning in several preclinical models, including leiomyoma tumor model (Chapter

4). Systemic injection of CYT-6091 4 hours prior to cryosurgery of tumors grown in nude mice resulted in significant tumor growth delay and in some cases complete remission compared to mice injected with an equivalent dose of native TNF-α or the control nanoparticle without TNF-α [93, 124]. Furthermore, mice administered with CYT-6091 displayed no overt toxicity whereas nearly 25% of mice injected with native TNF-α prior to cryosurgery died within several hours after the therapy. Importantly, our results show that nanoparticle pre-conditioning with 5 µg TNF-α delivered by CYT-6091 results in 100% of the tumor within the iceball being destroyed (i.e. an overlap between the edge of the iceball and the edge of tumor destruction), whereas less than 40% of the tumor within the iceball was effectively treated without pre-conditioning, and a high percentage of animals died of TNF-α administered in native form [93]. This CYT-6091 for enhancement of cryoinjury is dose dependant [93, 124]. In a pilot translational study using VX2 tumors grown in rabbit kidneys, we obtained a significant decrease in the rate of peritoneal carcinomatosis (metastases) in animals treated with cryosurgery and CYT-6091 compared to cryosurgery alone [144]. This was an unexpected finding and further investigations are underway in preclinical tumor models to interpret whether this was a direct effect on mechanisms of tumor spread or a stimulation of tumor immunity. CYT-6091 has already completed a Phase I clinical trial as a standalone anticancer therapeutic [161]. The significant findings of the trial include lack of dose limiting toxicities or drug related serious adverse events, even at a high dose of 600 µg TNF-α/m^2. In addition, an absence of a systemic hypotensive response was observed, a major limiting factor that has restricted the use of native TNF-α in the clinical setting to an isolated limb perfusion treatment of high-grade sarcomas and melanomas [284]. In addition, we are in discussions with our clinical colleagues about a possible clinical trial using CYT-6091 and cryosurgery on high grade localized prostate cancer (Personal communication Dr. Joel Slaton, Head of Research Department of Urology, UM).

5.2 Future Work

While our results show a compelling enhancement of cryosurgical injury using TNF-α or CYT-6091 there remain several challenges at the basic science level to effective translation and use of these results. Specifically further work in two main areas are envisioned: 1) continued investigation into mechanisms of TNF-α (or other adjuvants) in providing enhanced cryosurgery, and translation of this to long term clinical outcomes, and 2) the use of multifunctional nanoparticles to deliver these agents to effectively pre-condition the tissue and target the prostate cancer.

5.2.1 Mechanisms of TNF-α Pre-conditioning

Our work shows that the inflammatory infiltrate is the main mechanism by which TNF-α enhances cryosurgery, however, it is unclear if the role of TNF-α in cryosurgical enhancement ends here, and if other cellular and molecular mechanisms could be activated by TNF-α to play a critical role in cryosurgical enhancement. For instance, other than short term (day 1 to 7) tumor ablation investigated in this work, it's still unclear if TNF-α could impact the mechanisms linked to the long term clinical outcomes (local recurrence, metastasis, survival) of cryosurgery. Therefore, the future work to better understand the mechanisms of TNF-α pre-conditioning will be required and will include the following aspects: 1) systemic activation of leukocytes by TNF-α, 2) hypercoagulability in tumor vasculature induced by TNF-α, 3) cryo-immunologic response and cryoinjury enhancement by TNF-α and 4) demonstration of pre-conditioning with cryosurgery on an clinically relevant model of prostate cancer.

Systemic Activation of Leukocytes by TNF-α

We have demonstrated that the inflammatory infiltrate was significantly enhanced by TNF-α, and that local expression of adhesion molecules (VCAM) regulated by NF-κB

pathway within tumor vasculature is highly responsible for inflammatory infiltrate recruitment (Appexdix II). However, the degree to which TNF-α activation of circulating leukocytes is responsible for the enhancement of the cryosurgical injury is still unclear. It is hypothesized that TNF-α mediated enhancement of cryosurgery is dependent on systemic leukocyte activation and their interaction with tumor microvasculature [249]. In addition, although neutrophils are mainly studied in this work, macrophages are also observed to present in the inflammation band and play a critical role in phagocytosis of tumor debris especially at longer time points beyond 3 – 5 days [113, 179]. Macrophages as professional antigen presenting cells, may also initiate the early immune response, by secreting cytokines such as IL-1 and TNF-α, that attract and activate T cells, leading to infiltration of T cells [290]. Therefore, it is also worth determining the importance of specific leukocyte populations (neutrophils vs. macrophages) and their roles in TNF-α enhancement of prostate cryosurgery. Importantly, the bulk of our work thus far has been performed with a nude mouse host. To fully explore the role of T cells we will need to change to an immune competent host and new tumor model (See discussion below).

Hypercoagulability in Tumor Vasculature Induced by TNF-α

Microvascular shutdown due to thrombus formation and subsequent tissue ischemia is a well established mechanism of tissue injury following cryosurgery. We have shown that the microvascular stasis region that develops after cryosurgery (in the DSFC model) closely overlaps the region of histologically-assessed normal and tumor tissue cell death [94]. However, the exact role of pre-administration of TNF-α in enhancing the coagulation processes that lead to enhancement of cryosurgical injury is still unknown. We have demonstrated that NF-κB is the dominant molecular mechanism in TNF-α cryosurgical enhancement. NF-κB is known to regulate both inflammation (the pre-condition) for cryoinjury enhancement and thrombosis (the causal event in tumor killing). Therefore, further investigation of the relative relationship between inflammation and thrombosis and their relative importance in this treatment environment is critical to the understanding and optimization of TNF-α enhanced cryosurgery. Additionally,

neutrophils, monocytes and endothelial cells are known to play a role in the coagulation cascade through the modulation of blood levels of molecules that are part of the coagulation pathway (e.g. tissue factor, activated protein C) and activation of the endothelium following interaction via cell adhesion molecules [61]. TNF-α is known to activate these cell types, however, the specific impact of this TNF-α activation on the enhancement of coagulation processes that lead to enhancement of cryosurgical injury has never been studied. It is hypothesized that TNF-α enhanced cryoinjury by hypercoagulability in tumor microvasculature is predominantly tissue factor dependent.

Cryo-immunologic Response and Cryoinjury Enhancement by TNF-α

The "host mediated" inflammatory response induced by TNF-α is both vascular as explored above as well as immunological due to the participation of immune cells. The cryo-immunological mechanism is thought to be responsible for the long-term clinical outcome of cryosurgery, for instance, such as reduced local recurrence, metastatic foci regression and increased host survival [101, 117, 260, 266, 272]. Unfortunately, cryo-immunology is poorly understood and/or measurable after cryosurgery alone [235]. Nevertheless, if TNF-α could enhance the immunological response, making it more reproducible and measurable, there is a strong possibility that the mechanism could then be harnessed to improve clinical outcomes post cryosurgery. Recent studies have shown that TNF-α promotes the maturation of dendritic cells *in vivo* and their migration to draining lymph nodes [228], and in some cases, triggers the generation of a specific T cell-based immune response [13], and fosters long-lasting protective immunity [270, 312]. Some clinical studies have documented that patients with higher pre-treatment TNF-α levels have more significant rise in TNF-α and Th1/Th2 ratio after cryosurgery. Joosten et al. showed significant inhibition of secondary tumor growth with cryosurgery in colon 26 tumors in Balb/c mice correlated with high plasma level of TNF-α and IL-1α [130]. Thus, there exists an opportunity to use immunological pre-conditioning of the tumor by TNF-α which could enhance the immunostimulatory properties of cryosurgery to the point of generating a therapeutic immune response against tumors.

Clinically Relevant Model of Prostate Cancer

Until now, our work has been conducted primarily with a non-metastatic human prostate cancer cell lines grown subcutaneously in an immune compromised nude mouse. A model using cells capable of metastasizing in immunocompetent mice will more closely reflect the human situation and improve clinical application of cryoadjuvants. In particular, more work is needed using poorly differentiated metastatic prostate tumors since, in human, adjuvant enhanced cryosurgery will likely have its greatest and most immediate impact in patients with high grade tumors with significant probability for local failure (recurrence) and/or metastasis. Therefore, studies of adjuvant-enhanced cryosurgery need to be extended to: (1) an immunocompetent model and (2) poorly differentiated metastatic prostate cancer models.

One of the best characterized and widely used mouse models of prostate cancer is the TRAMP model. It targets the prostate epithelium using a tissue-specific probasin (PB) promoter that drives the expression of SV40 T antigen (Tg), and leads to progressive disease from epithelial hyperplasia to prostatic intraepithelial neoplasia (PIN) and adenocarcinoma with both local and disseminated disease [89, 121]. The versatility of the TRAMP model has been extended further by the establishment of several TRAMP-derived prostate tumor cell lines (including TRAMP-C2) that can be injected into the syngeneic male C57BL/6 host to induce ectopic prostate tumorigenesis [72]. TRAMP-C2 cells metastasize to regional lymph nodes and other organs following an interval of chronic primary tumor growth. Following primary tumor resection in this model, metastatic recurrence occurs at a high rate (i.e., >95% of mice) and in a predictable pattern [154]. Metastatic recurrence in this model emanates from the outgrowth of established nodal micrometastases that are present at the time of primary tumor resection. Hence, metastatic disease progression is not a consequence of seeding. Furthermore, this model mimics the clinical paradigm in which distant metastases represent the direst

consequence of surgical treatment failure. Because of these attributes, this model readily lends itself to the testing of adjuvant therapies for their ability to eliminate poorly differentiated metastatic prostate cancer in immunocompetent host.

5.2.2 Multi -functional Nanoparticle Pre-conditioning

We have shown the ability to use CYT-6091, a gold nanoparticle tagged with TNF-α, to pre-condition the tumor vasculature for enhancement of thermal (heat and cold) therapies without toxicity [205]. For CYT-6091, receptor targeting is facilitated since TNF-α acts as both the ligand and the therapeutic. The drug is manufactured by covalently linking molecules of TNF-α and thiolated polyethylene glycol (PEG-THIOL) onto the surface of the colloidal gold particles. Each component of the multivalent drug serves a specific function to facilitate tumor specific drug delivery. The PEG-THIOL moiety serves to hydrate the colloidal gold nanoparticles and in doing so, shields the nanoparticle drug from detection and clearance by the RES. Thus the rationale behind attaching the cytokine to a nanoparticle (CYT-6091) is to reduce systemic toxicity and improve the localization of TNF-α to the tumor tissue. Future work in this area may seek to improve local delivery (i.e. pre-conditioning) and reduce systemic toxicity by selecting other pre-conditioning agents with less toxicity and even further by using specific targeting agents to prostate or other tumors [50, 102, 309] (See below).

Selection of Pre-conditioning Agent

We chose TNF-α as the pre-conditioning agent/biomolecule due to its well-established mechanism of action against the tumor vasculature, potential for sensitizing tumor cells to thermal injury, potential for eliciting an antitumor immune response, and documented clinical success in solid tumor therapy (although currently limited in scope). *In vitro* studies conducted by our group have shown that pre-treatment with native TNF-α sensitizes various tumor cell lines to thermal (heat and cold) injury [125, 287, 288]; however, the effect is more pronounced in microvascular endothelial cells. This suggests that even though direct cytotoxicity of tumor cells may be enhanced following thermal

therapy the primary mechanism of pre-conditioning by TNF-α plays out within the tumor vasculature. Therefore, other vascular agents with improved efficacy and less toxicity could be designed as pre-conditioning agents as shown in Table (5-1).

Prostate Cancer Targeting

There are a growing number of targeting ligands available that can be used on prostate cancer including: fibronectin-mimetic peptides (PR_b) [50], antisense oligonucleotides (ASO) against specific molecular targets (e.g., Bcl-2 and Raf-1) [309], transferrin receptor and folate receptor [102], HER-2 receptor [152] and EGFR [143], FGF and FGRF aptamers [135]. However, these ligands are not specific to prostate cancer and many are relatively new and untested including peptides selected from phage that do specifically target the prostate [274]. Of the potential prostate specific targeting ligands, prostate-specific antigen (PSA), prostatic acid phosphatase (PAP), and prostate-specific membrane antigen (PSMA), are the most studied immunologic targets in the prostate [67]. The PSMA antibody (Ab) in particular, is one of the most mature as it targets prostate cancer and endothelial cells in angiogenic vessels of prostate cancer [27] and has been used successfully to target prostate cancer in the past [82]. It is plausible that coating of gold nanoparticles with one or more of these prostate specific ligands would improve active targeting of the nanoparticless to the prostate tumor. Additionally, passive targeting can be improved by testing various sizes of PEGylated gold nanoparticles (20 – 100 nm) by methods similar to those already performed by Perrault for breast cancer *in vivo* [213].

5.3 Conclusion

Overall, the concept of pre-conditioning the tumor microenvironment using adjuvant coated targeted nanoparticles opens up several avenues for basic science research in the field of thermal therapies in general and cryosurgery in particular. With the potential for

both vascular and immunological pre-conditioning of the tumor microenvironment, a collaborative research effort between cancer biologists, nanotechnology researchers and cryotherapy interest groups is essential to identify and exploit specific targets in the tumor microenvironment that are amenable to pre-conditioning. Some of the key challenges for researchers in the field are: selection of the appropriate nanoparticle and pre-conditioning agent for the specific tumor type; demonstration of safety and efficacy, timing of the nanoparticle administration prior to thermal therapy; and effective targeting of nanoparticle in prostate and other tumors. With the multitude of ongoing research projects in nanomedicine approaches for cancer therapy, it may be feasible to design multifunctional nanoparticles that incorporate several features – pre-treatment planning, selective delivery to tumor, absence of systemic toxicity, appropriate pre-conditioning agent, improved imaging contrast – to aid in the enhancement of thermal therapies with the ultimate goal of reducing local recurrence and distant metastases and reducing morbidity in patients. The need for basic science research notwithstanding, Phase I clinical trials based on the nanoparticle pre-conditioning concept may be initiated in the near future using standalone nanoparticle therapeutics already approved by the FDA for cancer treatments. There are many types of cancer in great need of better options after standards of care have failed and nanomedicine is poised to fill this gap with the able assistance of cryotherapy.

Table 5-1: Vascular agents from clinical trial (by Raghav Goel, unpublished)

Family	Possible Agents (From Clinical Trials)	Suggested Timing
COAGULANTS	Thrombin Fibrinogen Arginine Vasopressin	Before/After Cryosurgery
VASOCONSTRICTERS	Naphazoline Phenylephrine Phenylpropanolamine Oxymetazoline	Before/After Cryosurgery
OXIDATIVE STRESSERS	Tamoxifen Transition Metals Anticancer Drugs	Before/After Cryosurgery
VASCULAR AGENTS	ATO MN-029 DMXAA	Before Cryosurgery
ACID / BASE	ACETIC ACIC NaOH	Before / After Cryosurgery
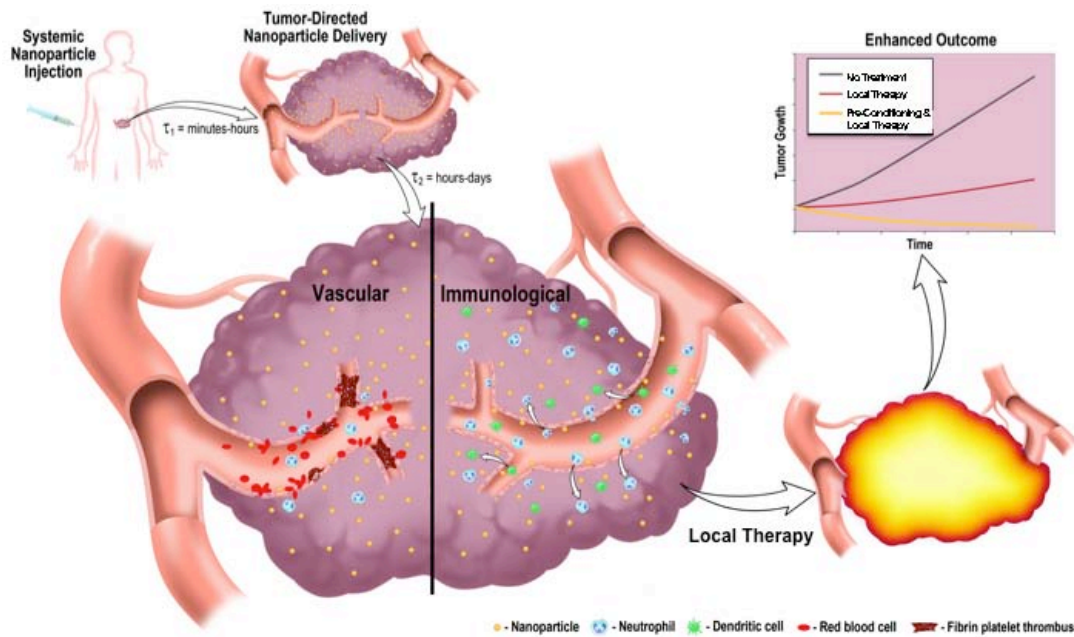
Figure 5-1: Nanoparticle pre-conditioning of tumor [252]. Illustration of the concept of pre-conditioning the tumor using a bio-conjugated nanoparticle prior to thermal therapy for achieving enhanced tumor destruction. Systemic injection of the nanoparticle leads to its accumulation in the tumor within a short timeframe (minutes-hours). Localization of the nanoparticle within the tumor initiates vascular and immunological pre-conditioning events (detailed in text) that reach peak response in a longer timeframe (hours-days). Thermal therapy (heat or cold) is then administered at an optimal time based on nanoparticle pre-conditioning to achieve superior tumor destruction over thermal therapy alone.

References

[1] National Cancer Institute

<http://www.cancer.gov/cancertopics/factsheet/Therapy/cryosurgery>.

[2] J.L. Abbruzzese, B. Levin, J.A. Ajani, J.S. Faintuch, R. Pazdur, S. Saks, C. Edwards, J.U. Gutterman, A phase II trial of recombinant human interferon-gamma and recombinant tumor necrosis factor in patients with advanced gastrointestinal malignancies: results of a trial terminated by excessive toxicity, J Biol Response Mod 1990 (9) 522-7.

[3] R.J. Ablin, M.J. Gonder, W.A. Soanes, Elution of cell-bound anti-prostatic epithelial antibodies after multiple cryotherapy of carcinoma of the prostate, Cryobiology 1974 (11) 218-21.

[4] J. Adams-Ray, S. Bellman, Vascular reactions after experimental cold injury; a microangiographic study of rabbit ears, Angiology 1956 (7) 339-67.

[5] G. Adanali, K. Ozer, M. Siemionow, Early and late effects of ischemic preconditioning on microcirculation of skeletal muscle flaps, Plastic and reconstructive surgery 2002 (109) 1344-51.

[6] G. Aliev, E. Ragazzi, M.A. Smith, A. Mironov, G. Perry, Morphological features of regeneration of rabbit aortic endothelium after cryoinduced vascular damage, J Submicrosc Cytol Pathol 1999 (31) 495-502.

[7] J. Arnott, Practical illustrations of the remedial efficacy of a very low or anaesthetic temperature. I. In cancer., Lancet 1850 (2) 257-9.

[8] G. Aus, Current status of HIFU and cryotherapy in prostate cancer--a review, Eur Urol 2006 (50) 927-34; discussion 34.

[9] G. Aus, Cryosurgery for prostate cancer, J Urol 2008 (180) 1882-3.

[10] B. Avitall, D. Lafontaine, G. Rozmus, N. Adoni, A. Dehnee, A. Urbonas, K.M. Le, D. Aleksonis, Ablation of atrial-ventricular junction tissues via the coronary sinus using cryo balloon technology, J Interv Card Electrophysiol 2005 (12) 203-11.

[11] P.A. Baeuerle, V.R. Baichwal, NF-kappa B as a frequent target for immunosuppressive and anti-inflammatory molecules, Adv Immunol 1997 (65) 111-37.

[12] R. Baissalov, G.A. Sandison, B.J. Donnelly, J.C. Saliken, J.G. McKinnon, K. Muldrew, J.C. Rewcastle, A semi-empirical treatment planning model for optimization of multiprobe cryosurgery, Phys Med Biol 2000 (45) 1085-98.

[13] E. Balza, L. Mortara, F. Sassi, S. Monteghirfo, B. Carnemolla, P. Castellani, D. Neri, R.S. Accolla, L. Zardi, L. Borsi, Targeted delivery of tumor necrosis factor-alpha to tumor vessels induces a therapeutic T cell-mediated immune response that protects the host against syngeneic tumors of different histologic origin, Clin Cancer Res 2006 (12) 2575-82.

[14] J.H. Barker, Bartlett, R., Funk, W., Hammersen, F., and Messmer, K., The effect of superoxide dismutase on the skin mircrocirculation after ischemia and reperfusion, Prog Appl Microcirc 1987 (12) 276-81.

[15] I.D. Bassukas, C. Gamvroulia, A. Zioga, K. Nomikos, C. Fotika, Cryosurgery during topical imiquimod: a successful combination modality for lentigo maligna, Int J Dermatol 2008 (47) 519-21.

[16] J.M. Baust, B. Van, J.G. Baust, Cell viability improves following inhibition of cryopreservation-induced apoptosis, In Vitro Cell Dev Biol Anim 2000 (36) 262-70.

[17] J.D. Belcher, P.H. Marker, J.P. Weber, R.P. Hebbel, G.M. Vercellotti, Activated monocytes in sickle cell disease: potential role in the activation of vascular endothelium and vaso-occlusion, Blood 2000 (96) 2451-9.

[18] B. Berman, M.H. Viera, S. Amini, R. Huo, I.S. Jones, Prevention and management of hypertrophic scars and keloids after burns in children, J Craniofac Surg 2008 (19) 989-1006.

[19] M.S. Berrada, J.C. Bischof, Evaluation of freezing effects on human microvascular-endothelial cells (HMEC), Cryo Letters 2001 (22) 353-66.

[20] G. Biasco, E. Derenzini, G. Grazi, G. Ercolani, M. Ravaioli, M.A. Pantaleo, G. Brandi, Treatment of hepatic metastases from colorectal cancer: many doubts, some certainties, Cancer Treat Rev 2006 (32) 214-28.

[21] J. Bischof, W. Fahssi, D. Smith, T. Nagel, D. Swanlund, A parametric study of freezing injury in ELT-3 uterine leiomyoma tumour cells, Hum Reprod 2001 (16) 340-8.

[22] T. Blankenstein, Z.H. Qin, K. Uberla, W. Muller, H. Rosen, H.D. Volk, T. Diamantstein, Tumor suppression after tumor cell-targeted tumor necrosis factor alpha gene transfer, J Exp Med 1991 (173) 1047-52.

[23] T.D. Brown, P. Goodman, T. Fleming, J.S. Macdonald, E.M. Hersh, T.J. Braun, A phase II trial of recombinant tumor necrosis factor in patients with adenocarcinoma of the pancreas: a Southwest Oncology Group study, J Immunother (1991) 1991 (10) 376-8.

[24] H.M. Carpenter, L.A. Hurley, E. Hardenbergh, R.B. Williams, Vascular injury due to cold. Affects of rapid rewarming, Arch Pathol 1971 (92) 153-61.

[25] E.A. Carswell, L.J. Old, R.L. Kassel, S. Green, N. Fiore, B. Williamson, An endotoxin-induced serum factor that causes necrosis of tumors, Proc Natl Acad Sci U S A 1975 (72) 3666-70.

[26] R.I. Ceilley, J.Q. Del Rosso, Current modalities and new advances in the treatment of basal cell carcinoma, Int J Dermatol 2006 (45) 489-98.

[27] S.S. Chang, V.E. Reuter, W.D. Heston, P.B. Gaudin, Comparison of anti-prostate-specific membrane antigen antibodies and other immunomarkers in metastatic prostate carcinoma, Urology 2001 (57) 1179-83.

[28] B.H. Chao, X. He, J.C. Bischof, Pre-treatment inflammation induced by TNF-alpha augments cryosurgical injury on human prostate cancer, Cryobiology 2004 (49) 10-27.

[29] D. Chauvier, S. Ankri, C. Charriaut-Marlangue, R. Casimir, E. Jacotot, Broad-spectrum caspase inhibitors: from myth to reality?, Cell death and differentiation 2007 (14) 387-91.

[30] T.D. Chung, H.J. Mauceri, D.E. Hallahan, J.J. Yu, S. Chung, W.L. Grdina, S. Yajnik, D.W. Kufe, R.R. Weichselbaum, Tumor necrosis factor-alpha-based gene therapy enhances radiation cytotoxicity in human prostate cancer, Cancer Gene Ther 1998 (5) 344-9.

[31] A. Ciavattini, D. Tsiroglou, P. Litta, M. Vichi, A.L. Tranquilli, Pregnancy outcome after laparoscopic cryomyolysis of uterine myomas: report of nine cases, J Minim Invasive Gynecol 2006 (13) 141-4.

[32] D.M. Clarke, J.M. Baust, R.G. Van Buskirk, J.G. Baust, Chemo-cryo combination therapy: an adjunctive model for the treatment of prostate cancer, Cryobiology 2001 (42) 274-85.

[33] D.M. Clarke, J.M. Baust, R.G. Van Buskirk, J.G. Baust, Addition of anticancer agents enhances freezing-induced prostate cancer cell death: implications of mitochondrial involvement, Cryobiology 2004 (49) 45-61.

[34] D.M. Clarke, A.T. Robilotto, R.G. VanBuskirk, J.G. Baust, A.A. Gage, J.M. Baust, Targeted induction of apoptosis via TRAIL and cryoablation: a novel strategy for the treatment of prostate cancer, Prostate Cancer Prostatic Dis 2007 (10) 175-84.

[35] R. Clynes, Y. Takechi, Y. Moroi, A. Houghton, J.V. Ravetch, Fc receptors are required in passive and active immunity to melanoma, Proc Natl Acad Sci U S A 1998 (95) 652-6.

[36] T. Collins, M.A. Read, A.S. Neish, M.Z. Whitley, D. Thanos, T. Maniatis, Transcriptional regulation of endothelial cell adhesion molecules: NF-kappa B and cytokine-inducible enhancers, FASEB J 1995 (9) 899-909.

[37] I.S. Cooper, Cryogenic surgery: a new method of destruction or extirpation of benign or malignant tissues, N Engl J Med 1963 (268) 743-9.

[38] I.S. Cooper, Cryobiology as Viewed by the Surgeon, Cryobiology 1964 (51) 44-51.

[39] I.S. Cooper, Cryogenic Surgery for Cancer, Fed Proc 1965 (24) S237-40.

[40] I.S. Copper, Cryogenic surgery: a new method of destruction or extirpation of benign or malignant tissues, N Engl J Med 1963 (268) 743-9.

[41] L.M. Coussens, Z. Werb, Inflammation and cancer, Nature 2002 (420) 860-7.

[42] B.D. Cowan, P.E. Sewell, J.C. Howard, R.M. Arriola, L.G. Robinette, Interventional magnetic resonance imaging cryotherapy of uterine fibroid tumors: preliminary observation, Am J Obstet Gynecol 2002 (186) 1183-7.

[43] E.T. Creagan, J.S. Kovach, C.G. Moertel, S. Frytak, L.K. Kvols, A phase I clinical trial of recombinant human tumor necrosis factor, Cancer 1988 (62) 2467-71.

[44] P.E. Davol, B.R. Fulmer, D.B. Rukstalis, Long-term results of cryoablation for renal cancer and complex renal masses, Urology 2006 (68) 2-6.

[45] S. de Kossodo, R. Moore, S. Gschmeissner, N. East, C. Upton, F.R. Balkwill, Changes in endogenous cytokines, adhesion molecules and platelets during cytokine-induced tumour necrosis, Br J Cancer 1995 (72) 1165-72.

[46] I.J. De Vries, D.J. Krooshoop, N.M. Scharenborg, W.J. Lesterhuis, J.H. Diepstra, G.N. Van Muijen, S.P. Strijk, T.J. Ruers, O.C. Boerman, W.J. Oyen, G.J. Adema, C.J. Punt, C.G. Figdor, Effective migration of antigen-pulsed dendritic cells to lymph nodes in melanoma patients is determined by their maturation state, Cancer Res 2003 (63) 12-7.

[47] L.A. Deane, R.V. Clayman, Review of minimally invasive renal therapies: Needle-based and extracorporeal, Urology 2006 (68) 26-37.

[48] R.J. Debs, N. Duzgunes, E.N. Brunette, B. Fendly, J. Patton, R. Philip, Liposome-associated tumor necrosis factor retains bioactivity in the presence of neutralizing anti-tumor necrosis factor antibodies, J Immunol 1989 (143) 1192-7.

[49] S. Demaria, N. Bhardwaj, W.H. McBride, S.C. Formenti, Combining radiotherapy and immunotherapy: a revived partnership, Int J Radiat Oncol Biol Phys 2005 (63) 655-66.

[50] D. Demirgoz, A. Garg, E. Kokkoli, PR_b-targeted PEGylated liposomes for prostate cancer therapy, Langmuir 2008 (24) 13518-24.

[51] M.H. den Brok, R.P. Sutmuller, S. Nierkens, E.J. Bennink, L.W. Toonen, C.G. Figdor, T.J. Ruers, G.J. Adema, Synergy between in situ cryoablation and TLR9 stimulation results in a highly effective in vivo dendritic cell vaccine, Cancer Res 2006 (66) 7285-92.

[52] E. Derenzini, M. Di Battista, M.C. Di Marco, S. Dell'Arte, M. Astorino, S. Bertolini, G. Brandi, G. Biasco, [Treatment of colorectal cancer liver metastases], Minerva Med 2006 (97) 107-19.

[53] T.G. Diacovo, M.D. Catalina, M.H. Siegelman, U.H. von Andrian, Circulating activated platelets reconstitute lymphocyte homing and immunity in L-selectin-deficient mice, J Exp Med 1998 (187) 197-204.

[54] I. Ding, J.Z. Sun, B. Fenton, W.M. Liu, P. Kimsely, P. Okunieff, W. Min, Intratumoral administration of endostatin plasmid inhibits vascular growth and perfusion in MCa-4 murine mammary carcinomas, Cancer Res 2001 (61) 526-31.

[55] A.E. Dirkx, M.G. Oude Egbrink, M.J. Kuijpers, S.T. van der Niet, V.V. Heijnen, J.C. Bouma-ter Steege, J. Wagstaff, A.W. Griffioen, Tumor angiogenesis modulates leukocyte-vessel wall interactions in vivo by reducing endothelial adhesion molecule expression, Cancer Res 2003 (63) 2322-9.

[56] X. Dolcet, D. Llobet, J. Pallares, X. Matias-Guiu, NF-kB in development and progression of human cancer, Virchows Arch 2005 (446) 475-82.

[57] T. Eberl, A. Amberger, M. Herold, P. Hengster, W. Steurer, B.W. Hochleitner, E. Gnaiger, R. Margreiter, Expression of stress proteins, adhesion molecules, and interleukin-8 in endothelial cells after preservation and reoxygenation, Cryobiology 1999 (38) 106-18.

[58] A.M. Eggermont, H. Schraffordt Koops, J.M. Klausner, B.B. Kroon, P.M. Schlag, D. Lienard, A.N. van Geel, H.J. Hoekstra, I. Meller, O.E. Nieweg, C. Kettelhack, G. Ben-Ari, J.C. Pector, F.J. Lejeune, Isolated limb perfusion with tumor necrosis factor and melphalan for limb salvage in 186 patients with locally advanced soft tissue extremity sarcomas. The cumulative multicenter European experience, Ann Surg 1996 (224) 756-64; discussion 64-5.

[59] S.A. Eming, T. Krieg, J.M. Davidson, Inflammation in wound repair: molecular and cellular mechanisms, J Invest Dermatol 2007 (127) 514-25.

[60] M.J. Eppihimer, D.N. Granger, Ischemia/reperfusion-induced leukocyte-endothelial interactions in postcapillary venules, Shock 1997 (8) 16-25.

[61] C.T. Esmon, The impact of the inflammatory response on coagulation, Thrombosis research 2004 (114) 321-7.

[62] C. Exacoustos, E. Zupi, D. Marconi, M.E. Romanini, B. Szabolcs, A. Piredda, D. Arduini, Ultrasound-assisted laparoscopic cryomyolysis: two- and three-dimensional findings before, during and after treatment, Ultrasound Obstet Gynecol 2005 (25) 393-400.

[63] V.A. Fadok, D.L. Bratton, A. Konowal, P.W. Freed, J.Y. Westcott, P.M. Henson, Macrophages that have ingested apoptotic cells in vitro inhibit proinflammatory cytokine production through autocrine/paracrine mechanisms involving TGF-beta, PGE2, and PAF, J Clin Invest 1998 (101) 890-8.

[64] W. Fiedler, W. Zeller, C.J. Peimann, H.J. Weh, D.K. Hossfeld, A phase II combination trial with recombinant human tumor necrosis factor and gamma interferon in patients with colorectal cancer, Klin Wochenschr 1991 (69) 261-8.

[65] W. Fiers, Tumor necrosis factor. Characterization at the molecular, cellular and in vivo level, FEBS Lett 1991 (285) 199-212.

[66] S.G. Fletcher, D. Theodorescu, Surgery or radiation: what is the optimal management for locally advanced prostate cancer?, Can J Urol 2005 (12 Suppl 1) 58-61; discussion 101-2.

[67] L. Fong, E.J. Small, Immunotherapy for prostate cancer, Semin Oncol 2003 (30) 649-58.

[68] V. Forest, M. Peoc'h, C. Ardiet, L. Campos, D. Guyotat, J.M. Vergnon, In vivo cryochemotherapy of a human lung cancer model, Cryobiology 2005 (51) 92-101.

[69] V. Forest, M. Peoc'h, L. Campos, D. Guyotat, J.M. Vergnon, Effects of cryotherapy or chemotherapy on apoptosis in a non-small-cell lung cancer xenografted into SCID mice, Cryobiology 2005 (50) 29-37.

[70] V. Forest, M. Peoc'h, L. Campos, D. Guyotat, J.M. Vergnon, Benefit of a combined treatment of cryotherapy and chemotherapy on tumour growth and late cryo-induced angiogenesis in a non-small-cell lung cancer model, Lung Cancer 2006 (54) 79-86.

[71] P.L. Friedman, Catheter cryoablation of cardiac arrhythmias, Curr Opin Cardiol 2005 (20) 48-54.

[72] G.I. Frost, J. Lustgarten, B. Dudouet, L. Nyberg, B. Hartley-Asp, P. Borgstrom, Novel syngeneic pseudo-orthotopic prostate cancer model: vascular, mitotic and apoptotic responses to castration, Microvasc Res 2005 (69) 1-9.

[73] D. Fukumura, H.A. Salehi, B. Witwer, R.F. Tuma, R.J. Melder, R.K. Jain, Tumor necrosis factor alpha-induced leukocyte adhesion in normal and tumor vessels: effect of tumor type, transplantation site, and host strain, Cancer Res 1995 (55) 4824-9.

[74] W.L. Furman, D. Strother, K. McClain, B. Bell, B. Leventhal, C.B. Pratt, Phase I clinical trial of recombinant human tumor necrosis factor in children with refractory solid tumors: a Pediatric Oncology Group study, J Clin Oncol 1993 (11) 2205-10.

[75] A.A. Gage, Cryosurgery for oral and pharyngeal carcinoma, Am J Surg 1969 (118) 669-72.

[76] A.A. Gage, Cryosurgery in the treatment of cancer, Surg Gynecol Obstet 1992 (174) 73-92.

[77] A.A. Gage, History of cryosurgery, Semin Surg Oncol 1998 (14) 99-109.

[78] A.A. Gage, J. Baust, Mechanisms of tissue injury in cryosurgery, Cryobiology 1998 (37) 171-86.

[79] A.A. Gage, J.G. Baust, Cryosurgery - a review of recent advances and current issues, Cryo letters 2002 (23) 69-78.

[80] S. Gallucci, M. Lolkema, P. Matzinger, Natural adjuvants: endogenous activators of dendritic cells, Nat Med 1999 (5) 1249-55.

[81] J.R. Gamble, J.M. Harlan, S.J. Klebanoff, M.A. Vadas, Stimulation of the adherence of neutrophils to umbilical vein endothelium by human recombinant tumor necrosis factor, Proc Natl Acad Sci U S A 1985 (82) 8667-71.

[82] X. Gao, Y. Cui, R.M. Levenson, L.W. Chung, S. Nie, In vivo cancer targeting and imaging with semiconductor quantum dots, Nat Biotechnol 2004 (22) 969-76.

[83] S. Gazzaniga, A. Bravo, S.R. Goldszmid, F. Maschi, J. Martinelli, J. Mordoh, R. Wainstok, Inflammatory changes after cryosurgery-induced necrosis in human melanoma xenografted in nude mice, J Invest Dermatol 2001 (116) 664-71.

[84] M.G. Geeslin, D.J. Swanlund, J.C. Bischof, A parametric study of freezing injury in BPH1CAFTD-2 human prostate tumor cells, Cryo Letters 2007 (28) 173-86.

[85] J.C. Gilbert, B. Rubinsky, M.S. Roos, S.T. Wong, K.M. Brennan, MRI-monitored cryosurgery in the rabbit brain, Magn Reson Imaging 1993 (11) 1155-64.

[86] I.S. Gill, A.C. Novick, Renal cryosurgery, Urology 1999 (54) 215-9.

[87] I.S. Gill, A.C. Novick, J.J. Soble, G.T. Sung, E.M. Remer, J. Hale, C.M. O'Malley, Laparoscopic renal cryoablation: initial clinical series, Urology 1998 (52) 543-51.

[88] I.S. Gill, E.M. Remer, W.A. Hasan, B. Strzempkowski, M. Spaliviero, A.P. Steinberg, J.H. Kaouk, M.M. Desai, A.C. Novick, Renal cryoablation: outcome at 3 years, J Urol 2005 (173) 1903-7.

[89] J.R. Gingrich, R.J. Barrios, R.A. Morton, B.F. Boyce, F.J. DeMayo, M.J. Finegold, R. Angelopoulou, J.M. Rosen, N.M. Greenberg, Metastatic prostate cancer in a transgenic mouse, Cancer Res 1996 (56) 4096-102.

[90] S.C. Glasgow, S. Ramachandran, K.A. Csontos, J. Jia, T. Mohanakumar, W.C. Chapman, Interleukin-1beta is prominent in the early pulmonary inflammatory response after hepatic injury, Surgery 2005 (138) 64-70.

[91] R. Goel, K. Anderson, J. Slaton, F. Schmidlin, G. Vercellotti, J. Belcher, J.C. Bischof, Adjuvant approaches to enhance cryosurgery, J Biomech Eng 2009 (131) 074003.

[92] R. Goel, N. Shah, R. Visaria, G.F. Paciotti, J.C. Bischof, Biodistribution of TNF-alpha-coated gold nanoparticles in an in vivo model system, Nanomedicine (Lond) 2009 (4) 401-10.

[93] R. Goel, D. Swanlund, J. Coad, G.F. Paciotti, J.C. Bischof, TNF-{alpha}-based accentuation in cryoinjury--dose, delivery, and response, Mol Cancer Ther 2007 (6) 2039-47.

[94] R. Goel, D. Swanlund, J. Coad, G.F. Paciotti, J.C. Bischof, TNF-alpha-based accentuation in cryoinjury--dose, delivery, and response, Mol Cancer Ther 2007 (6) 2039-47.

[95] F.W. Goetz, J.V. Planas, S. MacKenzie, Tumor necrosis factors, Dev Comp Immunol 2004 (28) 487-97.

[96] G.F. Graham, Cryosurgery in the management of cutaneous malignancies, Clin Dermatol 2001 (19) 321-7.

[97] D.J. Granville, J.R. Shaw, S. Leong, C.M. Carthy, P. Margaron, D.W. Hunt, B.M. McManus, Release of cytochrome c, Bax migration, Bid cleavage, and activation of caspases 2, 3, 6, 7, 8, and 9 during endothelial cell apoptosis, Am J Pathol 1999 (155) 1021-5.

[98] F.R. Greten, M. Karin, The IKK/NF-kappaB activation pathway-a target for prevention and treatment of cancer, Cancer Lett 2004 (206) 193-9.

[99] D.S. Gridley, J.R. Baer, J.D. Cao, G.M. Miller, D.W. Kim, T.M. Timiryasova, I. Fodor, J.M. Slater, TNF-alpha gene and proton radiotherapy in an orthotopic brain tumor model, Int J Oncol 2002 (21) 251-9.

[100] D.S. Gridley, T.M. Timiryasova, G.M. Miller, M.L. Andres, R. Dutta-Roy, E.J. Bayeta, I. Fodor, Evaluation of TNF-alpha/Bax gene therapy and radiation against C6 glioma xenografts, Technol Cancer Res Treat 2003 (2) 41-50.

[101] E. Gursel, M. Roberts, R.J. Veenema, Regression of prostatic cancer following sequential cryotherapy to the prostate, J Urol 1972 (108) 928-32.

[102] B. Haley, E. Frenkel, Nanoparticles for drug delivery in cancer treatment, Urol Oncol 2008 (26) 57-64.

[103] B. Han, J.C. Bischof, Direct cell injury associated with eutectic crystallization during freezing, Cryobiology 2004 (48) 8-21.

[104] B. Han, A. Iftekhar, J.C. Bischof, Improved cryosurgery by use of thermophysical and inflammatory adjuvants, Technol Cancer Res Treat 2004 (3) 103-11.

[105] K.R. Han, J.K. Cohen, R.J. Miller, A.J. Pantuck, D.G. Freitas, C.A. Cuevas, H.L. Kim, J. Lugg, S.J. Childs, B. Shuman, M.A. Jayson, N.D. Shore, Y. Moore, A. Zisman, J.Y. Lee, R. Ugarte, L.A. Mynderse, T.M. Wilson, S.D. Sweat, H. Zincke, A.S. Belldegrun, Treatment of organ confined prostate cancer with third generation cryosurgery: preliminary multicenter experience, J Urol 2003 (170) 1126-30.

[106] Y. Har-Shai, M. Amar, E. Sabo, Intralesional cryotherapy for enhancing the involution of hypertrophic scars and keloids, Plast Reconstr Surg 2003 (111) 1841-52.

[107] Y. Har-Shai, W. Brown, D. Labbe, A. Dompmartin, I. Goldine, T. Gil, I. Mettanes, N. Pallua, Intralesional cryosurgery for the treatment of hypertrophic scars and keloids following aesthetic surgery: the results of a prospective observational study, Int J Low Extrem Wounds 2008 (7) 169-75.

[108] E.A. Havell, W. Fiers, R.J. North, The antitumor function of tumor necrosis factor (TNF), I. Therapeutic action of TNF against an established murine sarcoma is indirect, immunologically dependent, and limited by severe toxicity, J Exp Med 1988 (167) 1067-85.

[109] T. Hehlgans, K. Pfeffer, The intriguing biology of the tumour necrosis factor/tumour necrosis factor receptor superfamily: players, rules and the games, Immunology 2005 (115) 1-20.

[110] U. Hieber, M.E. Heim, Tumor necrosis factor for the treatment of malignancies, Oncology 1994 (51) 142-53.

[111] M. Hiraoka, Y.P. Li, K. Tsutsui, M. Abe, Y. Miyachi, Effects of tumor necrosis factor and hyperthermia on Meth-A tumors, Jpn J Cancer Res 1991 (82) 1171-4.

[112] H. Hirata, A. Takahashi, S. Kobayashi, S. Yonehara, H. Sawai, T. Okazaki, K. Yamamoto, M. Sasada, Caspases are activated in a branched protease cascade and control distinct downstream processes in Fas-induced apoptosis, J Exp Med 1998 (187) 587-600.

[113] N.E. Hoffmann, J.C. Bischof, Cryosurgery of normal and tumor tissue in the dorsal skin flap chamber: Part II--injury response, J Biomech Eng 2001 (123) 310-6.

[114] N.E. Hoffmann, J.C. Bischof, The cryobiology of cryosurgical injury, Urology 2002 (60) 40-9.

[115] N.E. Hoffmann, Bischof, J.B, Mechanisms of injury caused by in vivo freezing., in Life in Frozen State, E. Benson, B. Fuller, and N. lane, editors., Taylor & Francis 2003) 437-81.

[116] J.P. Homasson, [Cryotherapy in pneumology. Review of basic and clinical data], Rev Pneumol Clin 1990 (46) 189-93.

[117] A.H. Horan, Sequential cryotherapy for prostatic carcinoma: does it palliate the bone pain?, Conn Med 1975 (39) 81-3.

[118] S.R. Howe, M.M. Gottardis, J.I. Everitt, T.L. Goldsworthy, D.C. Wolf, C. Walker, Rodent model of reproductive tract leiomyomata. Establishment and characterization of tumor-derived cell lines, Am J Pathol 1995 (146) 1568-79.

[119] Q. Huang, J.K. Hu, F. Lohr, L. Zhang, R. Braun, J. Lanzen, J.B. Little, M.W. Dewhirst, C.Y. Li, Heat-induced gene expression as a novel targeted cancer gene therapy strategy, Cancer Res 2000 (60) 3435-9.

[120] S. Huerta-Yepez, M. Vega, A. Jazirehi, H. Garban, F. Hongo, G. Cheng, B. Bonavida, Nitric oxide sensitizes prostate carcinoma cell lines to TRAIL-mediated

apoptosis via inactivation of NF-kappa B and inhibition of Bcl-xl expression, Oncogene 2004 (23) 4993-5003.

[121] A.A. Hurwitz, B.A. Foster, J.P. Allison, N.M. Greenberg, E.D. Kwon, The TRAMP mouse as a model for prostate cancer, Curr Protoc Immunol 2001 (Chapter 20) Unit 20 5.

[122] S. Ikekawa, K. Ishihara, S. Tanaka, S. Ikeda, Basic studies of cryochemotherapy in a murine tumor system, Cryobiology 1985 (22) 477-83.

[123] G. Jacob, A.K. Li, K.E. Hobbs, A comparison of cryodestruction with excision or infarction of an implanted tumor in rat liver, Cryobiology 1984 (21) 148-56.

[124] J. Jiang, J.C. Bischof, Effect of timing, dose and interstitial versus nanoparticle delivery of tumor necrosis factor alpha in combinatorial adjuvant cryosurgery treatment of ELT-3 uterine leiomyoma (fibroid) tumor, Cryoletters 2009).

[125] J. Jiang, R. Goel, M.A. Iftekhar, R. Visaria, J.D. Belcher, G.M. Vercellotti, J.C. Bischof, Tumor necrosis factor-{alpha}-induced accentuation in cryoinjury: mechanisms in vitro and in vivo, Mol Cancer Ther 2008 (7) 2547-55.

[126] J. Jiang, R. Goel, M.A. Iftekhar, R. Visaria, J.D. Belcher, G.M. Vercellotti, J.C. Bischof, Tumor necrosis factor-alpha-induced accentuation in cryoinjury: mechanisms in vitro and in vivo, Mol Cancer Ther 2008 (7) 2547-55.

[127] J.S. Jones, J.C. Rewcastle, Primary cryoablation for Gleason 8, 9, or 10 localized prostate cancer: Biochemical and local control outcomes from the Cryo OnLine database registry, Indian J Urol 2008 (24) 490-3.

[128] J.S. Jones, J.C. Rewcastle, B.J. Donnelly, F.M. Lugnani, L.L. Pisters, A.E. Katz, Whole gland primary prostate cryoablation: initial results from the cryo on-line data registry, J Urol 2008 (180) 554-8.

[129] J. Joosten, G. Jager, W. Oyen, T. Wobbes, T. Ruers, Cryosurgery and radiofrequency ablation for unresectable colorectal liver metastases, Eur J Surg Oncol 2005 (31) 1152-9.

[130] J.J. Joosten, G.N. Muijen, T. Wobbes, T.J. Ruers, In vivo destruction of tumor tissue by cryoablation can induce inhibition of secondary tumor growth: an experimental study, Cryobiology 2001 (42) 49-58.

[131] J.E. Jordan, Z.Q. Zhao, J. Vinten-Johansen, The role of neutrophils in myocardial ischemia-reperfusion injury, Cardiovasc Res 1999 (43) 860-78.

[132] J. Jorizzo, J. Weiss, K. Furst, C. VandePol, S.F. Levy, Effect of a 1-week treatment with 0.5% topical fluorouracil on occurrence of actinic keratosis after cryosurgery: a randomized, vehicle-controlled clinical trial, Arch Dermatol 2004 (140) 813-6.

[133] J.O. Karlsson, E.G. Cravalho, I.H. Borel Rinkes, R.G. Tompkins, M.L. Yarmush, M. Toner, Nucleation and growth of ice crystals inside cultured hepatocytes during freezing in the presence of dimethyl sulfoxide, Biophys J 1993 (65) 2524-36.

[134] S. Karthik, D.O. Kessel, Cryoplasty--where is the evidence?, Acta Chir Belg 2007 (107) 500-3.

[135] Y. Katoh, M. Katoh, FGFR2-related pathogenesis and FGFR2-targeted therapeutics (Review), Int J Mol Med 2009 (23) 307-11.

[136] A.E. Katz, J.C. Rewcastle, The current and potential role of cryoablation as a primary therapy for localized prostate cancer, Curr Oncol Rep 2003 (5) 231-8.

[137] C.S. Kaufman, B. Bachman, P.J. Littrup, L.A. Freeman-Gibb, M. White, K. Carolin, D. Francescatti, L.H. Stocks, J.S. Smith, C.A. Henry, L. Bailey, J.K. Harness, R. Simmons, Cryoablation treatment of benign breast lesions with 12-month follow-up, Am J Surg 2004 (188) 340-8.

[138] C.S. Kaufman, P.J. Littrup, L.A. Freeman-Gibb, J.S. Smith, D. Francescatti, R. Simmons, L.H. Stocks, L. Bailey, J.K. Harness, B.A. Bachman, C.A. Henry, Office-based cryoablation of breast fibroadenomas with long-term follow-up, Breast J 2005 (11) 344-50.

[139] E. Kedar, O. Palgi, G. Golod, I. Babai, Y. Barenholz, Delivery of cytokines by liposomes. III. Liposome-encapsulated GM-CSF and TNF-alpha show improved pharmacokinetics and biological activity and reduced toxicity in mice, J Immunother 1997 (20) 180-93.

[140] P. Khairy, M. Dubuc, Transcatheter cryoablation part I: preclinical experience, Pacing Clin Electrophysiol 2008 (31) 112-20.

[141] K. Khargi, B.A. Hutten, B. Lemke, T. Deneke, Surgical treatment of atrial fibrillation; a systematic review, Eur J Cardiothorac Surg 2005 (27) 258-65.

119

[142] D.W. Kim, M.L. Andres, J. Li, E.H. Kajioka, G.M. Miller, A.L. Seynhaeve, T.L. Ten Hagen, D.S. Gridley, Liposome-encapsulated tumor necrosis factor-alpha enhances the effects of radiation against human colon tumor xenografts, J Interferon Cytokine Res 2001 (21) 885-97.

[143] E.S. Kim, F.R. Khuri, R.S. Herbst, Epidermal growth factor receptor biology (IMC-C225), Curr Opin Oncol 2001 (13) 506-13.

[144] R. Kircheis, E. Ostermann, M.F. Wolschek, C. Lichtenberger, C. Magin-Lachmann, L. Wightman, M. Kursa, E. Wagner, Tumor-targeted gene delivery of tumor necrosis factor-alpha induces tumor necrosis and tumor regression without systemic toxicity, Cancer Gene Ther 2002 (9) 673-80.

[145] S.J. Klebanoff, M.A. Vadas, J.M. Harlan, L.H. Sparks, J.R. Gamble, J.M. Agosti, A.M. Waltersdorph, Stimulation of neutrophils by tumor necrosis factor, J Immunol 1986 (136) 4220-5.

[146] H. Kono, M.D. Wheeler, I. Rusyn, M. Lin, V. Seabra, C.A. Rivera, B.U. Bradford, D.T. Forman, R.G. Thurman, Gender differences in early alcohol-induced liver injury: role of CD14, NF-kappaB, and TNF-alpha, Am J Physiol Gastrointest Liver Physiol 2000 (278) G652-61.

[147] M. Korbelik, PDT-associated host response and its role in the therapy outcome, Lasers Surg Med 2006 (38) 500-8.

[148] H. Koushafar, L. Pham, C. Lee, B. Rubinsky, Chemical adjuvant cryosurgery with antifreeze proteins, J Surg Oncol 1997 (66) 114-21.

[149] H. Koushafar, B. Rubinsky, Effect of antifreeze proteins on frozen primary prostatic adenocarcinoma cells, Urology 1997 (49) 421-5.

[150] G. Kramer, G.E. Steiner, P. Sokol, A. Handisurya, H.C. Klingler, U. Maier, M. Foldy, M. Marberger, Local intratumoral tumor necrosis factor-alpha and systemic IFN-alpha 2b in patients with locally advanced prostate cancer, J Interferon Cytokine Res 2001 (21) 475-84.

[151] E.G. Kuflik, Re: Evidence-based review of the use of cryosurgery in treatment of basal cell carcinoma, Dermatol Surg 2004 (30) 478.

[152] R. Kumar, M. Mandal, R. Vadlamudi, New insights into anti-HER-2 receptor monoclonal antibody research, Semin Oncol 2000 (27) 84-91; discussion 2-100.

[153] B.S. Kuszyk, F.M. Corl, F.N. Franano, D.A. Bluemke, L.V. Hofmann, B.J. Fortman, E.K. Fishman, Tumor transport physiology: implications for imaging and imaging-guided therapy, AJR Am J Roentgenol 2001 (177) 747-53.

[154] E.D. Kwon, B.A. Foster, A.A. Hurwitz, C. Madias, J.P. Allison, N.M. Greenberg, M.B. Burg, Elimination of residual metastatic prostate cancer after surgery and adjunctive cytotoxic T lymphocyte-associated antigen 4 (CTLA-4) blockade immunotherapy, Proc Natl Acad Sci U S A 1999 (96) 15074-9.

[155] W.Y. Lau, T.W. Leung, S.C. Yu, S.K. Ho, Percutaneous local ablative therapy for hepatocellular carcinoma: a review and look into the future, Ann Surg 2003 (237) 171-9.

[156] P. Le Pivert, R.S. Haddad, A. Aller, K. Titus, J. Doulat, M. Renard, D.R. Morrison, Ultrasound guided combined cryoablation and microencapsulated 5-Fluorouracil inhibits growth of human prostate tumors in xenogenic mouse model assessed by luminescence imaging, Technol Cancer Res Treat 2004 (3) 135-42.

[157] S.J. Leibovich, P.J. Polverini, H.M. Shepard, D.M. Wiseman, V. Shively, N. Nuseir, Macrophage-induced angiogenesis is mediated by tumour necrosis factor-alpha, Nature 1987 (329) 630-2.

[158] K. Lemola, M. Dubuc, P. Khairy, Transcatheter cryoablation part II: clinical utility, Pacing Clin Electrophysiol 2008 (31) 235-44.

[159] A.B. Lentsch, P.A. Ward, Regulation of inflammatory vascular damage, J Pathol 2000 (190) 343-8.

[160] P.J. Leopard, Cryosurgery for facial skin lesions, Proc R Soc Med 1975 (68) 606-8.

[161] S.K. Libutti, G.F. Paciotti, L. Myer, R. Haynes, W. Gannon, M. Walker, G. Seidel, A. Byrnes, N. Yuldasheva, L. Tamarkin, Results of a completed phase I clinical trial of CYT-6091: A pegylated colloidal gold-TNF nanomedicine, J Clin Oncol (Meeting Abstracts) 2009 (27) 3586-.

[162] P.J. Littrup, L. Freeman-Gibb, A. Andea, M. White, K.C. Amerikia, D. Bouwman, T. Harb, W. Sakr, Cryotherapy for breast fibroadenomas, Radiology 2005 (234) 63-72.

[163] K. Liu, T. Iyoda, M. Saternus, Y. Kimura, K. Inaba, R.M. Steinman, Immune tolerance after delivery of dying cells to dendritic cells in situ, J Exp Med 2002 (196) 1091-7.

[164] J.P. Long, D. Bahn, F. Lee, K. Shinohara, D.O. Chinn, J.N. Macaluso, Jr., Five-year retrospective, multi-institutional pooled analysis of cancer-related outcomes after cryosurgical ablation of the prostate, Urology 2001 (57) 518-23.

[165] J.P. Long, D. Bahn, F. Lee, K. Shinohara, D.O. Chinn, J.N. Macaluso Jr, Five-year retrospective, multi-institutional pooled analysis of cancer-related outcomes after cryosurgical ablation of the prostate, Urology 2001 (57) 518-23.

[166] J.E. Lovelock, The haemolysis of human red blood-cells by freezing and thawing, Biochim Biophys Acta 1953 (10) 414-26.

[167] J.L. Luo, H. Kamata, M. Karin, IKK/NF-kappaB signaling: balancing life and death--a new approach to cancer therapy, J Clin Invest 2005 (115) 2625-32.

[168] S. Mabuchi, M. Ohmichi, Y. Nishio, T. Hayasaka, A. Kimura, T. Ohta, J. Kawagoe, K. Takahashi, N. Yada-Hashimoto, H. Seino-Noda, M. Sakata, T. Motoyama, H. Kurachi, J.R. Testa, K. Tasaka, Y. Murata, Inhibition of inhibitor of nuclear factor-kappaB phosphorylation increases the efficacy of paclitaxel in in vitro and in vivo ovarian cancer models, Clin Cancer Res 2004 (10) 7645-54.

[169] S. Mabuchi, M. Ohmichi, Y. Nishio, T. Hayasaka, A. Kimura, T. Ohta, M. Saito, J. Kawagoe, K. Takahashi, N. Yada-Hashimoto, M. Sakata, T. Motoyama, H. Kurachi, K. Tasaka, Y. Murata, Inhibition of NFkappaB increases the efficacy of cisplatin in in vitro and in vivo ovarian cancer models, J Biol Chem 2004 (279) 23477-85.

[170] M.O. Maiwand, J.M. Evans, J.E. Beeson, The application of cryosurgery in the treatment of lung cancer, Cryobiology 2004 (48) 55-61.

[171] O. Maiwand, R. Glynne-Jones, J. Chambers, G. Asimakopoulos, Direct cryosurgery for inoperable metastatic disease of the lung, Ann Thorac Surg 2006 (81) 718-21.

[172] O. Maiwand, A.R. Makey, Cryoanalgesia for relief of pain after thoracotomy, Br Med J (Clin Res Ed) 1981 (282) 1749-50.

[173] T. Mala, Cryoablation of liver tumours -- a review of mechanisms, techniques and clinical outcome, Minim Invasive Ther Allied Technol 2006 (15) 9-17.

[174] P.P. Manna, T. Mohanakumar, Human dendritic cell mediated cytotoxicity against breast carcinoma cells in vitro, J Leukoc Biol 2002 (72) 312-20.

[175] P.N. Manson, R. Jesudass, L. Marzella, G.B. Bulkley, M.J. Im, K.K. Narayan, Evidence for an early free radical-mediated reperfusion injury in frostbite, Free Radic Biol Med 1991 (10) 7-11.

[176] M. Marberger, P.R. Carroll, M.J. Zelefsky, J.A. Coleman, H. Hricak, P.T. Scardino, L.L. Abenhaim, New treatments for localized prostate cancer, Urology 2008 (72) S36-43.

[177] K. Maruyama, O. Ishida, T. Takizawa, K. Moribe, Possibility of active targeting to tumor tissues with liposomes, Adv Drug Deliv Rev 1999 (40) 89-102.

[178] L. Marzella, R.R. Jesudass, P.N. Manson, R.A. Myers, G.B. Bulkley, Morphologic characterization of acute injury to vascular endothelium of skin after frostbite, Plast Reconstr Surg 1989 (83) 67-76.

[179] R. Matsumoto, A.M. Selig, V.M. Colucci, F.A. Jolesz, MR monitoring during cryotherapy in the liver: predictability of histologic outcome, J Magn Reson Imaging 1993 (3) 770-6.

[180] H.J. Mauceri, N.N. Hanna, J.D. Wayne, D.E. Hallahan, S. Hellman, R.R. Weichselbaum, Tumor necrosis factor alpha (TNF-alpha) gene therapy targeted by ionizing radiation selectively damages tumor vasculature, Cancer Res 1996 (56) 4311-4.

[181] P. Mazur, Kinetics of Water Loss from Cells at Subzero Temperatures and the Likelihood of Intracellular Freezing, J Gen Physiol 1963 (47) 347-69.

[182] P. Mazur, The role of cell membranes in the freezing of yeast and other single cells, Ann N Y Acad Sci 1965 (125) 658-76.

[183] J.M. McCord, Oxygen-derived radicals: a link between reperfusion injury and inflammation, Fed Proc 1987 (46) 2402-6.

[184] O. Micheau, J. Tschopp, Induction of TNF receptor I-mediated apoptosis via two sequential signaling complexes, Cell 2003 (114) 181-90.

[185] C. Michiels, T. Arnould, J. Remacle, Endothelial cell responses to hypoxia: initiation of a cascade of cellular interactions, Biochim Biophys Acta 2000 (1497) 1-10.

[186] L.M. Mir, B. Rubinsky, Treatment of cancer with cryochemotherapy, Br J Cancer 2002 (86) 1658-60.

[187] S. Mocellin, C.R. Rossi, P. Pilati, D. Nitti, Tumor necrosis factor, cancer and anticancer therapy, Cytokine Growth Factor Rev 2005 (16) 35-53.

[188] S.C. Moten, E. Rodriguez, R.C. Cook, L.W. Nifong, W.R. Chitwood, Jr., New ablation techniques for atrial fibrillation and the minimally invasive cryo-maze procedure in patients with lone atrial fibrillation, Heart Lung Circ 2007 (16 Suppl 3) S88-93.

[189] V. Mouraviev, S. Joniau, H. Van Poppel, T.J. Polascik, Current status of minimally invasive ablative techniques in the treatment of small renal tumours, Eur Urol 2007 (51) 328-36.

[190] V. Mouraviev, J.M. Mayes, T.J. Polascik, Pathologic basis of focal therapy for early-stage prostate cancer, Nat Rev Urol 2009 (6) 205-15.

[191] K. Muldrew, J. Rewcastle, B.J. Donnelly, J.C. Saliken, S. Liang, S. Goldie, M. Olson, R. Baissalov, G. Sandison, Flounder antifreeze peptides increase the efficacy of cryosurgery, Cryobiology 2001 (42) 182-9.

[192] A. Nagayasu, K. Uchiyama, H. Kiwada, The size of liposomes: a factor which affects their targeting efficiency to tumors and therapeutic activity of liposomal antitumor drugs, Adv Drug Deliv Rev 1999 (40) 75-87.

[193] W.A. Nagle, B.L. Soloff, A.J. Moss, Jr., K.J. Henle, Cultured Chinese hamster cells undergo apoptosis after exposure to cold but nonfreezing temperatures, Cryobiology 1990 (27) 439-51.

[194] P.L. Naredi, P.G. Lindner, S.B. Holmberg, U. Stenram, A. Peterson, L.R. Hafstrom, The effects of tumour necrosis factor alpha on the vascular bed and blood flow in an experimental rat hepatoma, Int J Cancer 1993 (54) 645-9.

[195] P. Nawroth, D. Handley, G. Matsueda, R. De Waal, H. Gerlach, D. Blohm, D. Stern, Tumor necrosis factor/cachectin-induced intravascular fibrin formation in meth A fibrosarcomas, J Exp Med 1988 (168) 637-47.

[196] P.P. Nawroth, D.M. Stern, Modulation of endothelial cell hemostatic properties by tumor necrosis factor, J Exp Med 1986 (163) 740-5.

124

[197] A. Nii, D. Fan, I.J. Fidler, Cytotoxic potential of liposomes containing tumor necrosis factor-alpha against sensitive and resistant target cells, J Immunother (1991) 1991 (10) 13-9.

[198] T. Ninomiya, M. Mori, Histologic and histochemical changes in experimental carcinomas following cryosurgery, Int J Oral Surg 1985 (14) 362-70.

[199] J. Nurko, C.D. Mabry, P. Whitworth, D. Jarowenko, L. Oetting, T. Potruch, L. Han, M.J. Edwards, Interim results from the FibroAdenoma Cryoablation Treatment Registry, Am J Surg 2005 (190) 647-51; discussion 51-2.

[200] G. Onik, Image-guided prostate cryosurgery: state of the art, Cancer Control 2001 (8) 522-31.

[201] G. Onik, J. Gilbert, W. Hoddick, R. Filly, P. Callen, B. Rubinsky, L. Farrel, Sonographic monitoring of hepatic cryosurgery in an experimental animal model, AJR Am J Roentgenol 1985 (144) 1043-7.

[202] G. Onik, B. Rubinsky, R. Zemel, L. Weaver, D. Diamond, C. Cobb, B. Porterfield, Ultrasound-guided hepatic cryosurgery in the treatment of metastatic colon carcinoma. Preliminary results, Cancer 1991 (67) 901-7.

[203] G.M. Onik, J.K. Cohen, G.D. Reyes, B. Rubinsky, Z. Chang, J. Baust, Transrectal ultrasound-guided percutaneous radical cryosurgical ablation of the prostate, Cancer 1993 (72) 1291-9.

[204] K. Ozer, G. Adanali, M. Siemionow, Late effects of TNF-alpha-induced inflammation on the microcirculation of cremaster muscle flaps under intravital microscopy, J Reconstr Microsurg 2002 (18) 37-45.

[205] G.F. Paciotti, L. Myer, D. Weinreich, D. Goia, N. Pavel, R.E. McLaughlin, L. Tamarkin, Colloidal gold: a novel nanoparticle vector for tumor directed drug delivery, Drug Deliv 2004 (11) 169-83.

[206] H.D. Papenfuss, J.F. Gross, M. Intaglietta, F.A. Treese, A transparent access chamber for the rat dorsal skin fold, Microvasc Res 1979 (18) 311-8.

[207] M.I. Papisov, Theoretical considerations of RES-avoiding liposomes: Molecular mechanics and chemistry of liposome interactions, Adv Drug Deliv Rev 1998 (32) 119-38.

[208] H. Park, J.C. Lyons, R.J. Griffin, B.U. Lim, C.W. Song, Apoptosis and cell cycle progression in an acidic environment after irradiation, Radiat Res 2000 (153) 295-304.

[209] F. Partheniou, S.M. Kelsey, S.M. Srinivasula, A.C. Newland, E.S. Alnemri, L. Jia, c-IAP1 blocks TNFalpha-mediated cytotoxicity upstream of caspase-dependent and -independent mitochondrial events in human leukemic cells, Biochem Biophys Res Commun 2001 (287) 181-9.

[210] H.M. Patel, S.M. Moghimi, Serum-mediated recognition of liposomes by phagocytic cells of the reticuloendothelial system - The concept of tissue specificity, Adv Drug Deliv Rev 1998 (32) 45-60.

[211] G.R. Pease, S.T. Wong, M.S. Roos, B. Rubinsky, MR image-guided control of cryosurgery, J Magn Reson Imaging 1995 (5) 753-60.

[212] Y. Peng, D.A. Martin, J. Kenkel, K. Zhang, C.A. Ogden, K.B. Elkon, Innate and adaptive immune response to apoptotic cells, J Autoimmun 2007 (29) 303-9.

[213] S.D. Perrault, W.C. Chan, Synthesis and surface modification of highly monodispersed, spherical gold nanoparticles of 50-200 nm, J Am Chem Soc 2009 (131) 17042-3.

[214] C.A. Pettaway, S. Pathak, G. Greene, E. Ramirez, M.R. Wilson, J.J. Killion, I.J. Fidler, Selection of highly metastatic variants of different human prostatic carcinomas using orthotopic implantation in nude mice, Clin Cancer Res 1996 (2) 1627-36.

[215] L. Pham, R. Dahiya, B. Rubinsky, An in vivo study of antifreeze protein adjuvant cryosurgery, Cryobiology 1999 (38) 169-75.

[216] J.W. Pierce, R. Schoenleber, G. Jesmok, J. Best, S.A. Moore, T. Collins, M.E. Gerritsen, Novel inhibitors of cytokine-induced IkappaBalpha phosphorylation and endothelial cell adhesion molecule expression show anti-inflammatory effects in vivo, J Biol Chem 1997 (272) 21096-103.

[217] J.M. Rabb, M.L. Renaud, P.A. Brandt, C.W. Witt, Effect of freezing and thawing on the microcirculation and capillary endothelium of the hamster cheek pouch, Cryobiology 1974 (11) 508-18.

[218] T.S. Ravikumar, G.D. Steele, Jr., Hepatic cryosurgery, Surg Clin North Am 1989 (69) 433-40.

[219] J.H. Ravina, N.C. Vigneron, A. Aymard, O. Le Dref, J.J. Merland, Pregnancy after embolization of uterine myoma: report of 12 cases, Fertil Steril 2000 (73) 1241-3.

[220] V.Y. Reddy, P. Neuzil, A. d'Avila, M. Laragy, Z.J. Malchano, S. Kralovec, S.J. Kim, J.N. Ruskin, Balloon catheter ablation to treat paroxysmal atrial fibrillation: what is the level of pulmonary venous isolation?, Heart Rhythm 2008 (5) 353-60.

[221] P. Redondo, J. del Olmo, A. Lopez-Diaz de Cerio, S. Inoges, M. Marquina, I. Melero, M. Bendandi, Imiquimod enhances the systemic immunity attained by local cryosurgery destruction of melanoma lesions, J Invest Dermatol 2007 (127) 1673-80.

[222] J. Rees, B. Patel, R. MacDonagh, R. Persad, Cryosurgery for prostate cancer, BJU Int 2004 (93) 710-4.

[223] J. Rehman, J. Landman, D. Lee, R. Venkatesh, D.G. Bostwick, C. Sundaram, R.V. Clayman, Needle-based ablation of renal parenchyma using microwave, cryoablation, impedance- and temperature-based monopolar and bipolar radiofrequency, and liquid and gel chemoablation: laboratory studies and review of the literature, J Endourol 2004 (18) 83-104.

[224] O.B. Reite, Functional Qualities of Small Blood Vessels in Tissue Injured by Freezing and Thawing, Acta Physiol Scand 1965 (63) 111-20.

[225] N. Renard, D. Lienard, L. Lespagnard, A. Eggermont, R. Heimann, F. Lejeune, Early endothelium activation and polymorphonuclear cell invasion precede specific necrosis of human melanoma and sarcoma treated by intravascular high-dose tumour necrosis factor alpha (rTNF alpha), Int J Cancer 1994 (57) 656-63.

[226] G. Rigatelli, P. Cardaioli, M. Giordan, Endovascular treatment of femoro-popliteal obstructive disease, Minerva Cardioangiol 2007 (55) 125-32.

[227] M.L. Rivoire, E.J. Voiglio, P. Kaemmerlen, G. Molina, I. Treilleux, J. Finzy, E. Delay, F. Gory, Hepatic cryosurgery precision: evaluation of ultrasonography, thermometry, and impedancemetry in a pig model, J Surg Oncol 1996 (61) 242-8.

[228] J.A. Roake, A.S. Rao, P.J. Morris, C.P. Larsen, D.F. Hankins, J.M. Austyn, Dendritic cell loss from nonlymphoid tissues after systemic administration of lipopolysaccharide, tumor necrosis factor, and interleukin 1, J Exp Med 1995 (181) 2237-47.

[229] B. Robaye, R. Mosselmans, W. Fiers, J.E. Dumont, P. Galand, Tumor necrosis factor induces apoptosis (programmed cell death) in normal endothelial cells in vitro, Am J Pathol 1991 (138) 447-53.

[230] K.P. Roberts, D. Smith, H. Ozturk, A. Kazem, P.V. Pazhayannur, J.C. Hulbert, J.C. Bischof, Biochemical alterations and tissue viability in AT-1 tumor tissue after in vitro cryo-ablation, Cryo letters 1997 (18) 241-50.

[231] O.W. Rokhlin, A.V. Gudkov, S. Kwek, R.A. Glover, A.S. Gewies, M.B. Cohen, p53 is involved in tumor necrosis factor-alpha-induced apoptosis in the human prostatic carcinoma cell line LNCaP, Oncogene 2000 (19) 1959-68.

[232] B. Rubinsky, Cryosurgery, Annu Rev Biomed Eng 2000 (2) 157-87.

[233] T.J. Rutherford, Cryosurgery Is a Simple Modality for Endometrial Ablation, J Am Assoc Gynecol Laparosc 1996 (3) S44-5.

[234] T.J. Rutherford, T.G. Zreik, R.N. Troiano, S.F. Palter, D.L. Olive, Endometrial cryoablation, a minimally invasive procedure for abnormal uterine bleeding, J Am Assoc Gynecol Laparosc 1998 (5) 23-8.

[235] M.S. Sabel, Cryo-immunology: a review of the literature and proposed mechanisms for stimulatory versus suppressive immune responses, Cryobiology 2009 (58) 1-11.

[236] Y. Sakuhara, T. Shimizu, Y. Kodama, A. Sawada, H. Endo, D. Abo, T. Hasegawa, K. Miyasaka, Magnetic resonance-guided percutaneous cryoablation of uterine fibroids: early clinical experiences, Cardiovasc Intervent Radiol 2006 (29) 552-8.

[237] J.C. Saliken, B.J. Donnelly, J.C. Rewcastle, The evolution and state of modern technology for prostate cryosurgery, Urology 2002 (60) 26-33.

[238] G.A. Sandison, M.P. Loye, J.C. Rewcastle, L.J. Hahn, J.C. Saliken, J.G. McKinnon, B.J. Donnelly, X-ray CT monitoring of iceball growth and thermal distribution during cryosurgery, Phys Med Biol 1998 (43) 3309-24.

[239] S. Sarkar, V. Kalia, R.C. Montelaro, Caspase-mediated apoptosis and cell death of rhesus macaque CD4+ T-cells due to cryopreservation of peripheral blood mononuclear cells can be rescued by cytokine treatment after thawing, Cryobiology 2003 (47) 44-58.

[240] B. Sauter, M.L. Albert, L. Francisco, M. Larsson, S. Somersan, N. Bhardwaj, Consequences of cell death: exposure to necrotic tumor cells, but not primary tissue cells

or apoptotic cells, induces the maturation of immunostimulatory dendritic cells, J Exp Med 2000 (191) 423-34.

[241] J. Savill, I. Dransfield, C. Gregory, C. Haslett, A blast from the past: clearance of apoptotic cells regulates immune responses, Nat Rev Immunol 2002 (2) 965-75.

[242] V. Schacht, K. Becker, R.M. Szeimies, C. Abels, Apoptosis and leucocyte-endothelium interactions contribute to the delayed effects of cryotherapy on tumours in vivo, Arch Dermatol Res 2002 (294) 341-8.

[243] C.G. Schirren, K. Scharffetter, R. Hein, O. Braun-Falco, T. Krieg, Tumor necrosis factor alpha induces invasiveness of human skin fibroblasts in vitro, J Invest Dermatol 1990 (94) 706-10.

[244] G. Schuder, G. Pistorius, M. Fehringer, G. Feifel, M.D. Menger, B. Vollmar, Complete shutdown of microvascular perfusion upon hepatic cryothermia is critically dependent on local tissue temperature, Br J Cancer 2000 (82) 794-9.

[245] J.K. Seifert, T. Junginger, Cryotherapy for liver tumors: current status, perspectives, clinical results, and review of literature, Technol Cancer Res Treat 2004 (3) 151-63.

[246] J.K. Seifert, D.L. Morris, World survey on the complications of hepatic and prostate cryotherapy, World J Surg 1999 (23) 109-13; discussion 13-4.

[247] J.K. Seifert, A. Springer, P. Baier, T. Junginger, Liver resection or cryotherapy for colorectal liver metastases: a prospective case control study, Int J Colorectal Dis 2005 (20) 507-20.

[248] P. Selby, S. Hobbs, C. Viner, E. Jackson, A. Jones, D. Newell, A.H. Calvert, T. McElwain, K. Fearon, J. Humphreys, et al., Tumour necrosis factor in man: clinical and biological observations, Br J Cancer 1987 (56) 803-8.

[249] M.R. Shalaby, M.A. Palladino, Jr., S.E. Hirabayashi, T.E. Eessalu, G.D. Lewis, H.M. Shepard, B.B. Aggarwal, Receptor binding and activation of polymorphonuclear neutrophils by tumor necrosis factor-alpha, J Leukoc Biol 1987 (41) 196-204.

[250] M. Sharma, W.W. Chuang, Z. Sun, Phosphatidylinositol 3-kinase/Akt stimulates androgen pathway through GSK3beta inhibition and nuclear beta-catenin accumulation, J Biol Chem 2002 (277) 30935-41.

[251] H.T. Sharp, Assessment of new technology in the treatment of idiopathic menorrhagia and uterine leiomyomata, Obstet Gynecol 2006 (108) 990-1003.

[252] M.M. Shenoi, Shah, N. B., Griffin, R. J., Vercellotti, G. M., Bischof, J.C., Nanoparticle pre-conditioning for enhanced thermal therapies in cancer, Nanomedicine 2009 (Submitted).

[253] J.P. Shepherd, R.P. Dawber, Wound healing and scarring after cryosurgery, Cryobiology 1984 (21) 157-69.

[254] K. Shinohara, J.A. Connolly, J.C. Presti, Jr., P.R. Carroll, Cryosurgical treatment of localized prostate cancer (stages T1 to T4): preliminary results, J Urol 1996 (156) 115-20; discussion 20-1.

[255] T. Shirai, H. Yamaguchi, H. Ito, C.W. Todd, R.B. Wallace, Cloning and expression in Escherichia coli of the gene for human tumour necrosis factor, Nature 1985 (313) 803-6.

[256] A.C. Skanes, R. Yee, A.D. Krahn, G.J. Klein, Cryoablation of atrial arrhythmias, Card Electrophysiol Rev 2002 (6) 383-8.

[257] M. Skoberne, A.S. Beignon, N. Bhardwaj, Danger signals: a time and space continuum, Trends Mol Med 2004 (10) 251-7.

[258] S.T. Smiley, J.A. King, W.W. Hancock, Fibrinogen stimulates macrophage chemokine secretion through toll-like receptor 4, J Immunol 2001 (167) 2887-94.

[259] D.J. Smith, W.M. Fahssi, D.J. Swanlund, J.C. Bischof, A parametric study of freezing injury in AT-1 rat prostate tumor cells, Cryobiology 1999 (39) 13-28.

[260] W.A. Soanes, R.J. Ablin, M.J. Gonder, Remission of metastatic lesions following cryosurgery in prostatic cancer: immunologic considerations, J Urol 1970 (104) 154-9.

[261] J.M. Srinivasan, L.F. Fajardo, G.M. Hahn, Mechanism of antitumor activity of tumor necrosis factor alpha with hyperthermia in a tumor necrosis factor alpha-resistant tumor, J Natl Cancer Inst 1990 (82) 1904-10.

[262] J.P. Steinbach, J. Weissenberger, A. Aguzzi, Distinct phases of cryogenic tissue damage in the cerebral cortex of wild-type and c-fos deficient mice, Neuropathology and applied neurobiology 1999 (25) 468-80.

[263] P.L. Steponkus, Role of the plasma membrane in freezing injury and cold acclimation Ann Rev Plant Physiol 1984 (35) 543-84.

[264] C. Stroh, U. Cassens, A.K. Samraj, W. Sibrowski, K. Schulze-Osthoff, M. Los, The role of caspases in cryoinjury: caspase inhibition strongly improves the recovery of cryopreserved hematopoietic and other cells, FASEB J 2002 (16) 1651-3.

[265] L.M. Stuart, M. Lucas, C. Simpson, J. Lamb, J. Savill, A. Lacy-Hulbert, Inhibitory effects of apoptotic cell ingestion upon endotoxin-driven myeloid dendritic cell maturation, J Immunol 2002 (168) 1627-35.

[266] M. Suzuki, H. Asako, P. Kubes, S. Jennings, M.B. Grisham, D.N. Granger, Neutrophil-derived oxidants promote leukocyte adherence in postcapillary venules, Microvasc Res 1991 (42) 125-38.

[267] P.W. Szlosarek, F.R. Balkwill, Tumour necrosis factor alpha: a potential target for the therapy of solid tumours, Lancet Oncol 2003 (4) 565-73.

[268] A.M. Szpaderska, E.I. Egozi, R.L. Gamelli, L.A. DiPietro, The effect of thrombocytopenia on dermal wound healing, J Invest Dermatol 2003 (120) 1130-7.

[269] J. Tacke, G. Adam, P. Haage, B. Sellhaus, S. Grosskortenhaus, R.W. Gunther, MR-guided percutaneous cryotherapy of the liver: in vivo evaluation with histologic correlation in an animal model, J Magn Reson Imaging 2001 (13) 50-6.

[270] J.E. Talmadge, H.R. Tribble, R.W. Pennington, H. Phillips, R.H. Wiltrout, Immunomodulatory and immunotherapeutic properties of recombinant gamma-interferon and recombinant tumor necrosis factor in mice, Cancer Res 1987 (47) 2563-70.

[271] D. Tanaka, K. Shimada, Y. Rabin, Two-phase computerized planning of cryosurgery using bubble-packing and force-field analogy, J Biomech Eng 2006 (128) 49-58.

[272] S. Tanaka, Immunological aspects of cryosurgery in general surgery, Prog Clin Biol Res 1982 (107) 799-814.

[273] K.N. Tatsutani, J.D. Joye, R. Virmani, M.J. Taylor, In vitro evaluation of vascular endothelial and smooth muscle cell survival and apoptosis in response to hypothermia and freezing, Cryo letters 2005 (26) 55-64.

[274] T. Teesalu, K.N. Sugahara, V.R. Kotamraju, E. Ruoslahti, C-end rule peptides mediate neuropilin-1-dependent cell, vascular, and tissue penetration, Proc Natl Acad Sci U S A 2009 (106) 16157-62.

[275] N.R. Telfer, G.B. Colver, C.A. Morton, Guidelines for the management of basal cell carcinoma, Br J Dermatol 2008 (159) 35-48.

[276] C. Termeer, F. Benedix, J. Sleeman, C. Fieber, U. Voith, T. Ahrens, K. Miyake, M. Freudenberg, C. Galanos, J.C. Simon, Oligosaccharides of Hyaluronan activate dendritic cells via toll-like receptor 4, J Exp Med 2002 (195) 99-111.

[277] K. Theilgaard-Monch, S. Knudsen, P. Follin, N. Borregaard, The transcriptional activation program of human neutrophils in skin lesions supports their important role in wound healing, J Immunol 2004 (172) 7684-93.

[278] D.E. Townsend, A.J. Duleba, M.M. Wilkes, Durability of treatment effects after endometrial cryoablation versus rollerball electroablation for abnormal uterine bleeding: two-year results of a multicenter randomized trial, Am J Obstet Gynecol 2003 (188) 699-701.

[279] J.M. Trevejo, M.W. Marino, N. Philpott, R. Josien, E.C. Richards, K.B. Elkon, E. Falck-Pedersen, TNF-alpha -dependent maturation of local dendritic cells is critical for activating the adaptive immune response to virus infection, Proc Natl Acad Sci U S A 2001 (98) 12162-7.

[280] T.M. Turk, M.A. Rees, P. Pietrow, C.E. Myers, S.E. Mills, J.Y. Gillenwater, Determination of optimal freezing parameters of human prostate cancer in a nude mouse model, Prostate 1999 (38) 137-43.

[281] M. Udagawa, C. Kudo-Saito, G. Hasegawa, K. Yano, A. Yamamoto, M. Yaguchi, M. Toda, I. Azuma, T. Iwai, Y. Kawakami, Enhancement of immunologic tumor regression by intratumoral administration of dendritic cells in combination with cryoablative tumor pre-treatment and Bacillus Calmette-Guerin cell wall skeleton stimulation, Clin Cancer Res 2006 (12) 7465-75.

[282] T. Utsumi, M.C. Hung, J. Klostergaard, Preparation and characterization of liposomal-lipophilic tumor necrosis factor, Cancer Res 1991 (51) 3362-6.

[283] A.H. van der Veen, A.M. Eggermont, A.L. Seynhaeve, T. van, T.L. ten Hagen, Biodistribution and tumor localization of stealth liposomal tumor necrosis factor-alpha in soft tissue sarcoma bearing rats, Int J Cancer 1998 (77) 901-6.

[284] R. van Horssen, T.L. Ten Hagen, A.M. Eggermont, TNF-alpha in cancer treatment: molecular insights, antitumor effects, and clinical utility, Oncologist 2006 (11) 397-408.

[285] E.E. Varfolomeev, A. Ashkenazi, Tumor necrosis factor: an apoptosis JuNKie?, Cell 2004 (116) 491-7.

[286] J. Vilcek, V.J. Palombella, D. Henriksen-DeStefano, C. Swenson, R. Feinman, M. Hirai, M. Tsujimoto, Fibroblast growth enhancing activity of tumor necrosis factor and its relationship to other polypeptide growth factors, J Exp Med 1986 (163) 632-43.

[287] R. Visaria, J.C. Bischof, M. Loren, B. Williams, E. Ebbini, G. Paciotti, R. Griffin, Nanotherapeutics for enhancing thermal therapy of cancer, Int J Hyperthermia 2007 (23) 501-11.

[288] R.K. Visaria, R.J. Griffin, B.W. Williams, E.S. Ebbini, G.F. Paciotti, C.W. Song, J.C. Bischof, Enhancement of tumor thermal therapy using gold nanoparticle-assisted tumor necrosis factor-{alpha} delivery, Mol Cancer Ther 2006 (5) 1014-20.

[289] R.K. Visaria, R.J. Griffin, B.W. Williams, E.S. Ebbini, G.F. Paciotti, C.W. Song, J.C. Bischof, Enhancement of tumor thermal therapy using gold nanoparticle-assisted tumor necrosis factor-alpha delivery, Molecular cancer therapeutics 2006 (5) 1014-20.

[290] I.H. Vos, R. Govers, H.J. Grone, L. Kleij, M. Schurink, R.A. De Weger, R. Goldschmeding, T.J. Rabelink, NFkappaB decoy oligodeoxynucleotides reduce monocyte infiltration in renal allografts, FASEB J 2000 (14) 815-22.

[291] C.L. Walker, D. Hunter, J.I. Everitt, Uterine leiomyoma in the Eker rat: a unique model for important diseases of women, Genes Chromosomes Cancer 2003 (38) 349-56.

[292] P. Walsh, A. Retik, E. Vaughan, A. Wein, editors. Campbell's Urology: WB Saunders; 2002.

[293] T.A.S. Walter Schurch, and Giulio Gabbiani, Histology for Pathologists, Philadelphia, Lippincott-Raven Publishers, 1997.

[294] C.L. Wang, K.Y. Teo, B. Han, An amino acidic adjuvant to augment cryoinjury of MCF-7 breast cancer cells, Cryobiology 2008 (57) 52-9.

[295] N. Watanabe, Y. Niitsu, H. Umeno, H. Kuriyama, H. Neda, N. Yamauchi, M. Maeda, I. Urushizaki, Toxic effect of tumor necrosis factor on tumor vasculature in mice, Cancer Res 1988 (48) 2179-83.

[296] N. Watanabe, Y. Niitsu, H. Umeno, H. Sone, H. Neda, N. Yamauchi, M. Maeda, I. Urushizaki, Synergistic cytotoxic and antitumor effects of recombinant human tumor necrosis factor and hyperthermia, Cancer Res 1988 (48) 650-3.

[297] A. Waterston, M. Bower, TNF and cancer: good or bad?, Cancer Therapy 2004 (2) 131-48.

[298] S.M. Weber, F.T. Lee, Jr., D.O. Chinn, T. Warner, S.G. Chosy, D.M. Mahvi, Perivascular and intralesional tissue necrosis after hepatic cryoablation: results in a porcine model, Surgery 1997 (122) 742-7.

[299] C.J. Weight, J.H. Kaouk, N.J. Hegarty, E.M. Remer, C.M. O'Malley, B.R. Lane, I.S. Gill, A.C. Novick, Correlation of radiographic imaging and histopathology following cryoablation and radio frequency ablation for renal tumors, J Urol 2008 (179) 1277-81; discussion 81-3.

[300] S.J. Weiss, Tissue destruction by neutrophils, N Engl J Med 1989 (320) 365-76.

[301] S. West, R. Ruiz, W.H. Parker, Abdominal myomectomy in women with very large uterine size, Fertil Steril 2006 (85) 36-9.

[302] D.K. Whittaker, Vascular responses in the oral mucosa following cryosurgery, J Periodontal Res 1977 (12) 55-63.

[303] D.K. Whittaker, Mechanisms of tissue destruction following cryosurgery, Ann R Coll Surg Engl 1984 (66) 313-8.

[304] M.C. Woodle, Controlling liposome blood clearance by surface-grafted polymers, Adv Drug Deliv Rev 1998 (32) 139-52.

[305] Y.F. Xia, B.Q. Ye, Y.D. Li, J.G. Wang, X.J. He, X. Lin, X. Yao, D. Ma, A. Slungaard, R.P. Hebbel, N.S. Key, J.G. Geng, Andrographolide attenuates inflammation by inhibition of NF-kappa B activation through covalent modification of reduced cysteine 62 of p50, J Immunol 2004 (173) 4207-17.

[306] S.Q. Yang, H.Z. Lin, M.D. Lane, M. Clemens, A.M. Diehl, Obesity increases sensitivity to endotoxin liver injury: implications for the pathogenesis of steatohepatitis, Proc Natl Acad Sci U S A 1997 (94) 2557-62.

[307] W.L. Yang, T. Addona, D.G. Nair, L. Qi, T.S. Ravikumar, Apoptosis induced by cryo-injury in human colorectal cancer cells is associated with mitochondrial dysfunction, Int J Cancer 2003 (103) 360-9.

[308] F. Yuan, W. Zhou, J. Zhang, Z. Zhang, C. Zou, L. Huang, Y. Zhang, Z. Dai, Anticancer drugs are synergistic with freezing in induction of apoptosis in HCC cells, Cryobiology 2008 (57) 60-5.

[309] C. Zhang, J. Pei, D. Kumar, I. Sakabe, H.E. Boudreau, P.C. Gokhale, U.N. Kasid, Antisense oligonucleotides: target validation and development of systemically delivered therapeutic nanoparticles, Methods Mol Biol 2007 (361) 163-85.

[310] J. Zhang, G.A. Sandison, J.Y. Murthy, L.X. Xu, Numerical simulation for heat transfer in prostate cancer cryosurgery, J Biomech Eng 2005 (127) 279-94.

[311] F. Zhao, H. Xu, E.Q. He, Y.T. Jiang, K. Liu, Inhibitory effects of sesquiterpenes from Saussurea lappa on the overproduction of nitric oxide and TNF-alpha release in LPS-activated macrophages, J Asian Nat Prod Res 2008 (10) 1045-53.

[312] V.S. Zimmermann, A. Bondanza, A. Monno, P. Rovere-Querini, A. Corti, A.A. Manfredi, TNF-alpha coupled to membrane of apoptotic cells favors the cross-priming to melanoma antigens, J Immunol 2004 (172) 2643-50.

[313] N. Zook, J. Hussmann, R. Brown, R. Russell, J. Kucan, A. Roth, H. Suchy, Microcirculatory studies of frostbite injury, Ann Plast Surg 1998 (40) 246-53; discussion 54-5.

[314] T.G. Zreik, T.J. Rutherford, S.F. Palter, R.N. Troiano, E. Williams, J.M. Brown, D.L. Olive, Cryomyolysis, a new procedure for the conservative treatment of uterine fibroids, J Am Assoc Gynecol Laparosc 1998 (5) 33-8.

Appendix I Mathematic Modeling of NF-κB and Caspase Pathway Induced by TNF-α

To understand the mechanism of TNF-α enhanced cryoinjury, we need to elucidate the biological mechanism underlying cryosurgery, as well as the precise role TNF-α plays in the accentuation of injury. However, TNF-α can have a paradoxical effect on a cell depending on the cell type as well as signaling pathway activated in the cell, making it difficult to discern the ultimate effect. We simulated the TNF-α initiated apoptotic cascade, as well as nuclear transcription of IκB. These pathways play a crucial role in deciding cell fate in the response to inflammation and apoptosis respectively. The quantitative dynamic model based on [7] incorporates known specific protein-protein interactions (Table AI-3) as identified by experiments [2, 4], a set of ordinary differential chemical equations (Table AI-2) are built to describe the signal transduction process. The variables are the time dependent concentrations of participating molecules, initial values are shown in Table AI-1 [2, 4]. The parameters are reaction rate constants (Table AI-4). In this approach, where dependences on spatial location are neglected, except for the consideration of different cellular compartments such as cytoplasm or nucleus, reactions are assumed to occur homogeneously throughout the compartmental volume. When the number of molecules is large any two reactions can take place at the same time. The system of ordinary differential equations for concentrations thus represents a collection of reactions occurring simultaneously all through the reaction volume. The simplified pathway network behind this model is shown in Fig. AI-1. The model is constructed with 4 components:

1. Formation of the Early Complex

Binding of TNF-α to TNFR1 leads to the recruitment of the death domain proteins TRADD, TRAF2 and RIP-1 to the ligand-receptor complex [6]. These multi-protein complexes are referred to as early complexes. The early complex, the concentration of

which is represented by c_9, forms the pedestal for the two-sub-pathways: 1) transcription of NF-κB production; and 2) induction of enzymatic caspase cascade.

2. Activation of NF-κB

NF-κB is sequestered in inactive form in the cytoplasm through the interaction with inhibitory proteins, the IκB. Proteolytic degradation of IκB immediately precedes, and is required for NF-κB release and subsequent nuclear translocation [3]. The inactive inhibitory kinase IKK binds to the early complex, forming a survival complex c_{11},. Dissociation of this complex leads to activation of IKK and regeneration of the adaptor proteins. The phosphorylation of IκB and release of NF-κB is mediated by the activated IKK.

3. Activation of the Caspase Cascade

The early complex c_9 when bound to FADD and then procaspase 8, leads to activation of the apoptotic signaling machinery via the death-including signaling complex (DISC) [6], c_{21}. DISC consists of FADD, caspase 8, TRADD and TRAF2 but not TNFR1 [6], thus an additional reaction is involved to depict the formation of DISC without TNFR1. DISC release activated caspase 8 which is capable of activating caspase 3 [9].

4. Nuclear Activity

NF-κB in the nucleus binds to DNA and leads to the transcription of inhibitor of apoptosis protein (IAP) and its own inhibitor IκB among others. IAP arrests activated caspase 3 and thus prevents DNA fragmentation [5].

With this model implemented as described, we checked the dynamics of key molecules involved in the NF-κB and apoptosis pathways at different TNF-α dosage (Fig. AI-3). The oscillation response shown in Fig. AI-3A is because of the negative feedback loop of IκB-NF-κB signaling (Fig. AI-2) which is first modeled and validated by Hoffman et al, 2002 [4]. NF-κB is held inactive in the cytoplasm by three IκB isoforms. Cell stimulation activates the IKK complex, leading to phosphorylation and degradation of IκB proteins. Free NF-κB translocates to the nucleus, activating genes, including IκB and IAP. IκB allows for temporal control of NF-κB activation involving a negative feedback. IAP, on the other hand, inhibits apoptosis by arresting active caspase 3. The oscillation behavior in our model agrees with experimental data [4]. DNA fragmentation is a hall mark of the onset of apoptosis. The dynamics of DNA fragmentation for the apoptosis and full pathway is shown in Fig. AI-4. With TNF-α increases, the rate and amount of caspase 3 cleavage increases (DNA fragmentation dynamics monitors production of active caspse 3), and the process takes shorter time. With low dosage of TNF-α (ex. 1nM, 0.5nM), there is very little total DNA damage induced within 10 hours. Based on the model, DNA will be totally fragmented (800nM) whatever low dosage applied, though it will take much longer time to reach. This is not realistic because the long course of DNA fragmentation possibly allows time for other genes to come into play (ex. DNA repair system). In this case, the cell fate is not predictable only by the mathematical model.

Previous studies suggest that rather than tumor cells themselves, cells of the tumor stroma may be responsible for the observed antitumor effect of TNF-α in patients [8]. This hypothesis was confirmed by data from mice experiments revealing that TNF-α had a cytotoxic effect on tumor vasculature [10]. The activation of apoptosis and inflammation pathways in endothelial cells are responsible for the extravasation of erythrocytes and leukocytes to the interstitial space of tumor tissue, leading to hemorrhagic necrosis [8]. Therefore, TNF-α is considered as a vascular agent targeting the tumor-associated vasculature by inducing hyperpermeability and destruction of the vascular lining.

Table AI-1: Species and initial values [1, 2, 4]

Name	Species	Initial value (nM)
c1	TNF-α	a
c2	TNFR1	100
c3	TNF-α/ TNFR1	0
c4	TRADD	150
c5	TNF-α/ TNFR1/TRADD	0
c6	TRAF2	100
c7	TNF-α/ TNFR1/TRADD/ TRAF2	0
c8	RIP-1	100
c9	TNF-α/TNFR1/TRADD/TRAF2/RIP-1 (Early Complex)	0
c10	IKK	100
c11	TNF-α/ TNFR1/TRADD/ TRAF2/RIP-1/IKK (Survival Complex)	0
c12	IKK*	0
c13	IκB/NF-κB	250
c14	IκB/NF-κB/ IKK*	0
c15	IκB-P	0
c16	NF-κB	0
c17	FADD	100
c18	TNF-α/TNFR1/TRADD/TRAF2/RIP-1/FADD	0
c19	TRADD/TRAF2/RIP-1/FADD	0
c20	Caspase-8	80
c21	TRADD/TRAF2/RIP-1/FADD/ Caspase-8 (Death Complex)	0
c22	Caspase-8*	0
c23	Caspase-3	200
c24	Caspase-8*/ Caspase-3	0
c25	Caspase-3*	0
c26	DNA-fragmentation	0
c27	c-IAP	0
c28	Caspase-3*/c-IAP	0
c29	DNA (intact)	800
c30	Caspase-3*/DNA	0
c31	IκB	0

Table AI-2: Differential equations

$$\frac{dc_1}{dt} = -k_1.c_1.c_2 + k_2.c_3$$

$$\frac{dc_2}{dt} = -k_1.c_1.c_2 + k_2.c_3 + k_{17}.c_{18} + k_{11}.c_{11}$$

$$\frac{dc_3}{dt} = k_1.c_1.c_2 - k_2.c_3 - k_3.c_3.c_4 + k_4 c_5$$

$$\frac{dc_4}{dt} = -k_3.c_3.c_4 + k_4 c_5 + k_{11}.c_{11} + k_{20}.c_{21}$$

$$\frac{dc_5}{dt} = k_3.c_3.c_4 - k_4.c_5 - k_5.c_5.c_6 + k_6.c_7$$

$$\frac{dc_6}{dt} = -k_5.c_5.c_6 + k_6.c_7 + k_{11}.c_{11} + k_{20}.c_{21}$$

$$\frac{dc_7}{dt} = k_5.c_5.c_6 - k_6.c_7 - k_7.c_7.c_8 + k_8.c_9$$

$$\frac{dc_8}{dt} = -k_7.c_7.c_8 + k_8.c_9 + k_{11}.c_{11} + k_{20}.c_{21}$$

$$\frac{dc_9}{dt} = k_7.c_7.c_8 - k_8.c_9 - k_9.c_9.c_{10} + k_{10}.c_{11}$$
$$- k_{15}.c_9.c_{17} + k_{16}.c_{18}$$

$$\frac{dc_{10}}{dt} = -k_9.c_9.c_{10} + k_{10}.c_{11} + k_{14}.c_{14}$$

$$\frac{dc_{11}}{dt} = k_9.c_9.c_{10} - k_{10}.c_{11} - k_{11}.c_{11}$$

$$\frac{dc_{12}}{dt} = -k_{12}.c_{12}.c_{13} + k_{13}.c_{14} + k_{11}.c_{11}$$

$$\frac{dc_{13}}{dt} = -k_{12}.c_{12}.c_{13} + k_{13}.c_{14} + k_{29}.c_{16}.c_{31}$$

$$\frac{dc_{14}}{dt} = k_{12}.c_{12}.c_{13} - k_{13}.c_{14} - k_{14}.c_{14}$$

$$\frac{dc_{15}}{dt} = k_{14}.c_{14}$$

$$\frac{dc_{16}}{dt} = k_{14}.c_{14} - k_{29}.c_{16}.c_{31}$$

$$\frac{dc_{17}}{ct} = -k_{15}.c_9.c_{17} + k_{16}.c_{18} + k_{20}.c_{21}$$

$$\frac{dc_{18}}{dt} = k_{15}.c_9.c_{17} - k_{16}.c_{18} - k_{17}.c_{18}$$

$$\frac{dc_{19}}{ct} = k_{17}.c_{18} - k_{18}.c_{19}.c_{20} + k_{19}.c_{21}$$

$$\frac{dc_{20}}{dt} = -k_{18}.c_{19}.c_{20} + k_{19}.c_{21}$$

$$\frac{dc_{21}}{dt} = k_{18}.c_{19}.c_{20} - k_{19}.c_{21} - k_{20}.c_{21}$$

$$\frac{dc_{22}}{dt} = k_{20}.c_{21} - k_{21}.c_{22}.c_{23} + k_{22}.c_{24} + k_{23}.c_{24}$$

$$\frac{dc_{23}}{dt} = -k_{21}.c_{22}.c_{23} + k_{22}.c_{24} + k_{26}.c_{30}$$

$$\frac{dc_{24}}{dt} = k_{21}.c_{22}.c_{23} - k_{22}.c_{24} - k_{23}.c_{24}$$

$$\frac{dc_{25}}{dt} = k_{23}.c_{24} - k_{28}.c_{27}.c_{25} - k_{24}.c_{29}.c_{25} + k_{25}.c_{30}$$

$$\frac{dc_{26}}{dt} = k_{26}.c_{30}$$

$$\frac{dc_{27}}{dt} = p.c_{16}(t-\tau) - k_{28}.c_{27}.c_{25}$$

$$\frac{dc_{28}}{dt} = k_{28}.c_{27}.c_{25}$$

$$\frac{dc_{29}}{dt} = -k_{24}.c_{29}.c_{25} + k_{25}.c_{30}$$

$$\frac{dc_{30}}{dt} = k_{24}.c_{29}.c_{25} - k_{25}.c_{30} - k_{26}.c_{30}$$

$$\frac{dc_{31}}{dt} = p.c_{16}(t-\tau) - k_{29}.c_{16}.c_{31}$$

140

Table AI-3: Reactions involved in the pathway

Module 1: Formation of the early complex	Node Equation
TNF-α+TNFR1⇔TNF-α/TNFR1	J1=k1c1c2-k2c3
TNF-α/TNFR1+TRADD⇔TNF-α/TNFR1/TNFDD	J2=k3c3c4-k4c5
TNF-α/TNFR1/TNFDD+TRAF2⇔TNF-α/TNFR1/TNFDD/TRAF2	J3=k5c5c6-k6c7
TNF-α/TNFR1/TNFDD/TRAF2+RIP-1⇔TNF-α/TNFR1/TNFDD/TRAF2/RIP-1	J4=k7c7c8-k8c9
Module 2: Activation of NF-κB by the multi-protein complexes	
TNF-α/TNFR1/TNFDD/TRAF2/RIP-1+IKK⇔TNF-α/TNFR1/TNFDD/TRAF2/RIP-1/IKK	J5=k9c10c9-k10c11
TNF-α/TNFR1/TNFDD/TRAF2/RIP-1/IKK=>TNFR1+TRADD+TRAF2+RIP-1+IKK*	J6=k11c11
IKK*+IκB/NF-κB⇔IκB/NF-κB/IKK*	J7=k12c12c13-k13c14
IκB/NF-κB/IKK* =>IKK+IκB-P+NF-κB	J8=k14c14
Module 3: Activation of Caspases by multi-protein complexes	
TNF-α/TNFR1/TNFDD/TRAF2/RIP-1+FADD⇔TNF-α/TNFR1/TNFDD/TRAF2/RIP-1/FADD	J9=k15c9c17-k16c18
TNF-α/TNFR1/TNFDD/TRAF2/RIP-1/FADD=>TNFDD/TRAF2/RIP-1/FADD+TNFR1	J10=k17c18
TNFDD/TRAF2/RIP-1/FADD+Caspase-8⇔TRADD/TRAF2/RIP-1/FADD/Caspase-8	J11=k18c19c20-k19c21
TRADD/TRAF2/RIP-1/FADD/Caspase-8=>Caspase-8* +TRADD+FADD+RIP-1+TRAF2	J12=k20c21
Caspase-8* + Caspase-3⇔ Caspase-8*/Caspase-3	J13=k21c22c23-k22c24
Caspase-8*/Caspase-3=>Caspase-3* + Caspase-8*	J14=k23c24
Module 4: Nuclear activity	
Caspase-3* + DNA⇔Caspase-3*/DNA	J15=k24c25c29-k25c30
Caspase-3*/DNA =>DNA-fragmentation+Caspase-3	J16=k26c30
NF-κB=>c-IAP+IκB	*J17=pc16(t-τ)
Caspase-3* + c-IAP=>Caspase-3*/c-IAP	J18=k28c27c25
IκB+NF-κB=>IκB/NF-κ	J19=k19c16c31

Table AI-4: Kinetic parameters (Concentration is in nM and time in seconds) [2, 4]
The first order rate constants have units of s^{-1} and the second order rate constants have units of $nM^{-1}.s^{-1}$

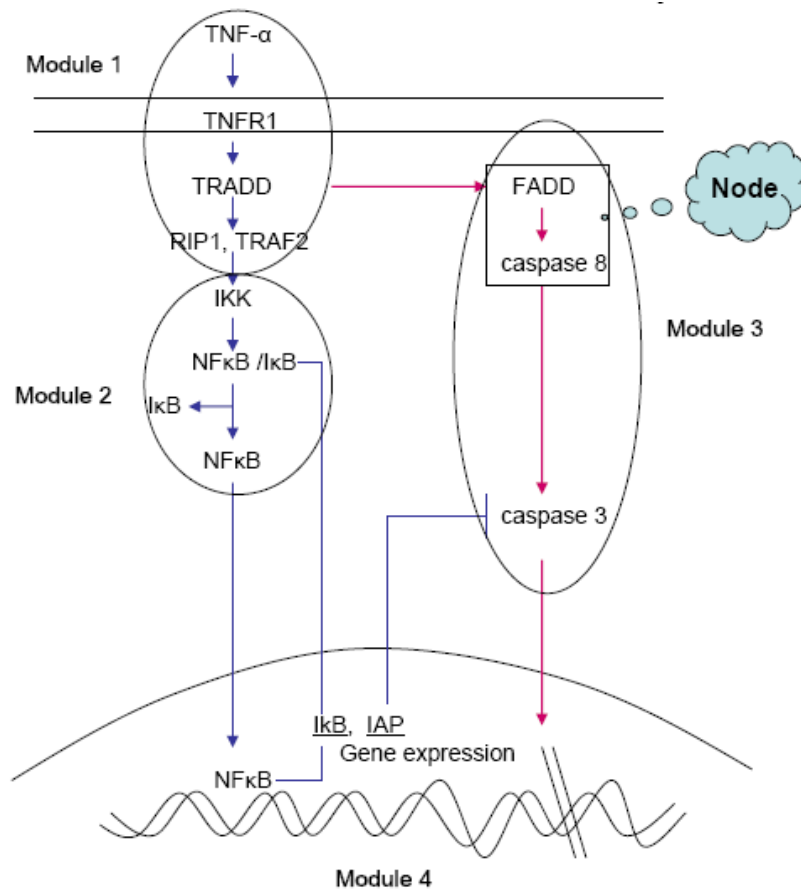| Kinetic Parameter	Value*10^3	Kinetic Parameter	Value*10^3
k1	0.185	k15	0.185
k2	0.00125	k16	0.00125
k3	0.185	k17	0.37
k4	0.00125	k18	0.5
5	0.185	k19	0.2
k6	0.00125	k20	0.1
k7	0.185	k21	0.1
k8	0.00125	k22	0.06
k9	0.185	k23	100
k10	0.00125	k24	0.185
k11	0.37	k25	0.00125
k12	0.014	k26	0.37
k13	0.00125	k27	0.37
k14	0.37	k28	0.5
p	1.75	k29	750

Figure AI-1: Pathway network for the mathematic model. In this network, each protein-protein interaction is defined as a "node", ex. interaction of FADD and capsese 8 is considered as node 11 (J11), association rate k18 and disassociation rate k19 are node parameters. See Table 3-2 for detail and Table 3-3 for initial value.
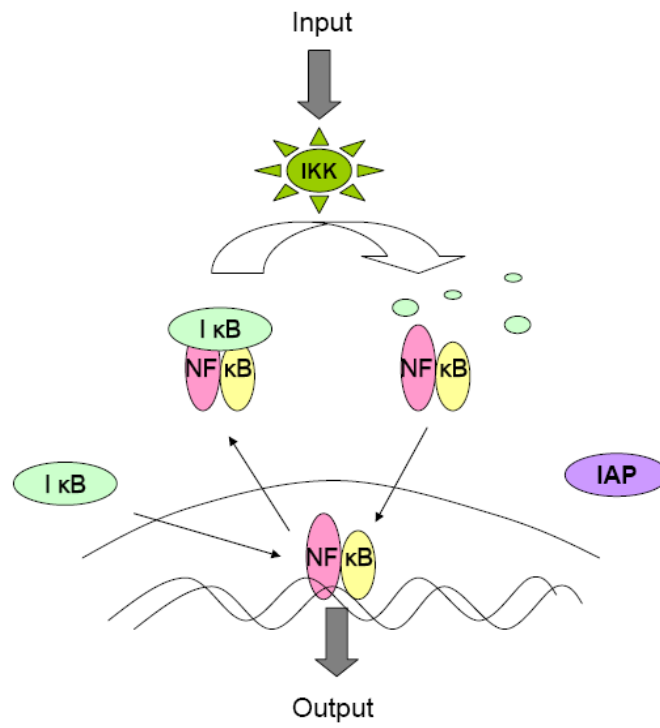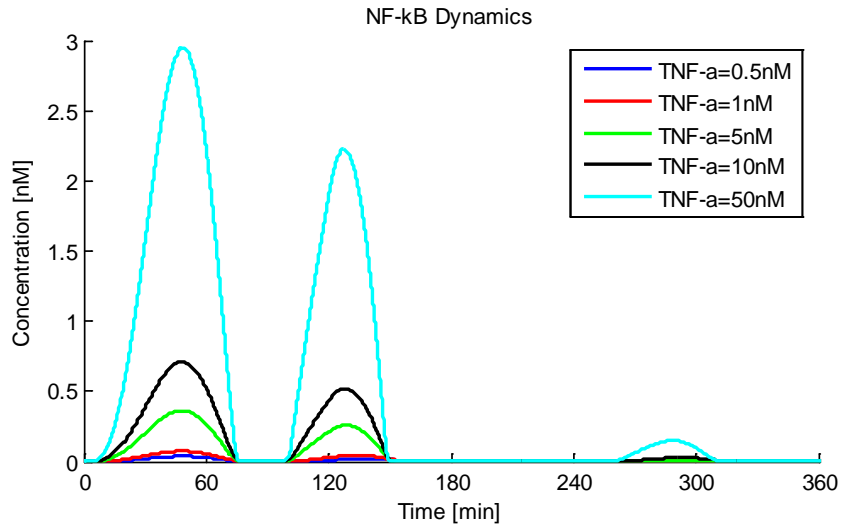
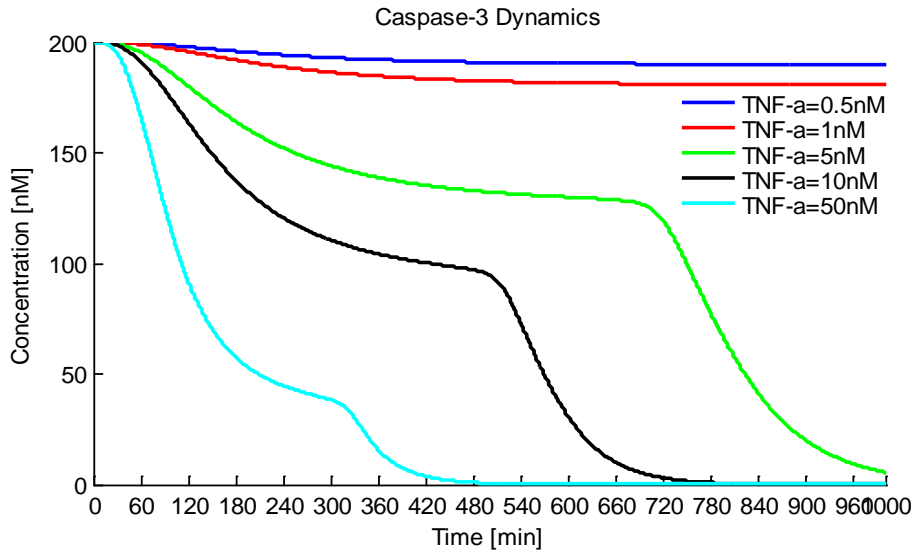Figure AI-2: Negative feedback loop of IκB-NF-κB signaling

A

B

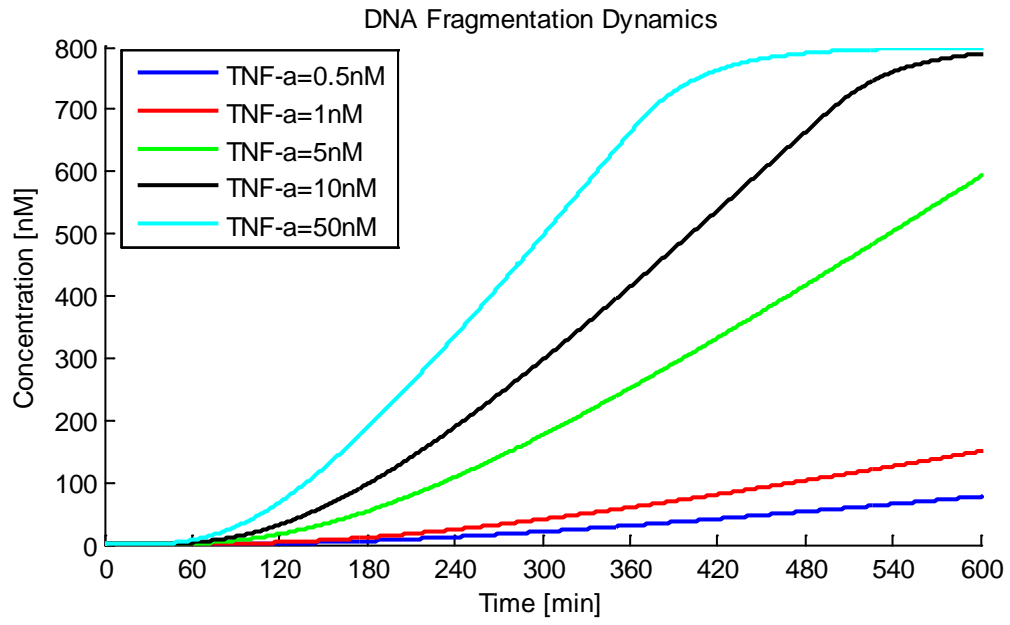Figure AI-3: Response of NF-κB (A) and caspase-3 (B) to TNF-α concentration

Figure AI-4: DNA fragmentation dynamics post TNF-α treatment

References

[1] T. Eissing, H. Conzelmann, E.D. Gilles, F. Allgower, E. Bullinger, P. Scheurich, Bistability analyses of a caspase activation model for receptor-induced apoptosis, J Biol Chem 2004 (279) 36892-7.

[2] M. Fussenegger, J.E. Bailey, J. Varner, A mathematical model of caspase function in apoptosis, Nat Biotechnol 2000 (18) 768-74.

[3] F.R. Greten, M. Karin, The IKK/NF-kappaB activation pathway-a target for prevention and treatment of cancer, Cancer Lett 2004 (206) 193-9.

[4] A. Hoffmann, A. Levchenko, M.L. Scott, D. Baltimore, The IkappaB-NF-kappaB signaling module: temporal control and selective gene activation, Science 2002 (298) 1241-5.

[5] M. Holcik, R.G. Korneluk, XIAP, the guardian angel, Nat Rev Mol Cell Biol 2001 (2) 550-6.

[6] O. Micheau, J. Tschopp, Induction of TNF receptor I-mediated apoptosis via two sequential signaling complexes, Cell 2003 (114) 181-90.

[7] P. Rangamani, L. Sirovich, Survival and apoptotic pathways initiated by TNF-alpha: modeling and predictions, Biotechnol Bioeng 2007 (97) 1216-29.

[8] R. van Horssen, T.L. Ten Hagen, A.M. Eggermont, TNF-alpha in cancer treatment: molecular insights, antitumor effects, and clinical utility, The oncologist 2006 (11) 397-408.

[9] F. Wang, T.S. Chen, D. Xing, J.J. Wang, Y.X. Wu, Measuring dynamics of caspase-3 activity in living cells using FRET technique during apoptosis induced by high fluence low-power laser irradiation, Lasers Surg Med 2005 (36) 2-7.

[10] N. Watanabe, Y. Niitsu, H. Umeno, H. Kuriyama, H. Neda, N. Yamauchi, M. Maeda, I. Urushizaki, Toxic effect of tumor necrosis factor on tumor vasculature in mice, Cancer Res 1988 (48) 2179-83.

Appendix II TNF-α Induced Leukocyte-Endothelium Interaction on Cryosurgical Enhancement

Our previous results suggests that the main effect of TNF-α is to pre-condition the vasculature by activating vascular endothelial cells to recruit inflammatory cells and promote their extravasation. NF-κB pathway activation and the subsequent vascular adhesion molecule (VCAM) expression were mainly responsible for the inflammatory cells (leukocytes) recruitment. In particular, it is VCAM expression on endothelial surface directly mediates the leukocyte-endothelium interaction [2, 3]. Combined with cryosurgery, both NF-κB translocation and VCAM activation were significantly enhanced by TNF-α pre-treatment at day 1 (Fig. 3-4B). NF-κB inhibition significantly reduced inflammatory infiltration (Fig. 3-4C and D) and vascular injury (Fig. 2-5B) enhance by TNF-α pre-treatment at day 3 post cryosurgery. However, it still remains unknown if VCAM expression plays a role in cryosurgical enhancement by TNF-α. Therefore, VCAM inhibition study was performed to block the leukocyte-endothelium interaction post TNF-α pre-conditioning, which was expected to reduce both vascular injury (measured by stasis radius) and inflammatory infiltrate enhancement by TNF-α post cryosurgery.

The dorsal skin fold chamber (DSFC) was implanted and LNCaP tumor was implanted in male nude mouse (see DSFC implantation, tumor implantation, Chapter 2). 200 ng/mouse of TNF-α (a gift from CytImmune Science, Inc., Rockville, MD; dissolved in 30 µl saline) were topically applied for 15 min. At 4 hours after TNF-α treatment, nude mouse with implanted DSFC was topically injected with 60 µg of anti-mouse VCAM-1 monoclonal antibody (MAb) (Vector Laboratories, Burlingame, CA) [1]. The anti VCAM-1 MAb blocks the binding of $\alpha_4\beta_1$ integrin counterreceptors to VCAM-1. Cryosurgery procedure was performed 15 min after VCAM inhibition (see freeze/thaw (FT) of the DSFC, Chapter 2). Stasis radius was measured at day 3 post cryosurgery (see intravital measurements of vascular flow, Chapter 3). Animals were sacrificed at day 3 after stasis

radius measurement. The entire tumor tissue within DSFC was processed and stained with hematoxylin-eosin (H&E) (see Histology and Immunohistochemistry, Chapter 3).

VCAM inhibition significantly reduced the TNF-α enhancement on stasis radius post cryosurgery (Fig. AII-1). The stasis radius was reduced to 3.04 ± 0.25 mm with VCAM inhibition, compared to 3.95 ± 0.25 mm without VCAM inhibition (*, $p < 0.01$). The stasis radius with VCAM inhibition was comparable to the cryosurgery alone without TNF-α pre-treatment and VCAM inhibition (3.29 ± 0.20 mm).VCAM inhibition also reduced TNF-α enhancement on inflammatory infiltrate post cryosurgery determined by histology (Fig. AII-2). The width and cell intensity of the inflammation band post TNF-α and cryosurgery were dramatically reduced by VCAM inhibition. Accordingly, the edge of the cryolesion post TNF-α and cryosurgery also shrank due to VCAM inhibition.

To conclude, VCAM expression induced by TNF-α pre-treatment plays a significant role in TNF-α enhancement of inflammatory infiltrate and vascular injury post cryosurgery. This indicates that TNF-α pre-conditions the tumor tissue by inducing VCAM expression, which further enhance inflammatory infiltrate and vascular injury after cryosurgery, thereby enhancing the cryolesion.
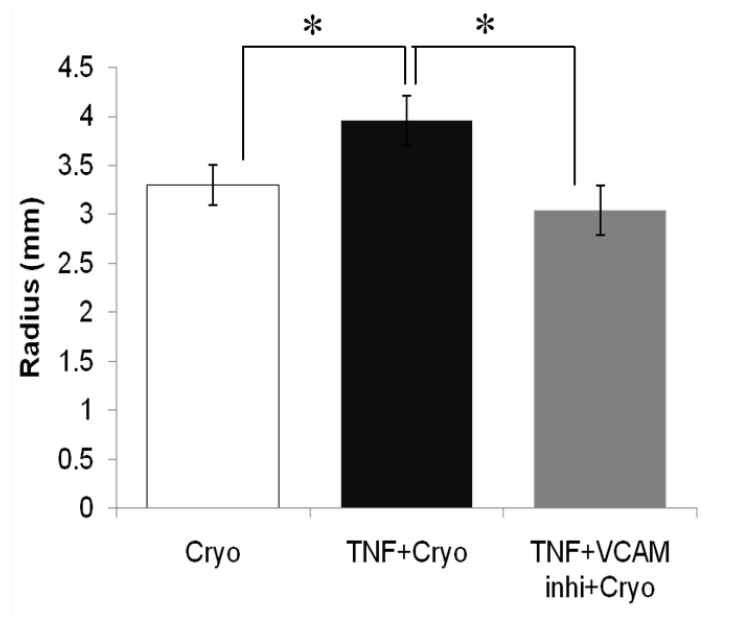
Figure AII-1: *In vivo* effect of VCAM inhibition on tumor grown in a dorsal skin fold chamber. The inhibition was performed at TNF-α pretreated dose of 200 ng. Values presented are mean ± standard error from 5-8 animals in each group. Groups were statistically different than groups pretreated with TNF-α (*, $p < 0.01$).
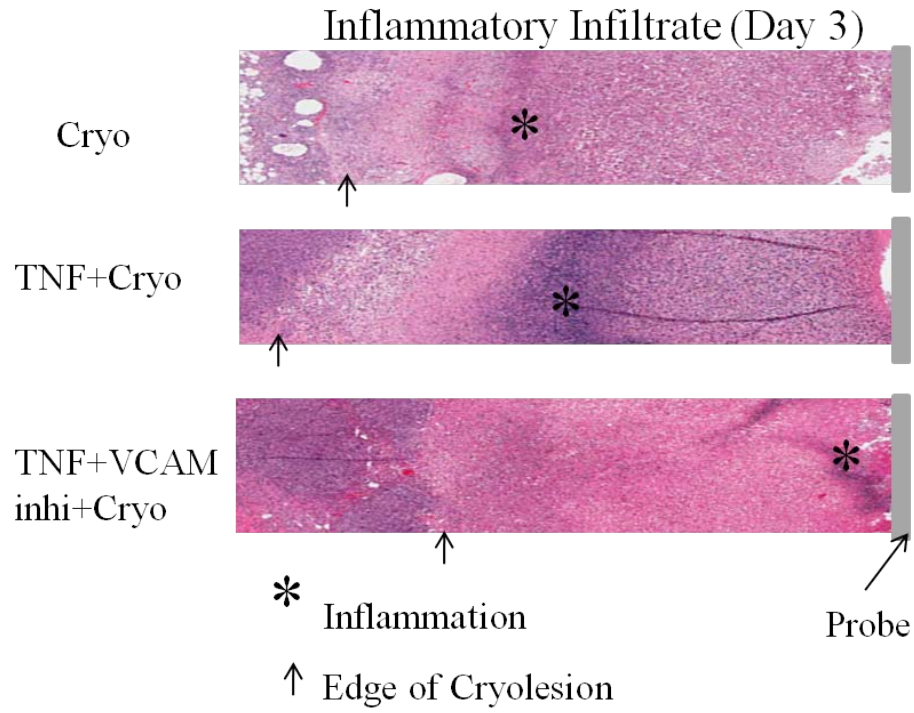
Figure AII-2: Histological analysis at day 3 post cryosurgery with or without VCAM inhibition. Stars indicate the inflammatory infiltrate post cryosurgery. And arrows indicate the cryolesion edge determined by histology.

References

[1] J.D. Belcher, H. Mahaseth, T.E. Welch, A.E. Vilback, K.M. Sonbol, V.S. Kalambur, P.R. Bowlin, J.C. Bischof, R.P. Hebbel, G.M. Vercellotti, Critical role of endothelial cell activation in hypoxia-induced vasoocclusion in transgenic sickle mice, Am J Physiol Heart Circ Physiol 2005 (288) H2715-25.

[2] T.M. Carlos, J.M. Harlan, Leukocyte-endothelial adhesion molecules, Blood 1994 (84) 2068-101.

[3] M. Morigi, S. Angioletti, B. Imberti, R. Donadelli, G. Micheletti, M. Figliuzzi, A. Remuzzi, C. Zoja, G. Remuzzi, Leukocyte-endothelial interaction is augmented by high glucose concentrations and hyperglycemia in a NF-kB-dependent fashion, J Clin Invest 1998 (101) 1905-15.